FYRSKEPPET
OFFSHORE AB

skyborn

Fyrskeppet Offshore

Liite E4: Hydrodynamic Pressure

Fyrskeppet Offshore Wind Farm

Hydrodynamic Pressure

Fyrskeppet Offshore AB

Date: 06 June 2023

Rev.no.	Date	Description	Prepared by	Verified by	Approved by
1	2023-02-24	Draft	TEB/GVIG	RUGA	TEB
2	2023-06-06	Final	TEB	RUGA	TEB

Contents

Appendix

1. Introduction

Fyrskeppet Offshore AB has appointed NIRAS to quantify the impact on the hydrodynamics of the planned Fyrskeppet Offshore Wind Farm (Fyrskeppet OWF)in the operation phase for a case with 187 turbines with 15MW rated power, corresponding to a worst-case scenario for the hydrodynamic impacts of fundaments and a representative scenario for wind speed reductions (compared to e.g., 93 turbines with 30MW rated power).

2. Scope of Work

The purpose of the hydrodynamic study is to present the present situation (Baseline) and the potential impact in the operation phase of the wind farm on:

- The general current pattern and eventual blocking;
- The wave pattern;

3. Abbreviation

GBS	Gravity Based Structure
Hm0	Significant wave height
IAC	Inter array cable
MW	Mega Watt
OWF	Offshore Wind Farm
OSS	Offshore substation
WTG	Wind turbine generator

4. Summary

To address the impact on the hydrodynamics a hydrodynamic and spectral wave model of the Gulf of Bothnia has been calibrated on public data of water levels, and project data of current, temperature, salinity and waves. Based on data from SMHI's 3D model of the Baltic Sea the year-to-year variations were investigated and the year 2021 was found to be close to an average year and thus to be used as a baseline for description of the potential impact. In general, the year-to-year variation is small and unlikely to impact the conclusion.

Baseline, general description:

The Bothnian Sea, where Fyrskeppet OWF is located, constitutes the southern part of the Gulf of Bothnia, and is separated from the Baltic Proper by a strait at the Åland Sea. Hydrographic conditions are characterised by a low salinity (3-6 PSU) and a weak vertical salinity gradient (halocline). Sea surface temperature varies from 0-2°C during the winter to somewhat over 20°C between June and August. Temperature is strongly stratified during the summer with a thermocline (zone of maximum temperature gradient) around 10-30m depth. Deeper temperature, below 30m, varies less during the year, between 2°C at the end of the winter to 7°C at the end of the autumn. Due to the absence of tides, water levels experience relatively small variations, generally between ±50cm around their average during the year. These variations are mostly driven by variations at the Åland boundary, wind and pressure differences (meteorological surge). Due to the limited variations in water levels, currents are generally weak, around 0.15m/s at the surface (maximum of 0.5m/s) and less than 0.07m/s below 30m, and mostly driven by wind as well as temperature and salinity differences. Average circulation in the Bothnian Sea is counter-clockwise with dominant northward currents along the east coast, southwards along the west coast, and relatively large (≥10km radius) eddies at the centre of the sea. Waves are fetch limited with under 1m significant wave height on average over the year. Maximum waves are observed in October, 1.5m on average, with higher waves in the northward direction.

The impact in the operation phase is evaluated for the obstruction from 187 15MW power rated wind turbines given by the foundations and the wake from the turbines.

Operation Phase, Hydrodynamic pressure – 187 turbines

The operation of the 187 wind turbines is expected to reduce average wind speed by 0.05 m/s at a maximum distance of 5 km around the wind farm.

Following the reduction in wind speeds, the average significant wave height is expected to decrease by at 0.02 m close to the foundations, by generally less than 0.01 m within the footprint of the wind farm (except in the direct vicinity of the foundations), and by less than 0.005 m outside the wind farm. The impact on the maximum wave height is also limited, at most 0.03 m around the foundations and between 0.005-0.01 m around and up to 15 km northwest of the wind farm.

Potential effects on longshore sediment are not expected due to the limited magnitude and extent of the reduction in the wave heights.

Increase in yearly average temperature of just under 0.1°C due to the operation of the 187 turbines are observed only for a very limited area west of the wind farm for the 10-20 m layer (Figure 8.8 to Figure 8.10). No change greater than 0.1 °C is observed in the Bothnian Sea, indicating a negligible impact on yearly temperatures in comparison to the

natural variability. Impacts on monthly temperatures of more than 0.3°C are expected only during the summer months (June – September), and are caused by slight lowering or highering of the thermocline depth. These changes ranges between -0.6 to 0.5 °C over limited areas, and are small in comparison of natural variability. No change in salinity of more than 0.05 PSU (1% of the natural salinity) is expected due to the operation of the wind farm.

Impacts on currents are seen mostly within and in the direct vicinity of the wind farm, with decreases of at most 0.003 m/s within the footprint area (7% of the current speed). Increases on the east, west and north side of the wind farm can be expected, linked to the somewhat decreased water flow through the wind farm, and are generally lower than 0.001 m/s and at most 0.0023 m/s in the 10-20 m layer, corresponding to a maximum increase of 6%.

Overall, impacts on hydrodynamics and waves are very limited and the impacts are mostly located at and in the direct vicinity of the wind farm. No impacts on currents, salinity, temperature, and wave at Finngrundet, directly south of the wind farm, are expected.

5. Methodology

To estimate the pressure on the hydrodynamics 2 types of numerical models are used:

1) A 3D hydrodynamic model to simulate the water level and currents and
2) A wave model to simulate the wave climate

Before any evaluation of potential impacts the 2 base models; the hydrodynamic model and the wave model, are calibrated toward the data collected by the project (wave, current, salinity and temperature) and publicly available water level data from Sweden and Finland.

Based on 10 years of data the Baseline is described and an average year is identified for input to the Construction and Operation Phase.

The numerical models used to simulate the baseline and the pressure from the wind farm are described shortly below and further information can be found here: https://www.mikepoweredbydhi.com/products.

Bathymetric data for the model domain will be extracted from C-Map which contains digitalized sea maps across the globe and EMODnet. Freely available boundary data of water level and wave conditions will be applied at the boundary towards the Baltic Sea combined with wind fields at the surface of the model domain. Wind data is anticipated to be obtained from ECMWF, ERA5 and wave data from SMHI.

Two models will be set up

1) A general model of the Gulf of Bothnia (regional model) and
2) A local high-resolution model forced by boundary data extracted from the regional model.

The combined MIKE3 HD & MIKE21 SW will be applied to assess the time series of the wave, current and water level conditions taking wave radiation stresses and wave transformation into consideration.

5.1.1. Hydrodynamic model

MIKE 3 HD FM (Hydrodynamics) is a hydrodynamic model with a flexible mesh. Based on tidal and current inputs along the open boundaries together with the wind conditions at the sea surface, the model simulates tide and depth-integrated current speed and direction throughout the model domain. The benefit of a flexible mesh is the possibility of using varying sizes of the mesh across the domain. Therefore, the focus area can have a high resolution, and areas further away can have a coarser resolution. This makes the model run faster, with a negligible impact on the simulation results.

5.1.2. Spectral wave model

MIKE 21 SW FM (Spectral Waves) is a spectral wave model which models wave growth and decay due to wind forcing, wave transformation, wave dissipation (from white capping, bottom friction and depth-induced wave breaking), refraction and shoaling.

6. Background data

In the present chapter, the background data used in the numerical modelling and the description of the morphological, oceanographic and hydraulic conditions site are presented. This includes Metocean data, grab samples and bathymetric surveys.

6.1. Fyrskeppet OWF, Project description

6.1.1. Wind Farm Layout

The layout of Fyrskeppet OWF is illustrated in Figure 6.1. The footprint covers an area of 488 km^2, the total number of turbines are 187, 4 offshore substation and 450 km infield cables (380 km inter-array cable and 70 km redundancy cables).

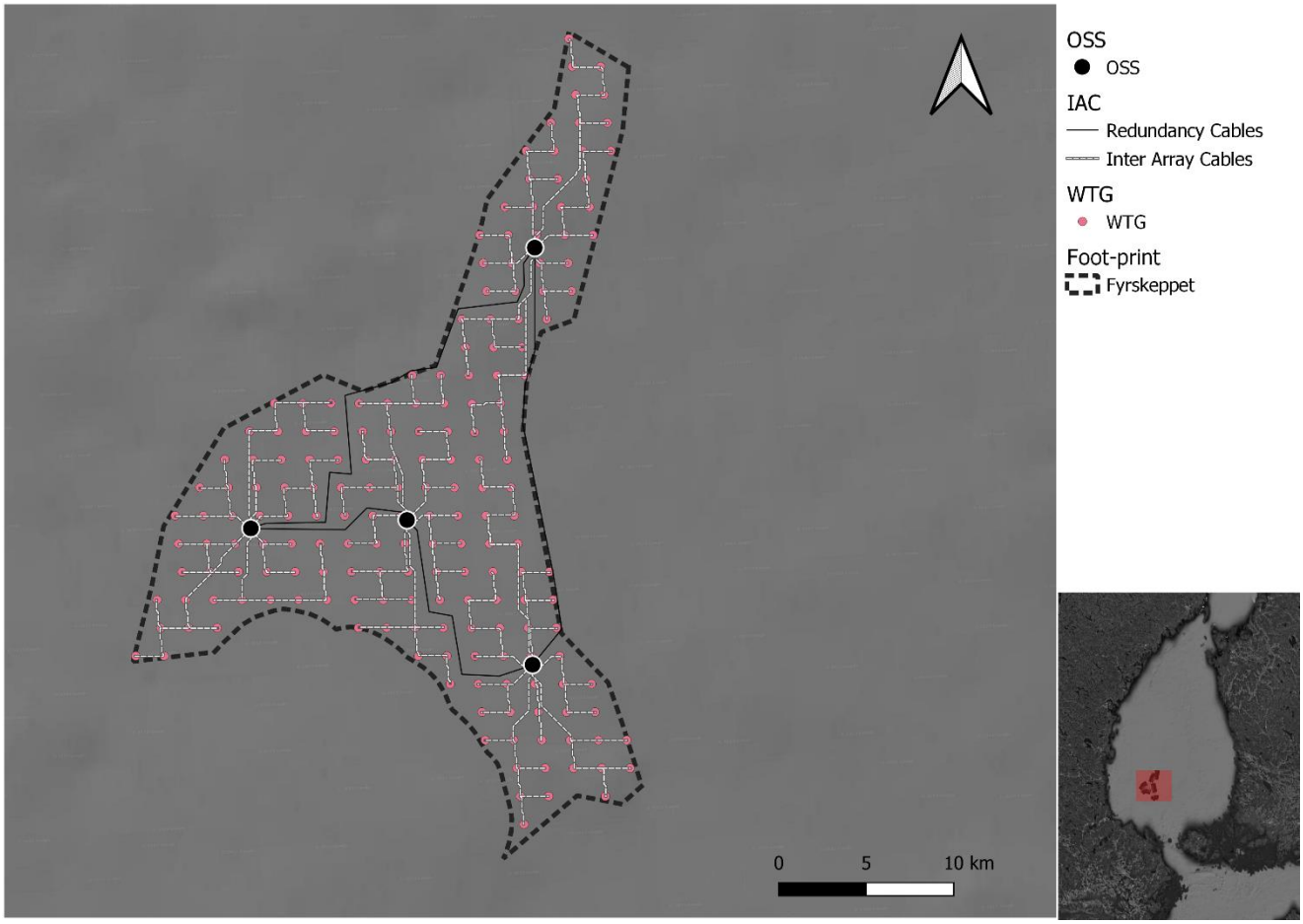

Figure 6.1: Fyskeppet OWF, layout: Map: Google Earth.

6.1.2. Dimensions

In Table 6.1 the dimensions of the wind turbines and supporting structures are listed and a sketch illustrating the shape of the GBS can be found in Figure 6.2.

Table 6.1: Substructure dimension

Case	**-**	**15MW GBS**
Capacity	**MW/Unit**	**15**
Rotor diameter	**[m]**	**245**
Hub Height	**[m]**	**142.5**
Substructure	-	GBS
Capacity, total	MW	2805
Nos	#	187
Bottom diameter, base	m	40
Top diameter, base	m	10.6
No. OSS	#	4
Bottom diameter, base	m	48

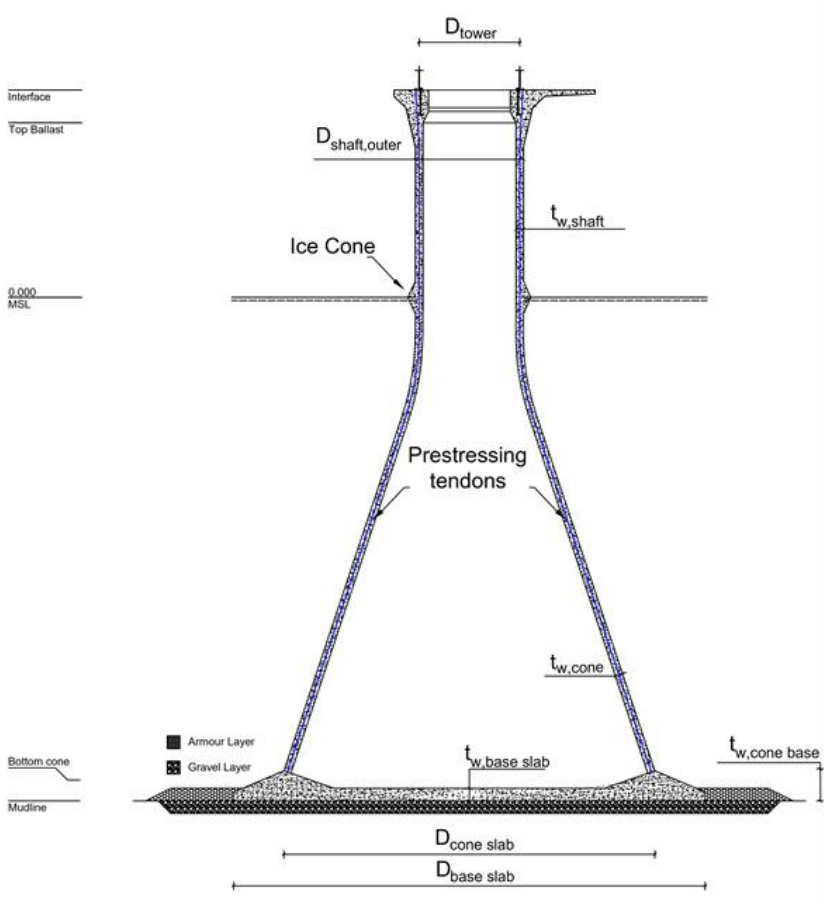

Figure 6.2: Sketch of the GBS

6.2. Bathymetry data

The water depths in the model are based on survey data provided by the project and EMODnet, (EMODnet, 2021) and presented in Figure 7.1 (together with the mesh).

6.3. Observations

6.3.1. Water levels

Water levels with an hourly resolution have been obtained from the SMHI stations Holmsund (lat: 63.6803, long: 20.3331), FORSMARK (lat: 60.4086, long: 18.2108), KALIX-STORÖN (lat: 65.6969, long: 23.0961) and SPIKARNA (lat: 62.3633, long: 17.5311), extracted for the years 2020-2022. The locations of the water level stations are displayed in Figure 6.3. Water levels for these stations are displayed in Figure 6.4.

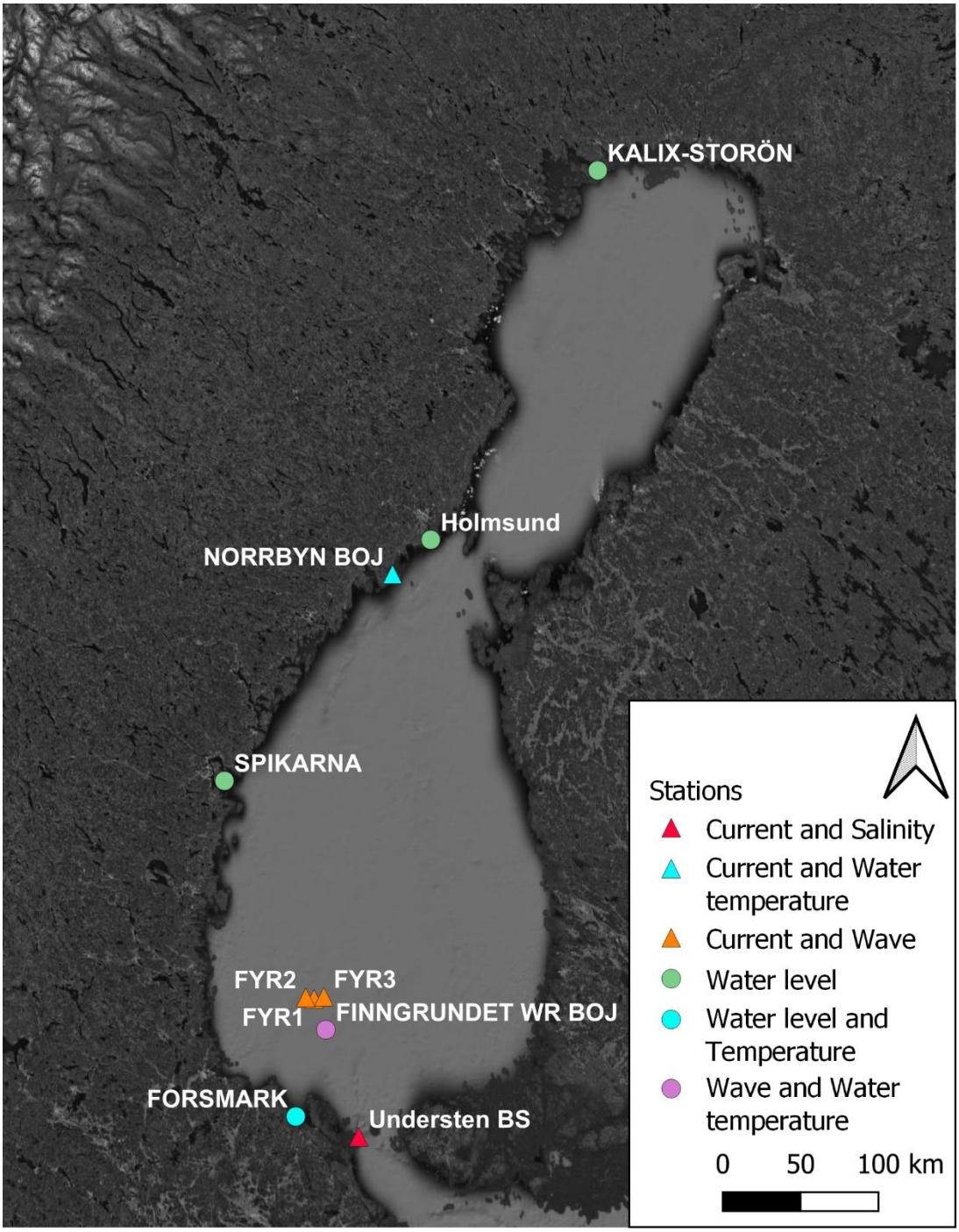

Figure 6.3: Location of water level, wave, current and water temperature monitoring stations used for calibration and validation of the hydrodynamic model. FYR1, FYR2 and FYR3 are project defined stations. Map: ESRI.

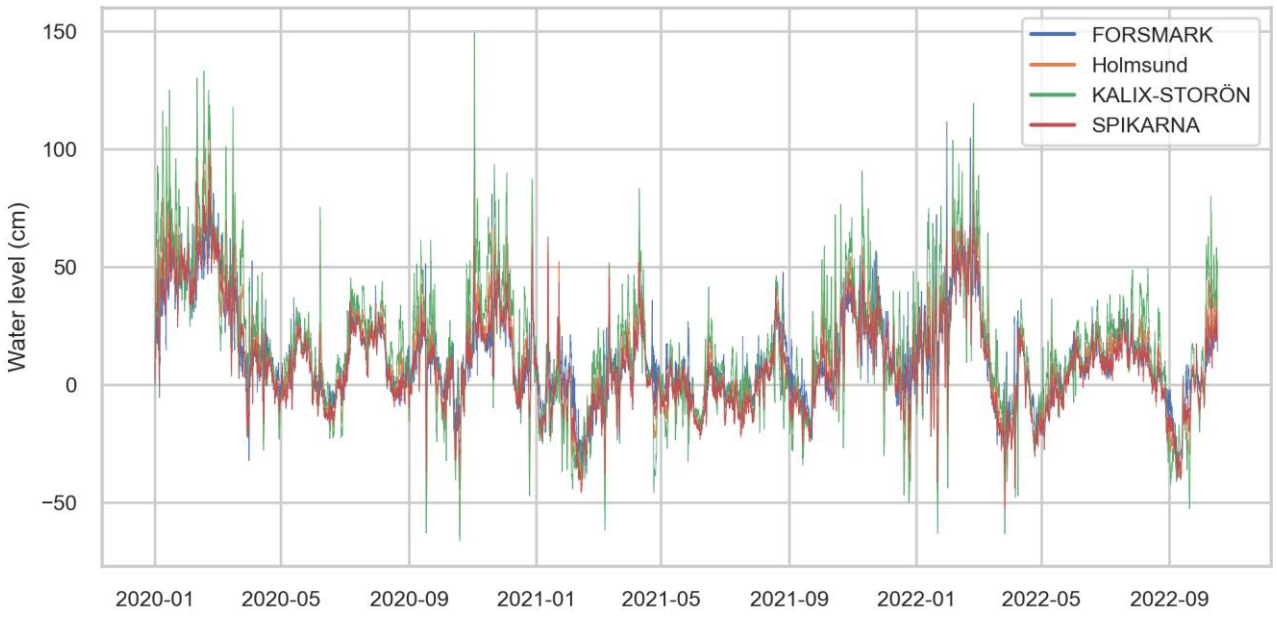

Figure 6.4: Water levels (cm) at the Forsmark, Holmsund, Kalix-Storön and Spikarna monitoring stations

6.3.2. Currents

Current speeds and directions with an hourly resolution have been obtained from the SMHI stations NORRBYN BOJ (lat: 63.499, long: 19.8044) at 5m, 15m and 25m depths for the period 2016-2021 and Understen BS (lat: 60.2715, long: 18.9302) at 219m depth for the year 2021.

Current speeds and directions with an hourly resolution have also been obtained from the project stations Fyrskeppet position 1 (61°4.924'N, 18°29.767'E), Fyrskeppet position 2 (61°5.498'N, 18°23.922'E) and Fyrskeppet position 3 (61°5.486'N, 18°36.863'E) for the period 2022/06/29 – 2022/10/01, extracted at 5m, 15m and 25m depths (FYR1, FYR2 and FYR3). The locations of the current stations are displayed in Figure 6.3. The current speeds and directions for the Fyrskeppet positions are shown in Figure 6.5 and Figure 6.6, respectively. The current speeds and directions for the SMHI stations are shown in Appendix 1.

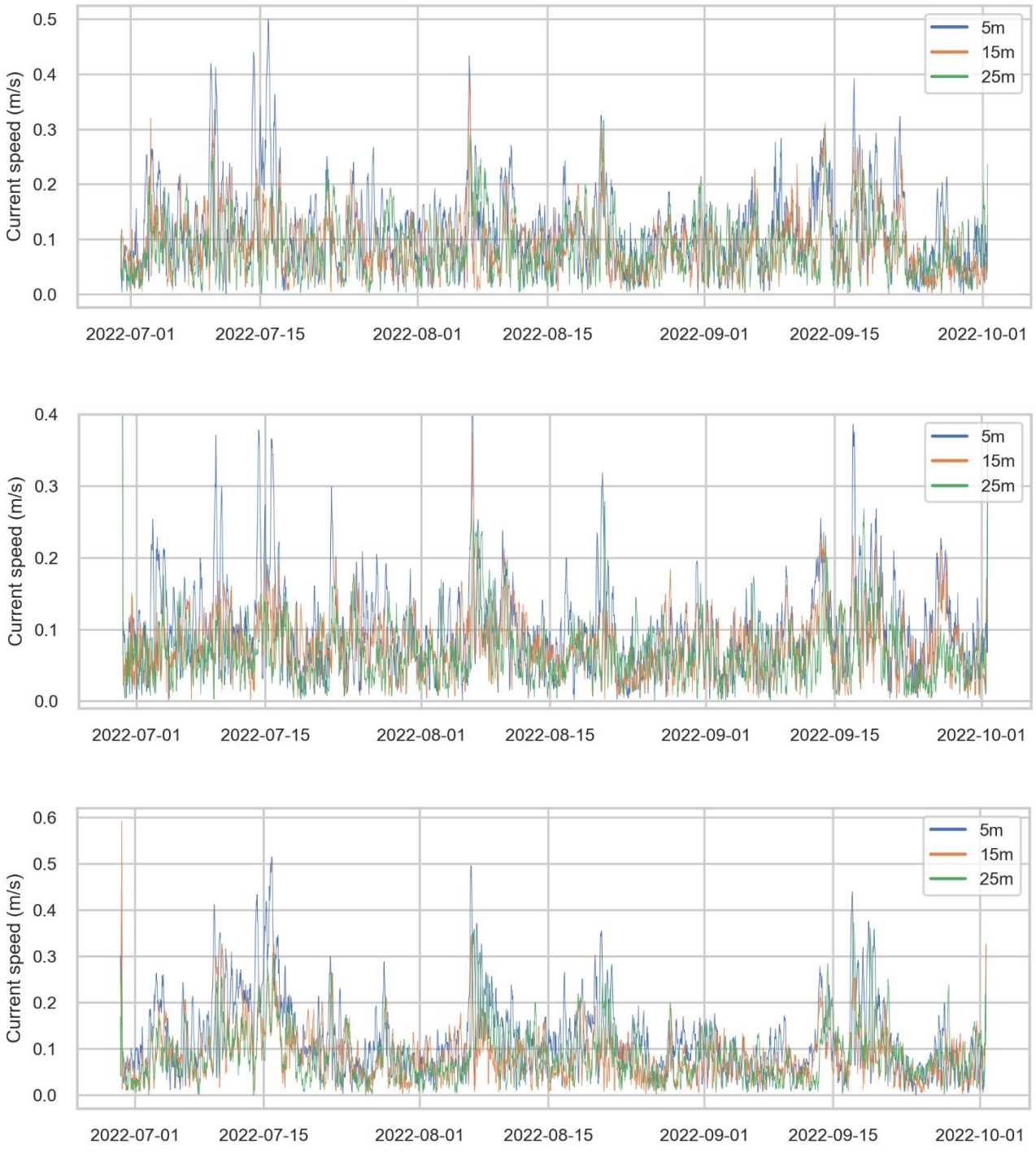

Figure 6.5: Current speeds (m/s) at 5, 15 and 25m for FYR1 (top), FYR2 (middle), and FYR3 (bottom).

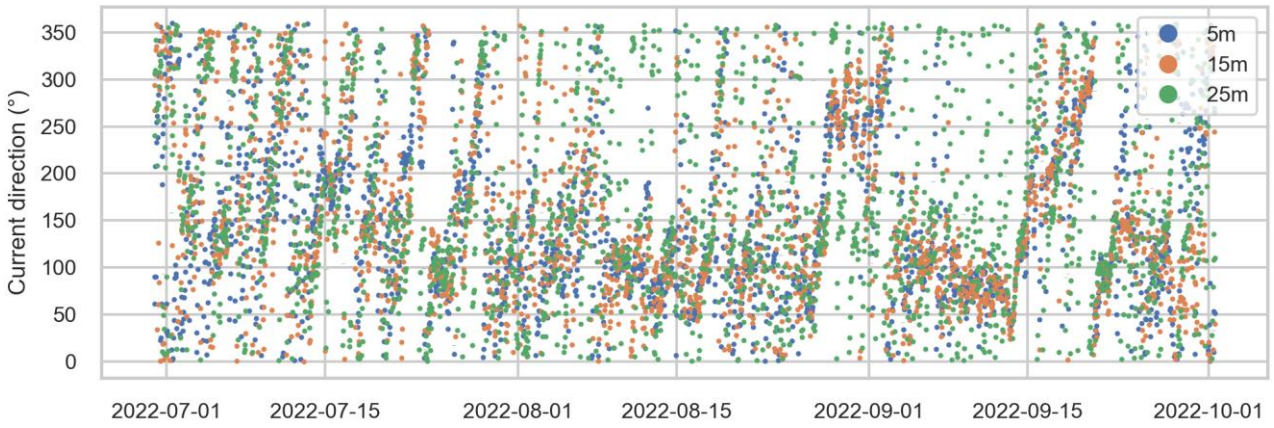
Current direction (°)
350
300
250
200
150
100
50
0
2022-07-01
2022-07-15
2022-08-01
2022-08-15
2022-09-01
2022-09-15
2022-10-01
5m
15m
25m

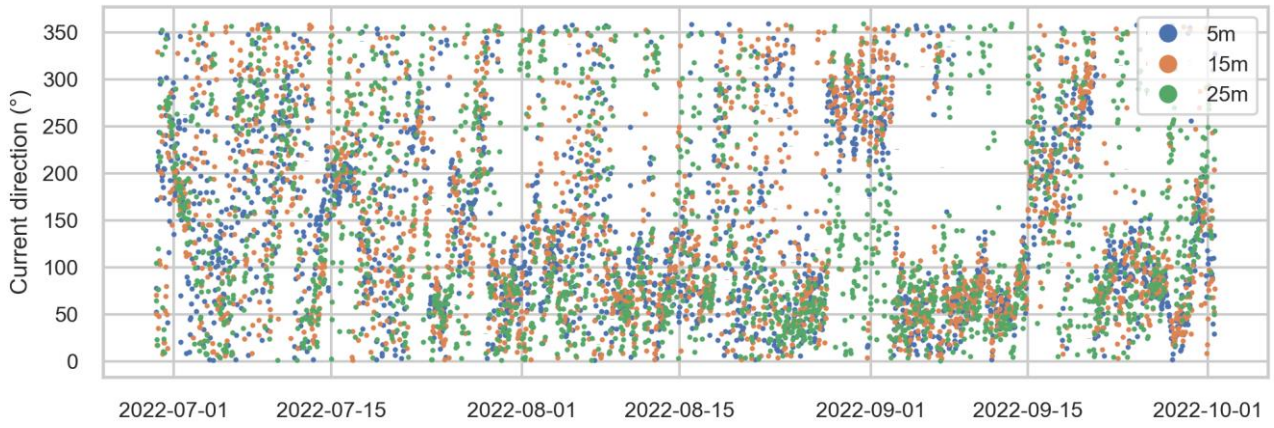
Current direction (°)
350
300
250
200
150
100
50
0
2022-07-01
2022-07-15
2022-08-01
2022-08-15
2022-09-01
2022-09-15
2022-10-01
5m
15m
25m

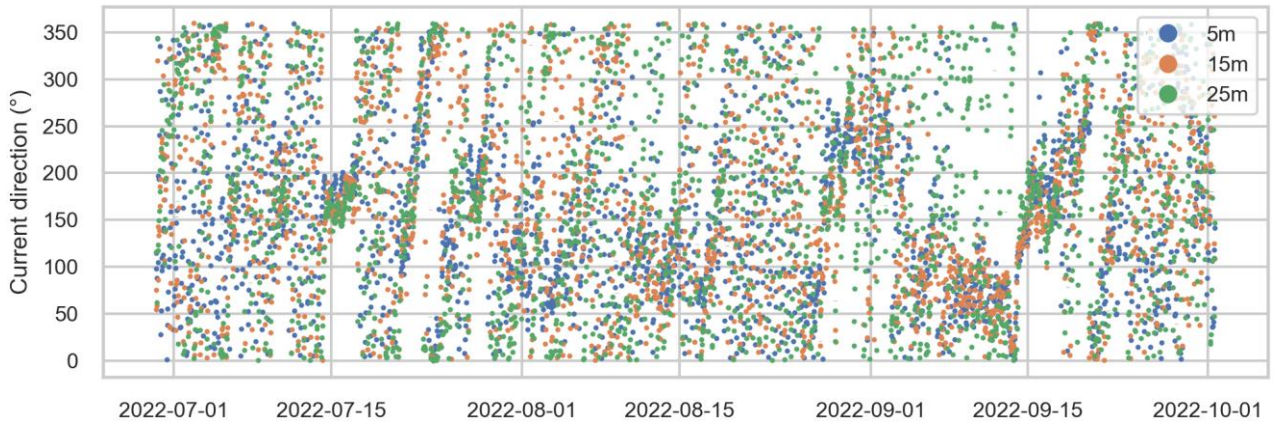

Figure 6.6: Current directions (°, going to) at 5, 15 and 25m for FYR1 (top), FYR2 (middle), and FYR3 (bottom).

6.3.3. Waves

Significant wave heights and mean wave directions with an hourly resolution have been obtained from the SMHI stations FINNGRUNDET WR BOJ (lat: 60.9, long: 18.6167) for the period 2020-2022.

Significant wave heights and mean wave directions with an hourly resolution have also been obtained from the project stations Fyrskeppet position 1 (61°4.924'N, 18°29.767'E), Fyrskeppet position 2 (61°5.498'N, 18°23.922'E) and Fyrskeppet position 3 (61°5.486'N, 18°36.863'E) for the period 2022/06/29 – 2022/10/01 (FYR1, FYR2 and FYR3). The locations of the wave stations are displayed in Figure 6.3.

Time series of significant wave heights and mean wave directions for the stations are displayed in Figure 6.7 and Figure 6.8.

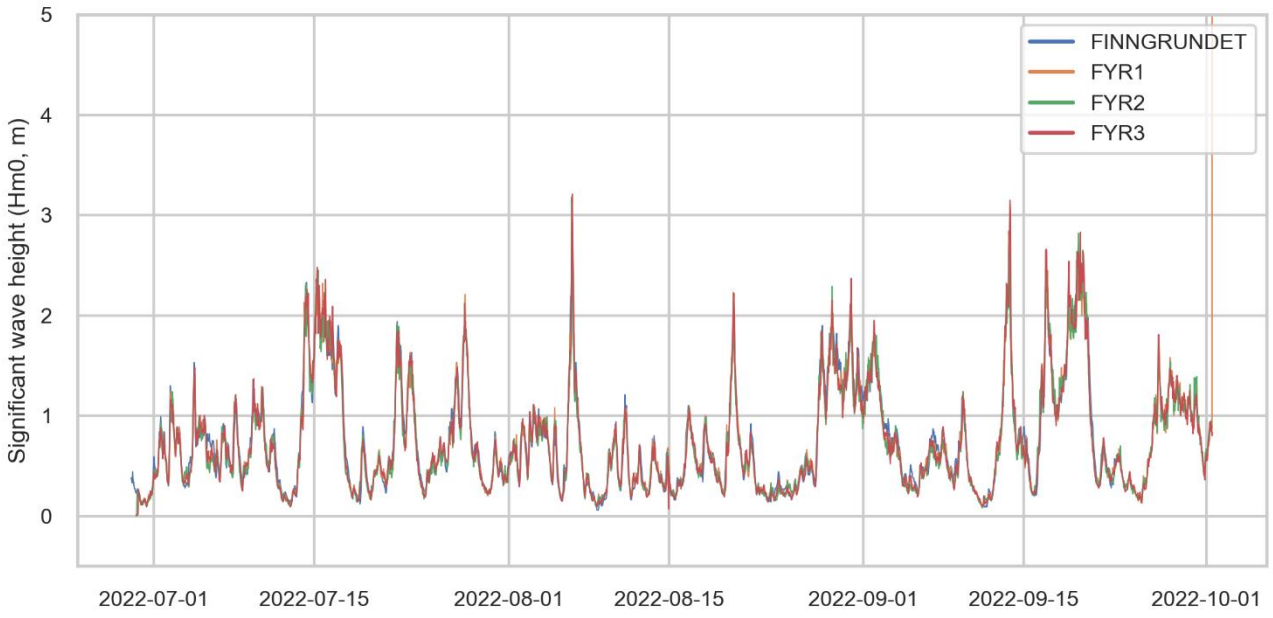

Figure 6.7: Significant wave height (Hm0, m) for the Fyrskeppet positions 1, 2 and 3, and SMHI station Finngrundet

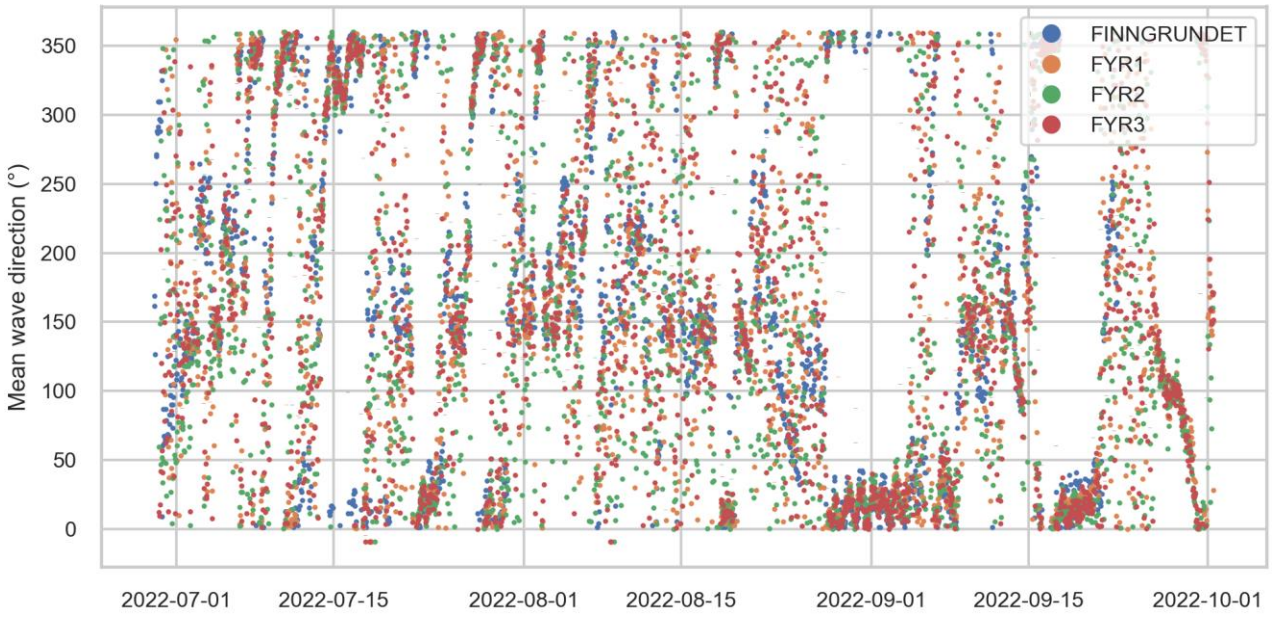

Figure 6.8: Mean wave direction (°, coming from) for the Fyrskeppet positions 1, 2 and 3, and SMHI station Finngrundet

6.3.4. Salinity and Temperature

Surface water temperatures (0m) with an hourly resolution have been obtained from the SMHI FINNGRUNDET WR BOJ (lat: 60.9, long: 18.6167), FORSMARK (lat: 60.41, long: 18.2108) and NORBYN (lat: 63.5642, long: 19.8331) stations for the period 2020-2022. Salinity at the surface (1m) from NORBYN BOJ and at the bottom (219m) from Understen BS has also been obtained from SMHI. The locations of the temperature and salinity stations are displayed in Figure 6.3. The time series of temperature and salinity are shown in Figure 6.9 and Figure 6.10, respectively.

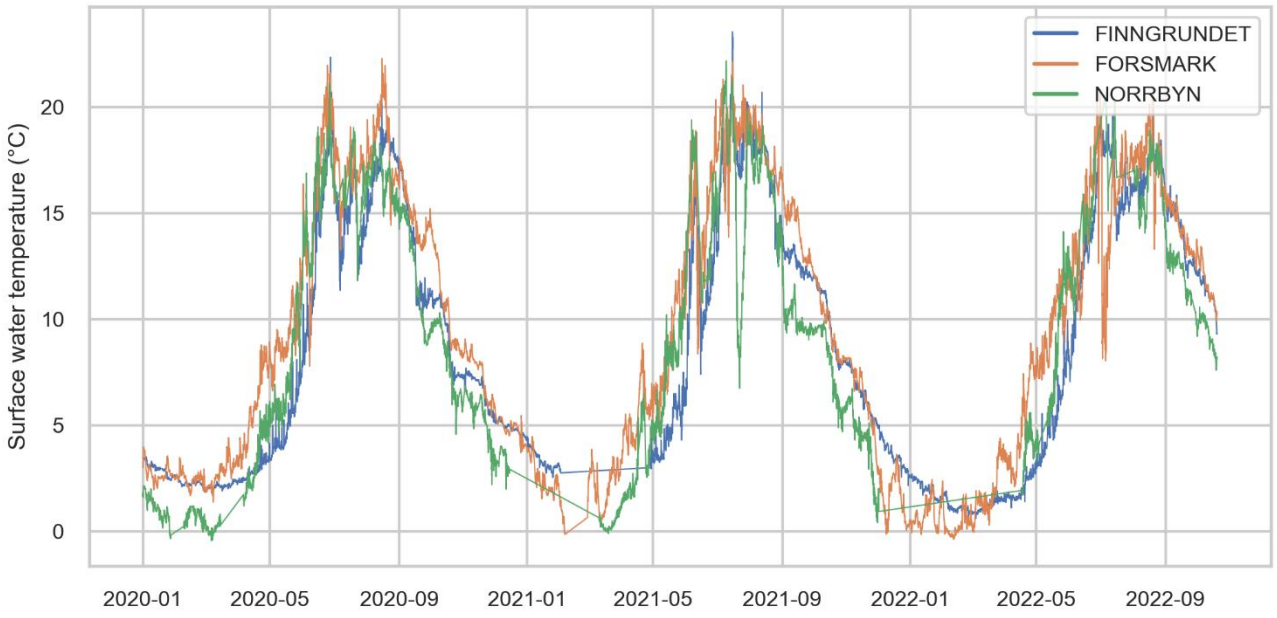

Figure 6.9: Surface water temperature (°C) at Finngrundet, Forsmark and Norrbyn monitoring stations

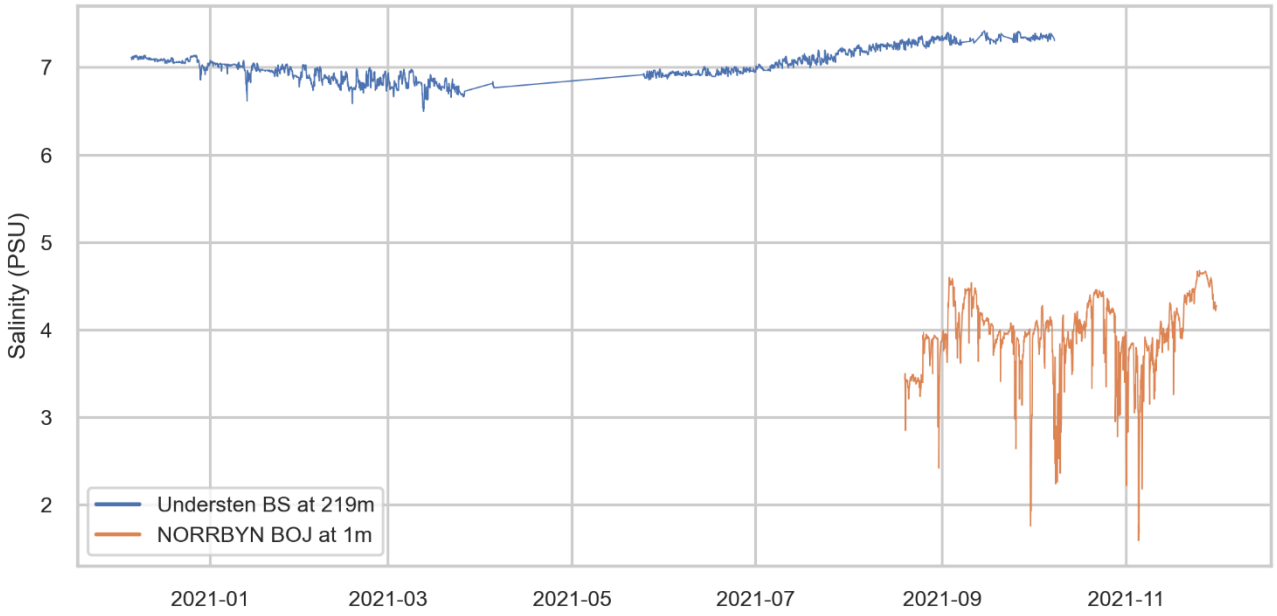

Figure 6.10: Salinity (PSU) at Understen BS (219m) and Norrbyn Boj (1m) stations

6.4. Hydrodynamic data from models

6.4.1. Water levels

Data from the 2km by 2km SMHI 3D Baltic Sea model are used at the Åland Sea boundary conditions to feed the Mike model (Copernicus, Baltic Sea Physics Analysis and Forecast, 2x2km, 2022) and (Copernicus, Baltic Sea Physics Reanalysis 4x4km, 2022).

6.4.2. Currents

To identify an average year for simulating impacts on hydrodynamics, SMHI 3D Baltic Sea model results at Fyrskeppet OWF (Copernicus, Baltic Sea Physics Analysis and Forecast, 2x2km, 2022) and (Copernicus, Baltic Sea Physics Reanalysis 4x4km, 2022) are presented in Appendix 4 and Appendix 5.

6.4.3. Salinity and Temperature

For initialisation and to feed the model at the boundary, data from SMHI's numerical model of the Baltic Sea are used, (Copernicus, Baltic Sea Physics Analysis and Forecast, 2x2km, 2022) and (Copernicus, Baltic Sea Physics Reanalysis 4x4km, 2022).

Data from selected years are presented in Appendix 2 and Appendix 3.

6.5. Wind, Air Pressure, Air Temperature, Net long and short-wave radiations

Atmospheric data in the form of instantaneous wind speed at 10 mMSL in x and y-directions, air pressure at the surface, air temperature at 2 m above the surface, relative air humidity, and net long and short-wave radiation at the surface have been extracted from ECMWF (ECMWF, 2022). The data have a horizontal resolution of 0.25 degrees and a temporal resolution of 1 hour.

6.6. Sea ice

The presence of sea ice is based on data produced by SMHI, (Copernicus, Baltic Sea Physics Analysis and Forecast, 2x2km, 2022) and (Copernicus, Baltic Sea Physics Reanalysis 4x4km, 2022) as ice thickness and concentration.

6.7. Run-off

The following major freshwater discharges (average discharge greater than 100m^3/s) to the Gulf of Bothnia are used as input to the model:

- Kokemäenjoki (Harjavalta station, lat: 61.34, long: 22.11; Finland)
- Oulujoki (Merikoski station, lat: 65.023, long: 25.47; Finland)
- Iijoki (Raasakka station, lat: 65.33, long: 25.41; Finland)
- Kemijoki (Taivalkoski station, lat: 65.93, long: 24.71; Finland)
- Tornionjoki (Karunki station, lat: 66.03, long: 24.02; Finland)
- Kalixälven (lat: 65.8, long: 23.25; Sweden)
- Luleälven (lat: 65.56, long: 22.05; Sweden)
- Piteälven (lat:65.30, long: 21.44; Sweden)
- Skellefteälven (lat: 64.71, long: 21.18; Sweden)
- Umeälven (lat: 63.74, long: 20.36; Sweden)
- Ångerman (lat: 63.03, long: 17.78; Sweden)
- Indalsälven (lat: 62.5, long: 17.5; Sweden)
- Ljungan (lat: 62.28, long: 17.4; Sweden)
- Ljusnan (lat: 61.2, long: 17.13; Sweden)
- Dalälven (lat: 60.62, long: 17.49; Sweden)

For the Swedish rivers, modelled and station-corrected daily discharges and temperatures have been obtained from the SMHI VattenWebb platform for the years 2020-2022. For the Finnish rivers, observed daily discharges have been obtained from the Finnish environmental institute Ymparisto, and water temperatures have been assumed similar to those of the Swedish river at the closest latitude. The discharges and temperatures of the main rivers are shown in

Figure 6.12 and Figure 6.14, respectively, the total river discharge in Figure 6.13 and their location in Figure 6.11.

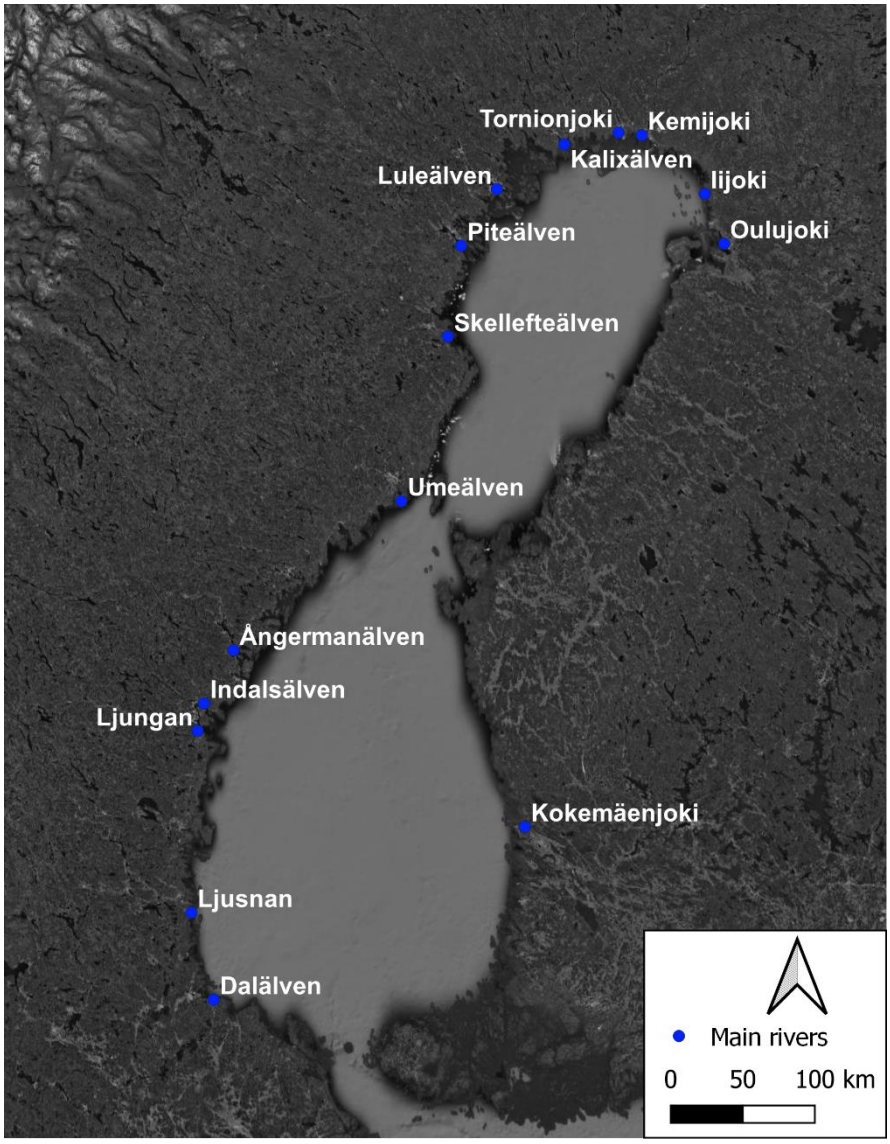

Figure 6.11: Location of the main rivers included in the model. Map: ESRI.

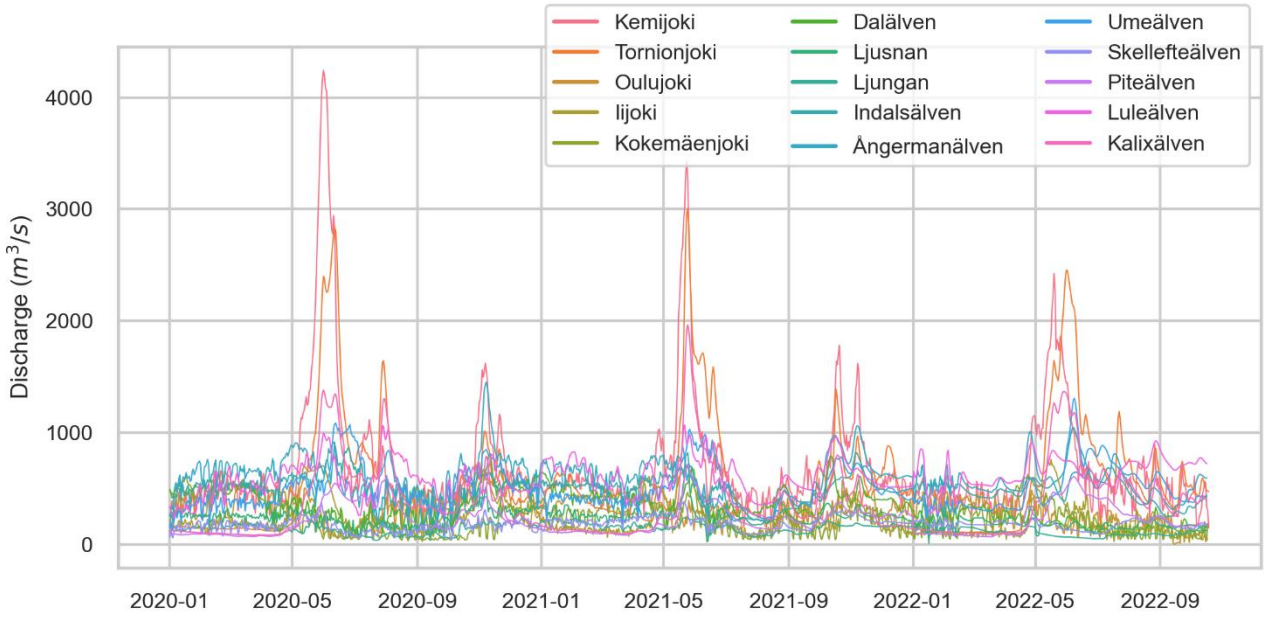

Figure 6.12: Daily discharges (m^3/s) for the main rivers considered in the model.

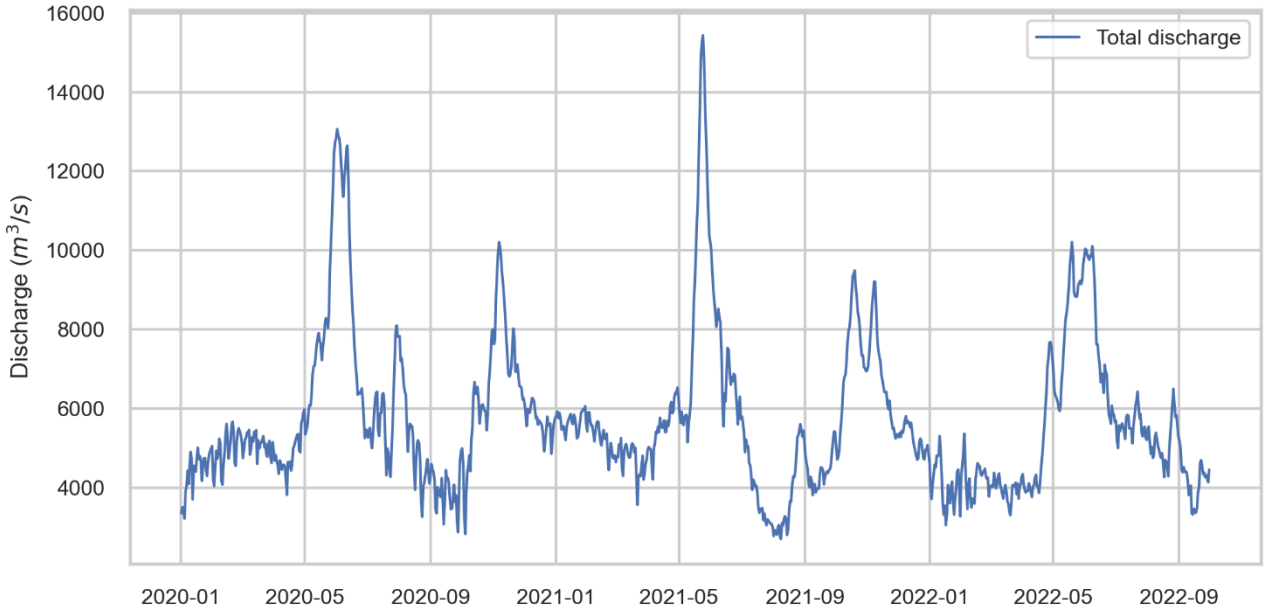

Figure 6.13: Total river discharge (m^3/s) into the model.

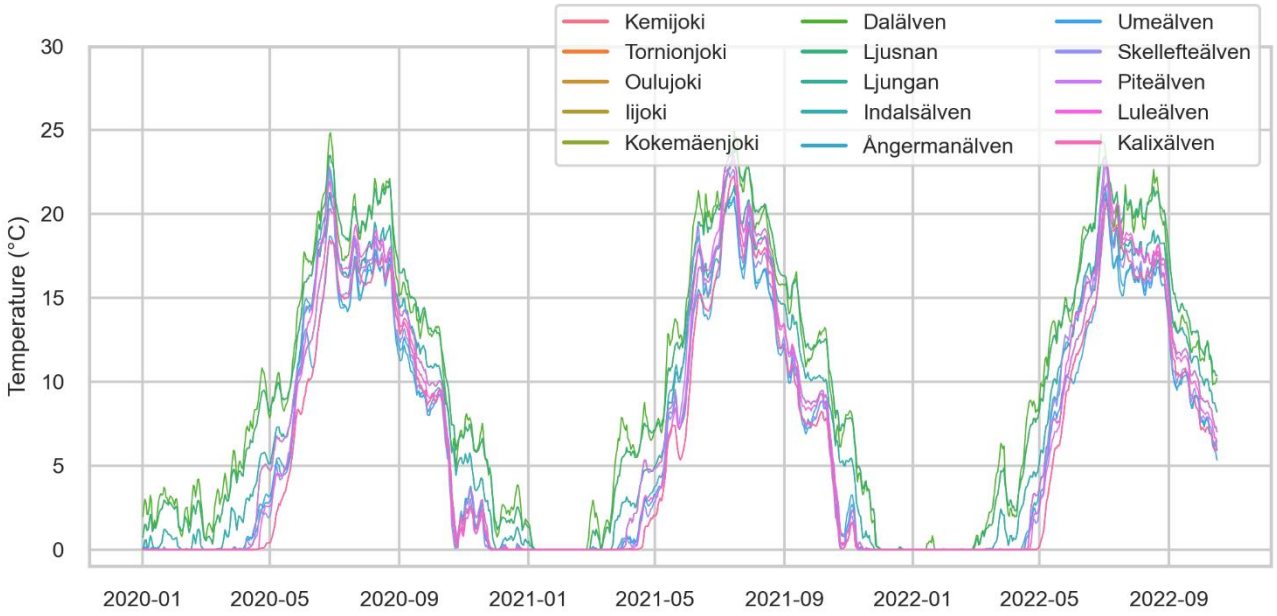

Figure 6.14: Daily water temperatures (°C) for the main rivers considered in the model.

6.8. Baseline description

The Bothnian Sea, where Fyrskeppet OWF is located, constitutes the southern part of the Gulf of Bothnia, and is separated from the Baltic Proper by a strait at the Åland Sea. Hydrographic conditions are characterised by a low salinity (3-6 PSU) and a weak vertical salinity gradient (halocline). Sea surface temperature varies from 0-2°C during the winter to somewhat over 20°C between June and August. Temperature is strongly stratified during the summer with a thermocline (zone of maximum temperature gradient) around 10-30m depth. Deeper temperature, below 30m, varies less during the year, between 2°C at the end of the winter to 7°C at the end of the autumn. Due to the absence of tides, water levels experience relatively small variations, generally between ±50cm around their average during the year. These variations are mostly driven by variations at the Åland boundary, wind and pressure differences. Due to the limited variations in water levels, currents are generally weak, around 0.15m/s at the surface (maximum of 0.5m/s) and less than 0.07m/s below 30m, and mostly driven by wind as well as temperature and salinity differences. Average circulation in the Bothnian Sea is counter-clockwise with dominant northward currents along the east coast, southwards along the west coast, and relatively large (≥10km radius) eddies at the centre of the sea. Waves are moderate due to the relatively small area of the sea (under 1m height on average over the year) and are maximum in October (1.5m on average), with higher waves in the northward direction (long side of the sea).

7. Hydrodynamic model

7.1. Bathymetry and mesh

7.1.1. Regional model

To account for regional circulation patterns, the regional 3D hydrodynamic model encompasses the whole Gulf of Bothnia (Bothnian Sea and Bothnian Bay). The boundary with the Baltic Proper has been placed at the narrowest zone of the Åland Sea. The regional model is used for calibration and validation of hydrodynamic processes, and to force the local pressure model (see below). To maintain reasonable simulation times, the model has a relatively coarse horizontal resolution (16km^2) and is constituted of 14240 elements and 8182 nodes.

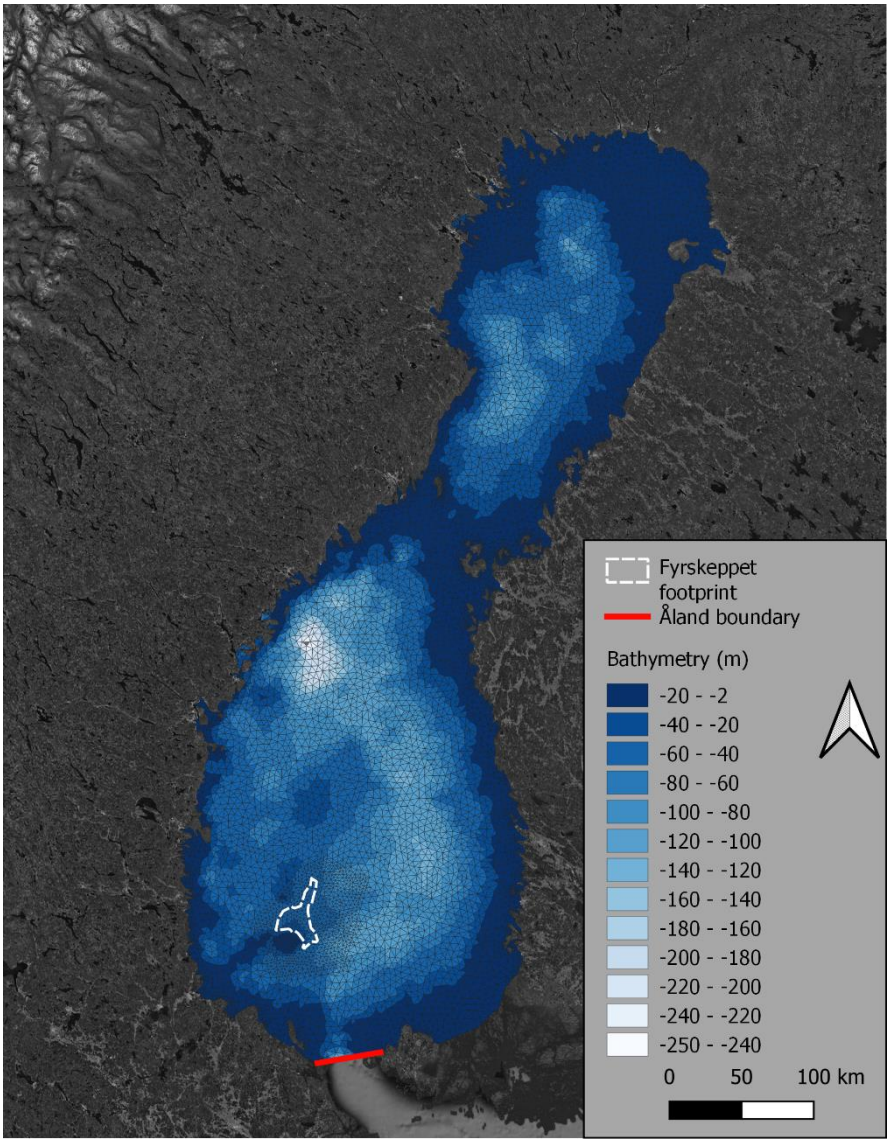

Figure 7.1: Mesh and associated bathymetry (MSL) of the regional hydrodynamic model for calibration and validation. Map: ESRI.

The horizontal resolution has been increased around the Fyrskeppet OWF project area to 5km^2 for comparison with project specific monitoring data. To capture temperature and salinity stratification, which are more pronounced in the surface layer, the water column is divided into 10 vertical elements for depths up to 30 meters (hybrid sigma layers), giving a minimum vertical resolution of 3 meters. The part of the water column deeper than 30 meters is described using constant depth layers of 12 meters. The bathymetry in the Gulf of Bothnia varies between 0 meter at the coast to 250 meters for the north-western Bothnian Sea. The Bothnian Sea is separated from the Bothnian Bay by a relatively shallow area (the Quark, shallower than 40 meters). The Fyrskeppet OWF project area is generally shallower than its surrounding area, with depth varying between 20 to 80 meters.

7.1.2. Local pressure model

To account for the propagation of hydrodynamic impacts and circulation patterns, the local pressure model encompasses the whole Bothnian Sea.

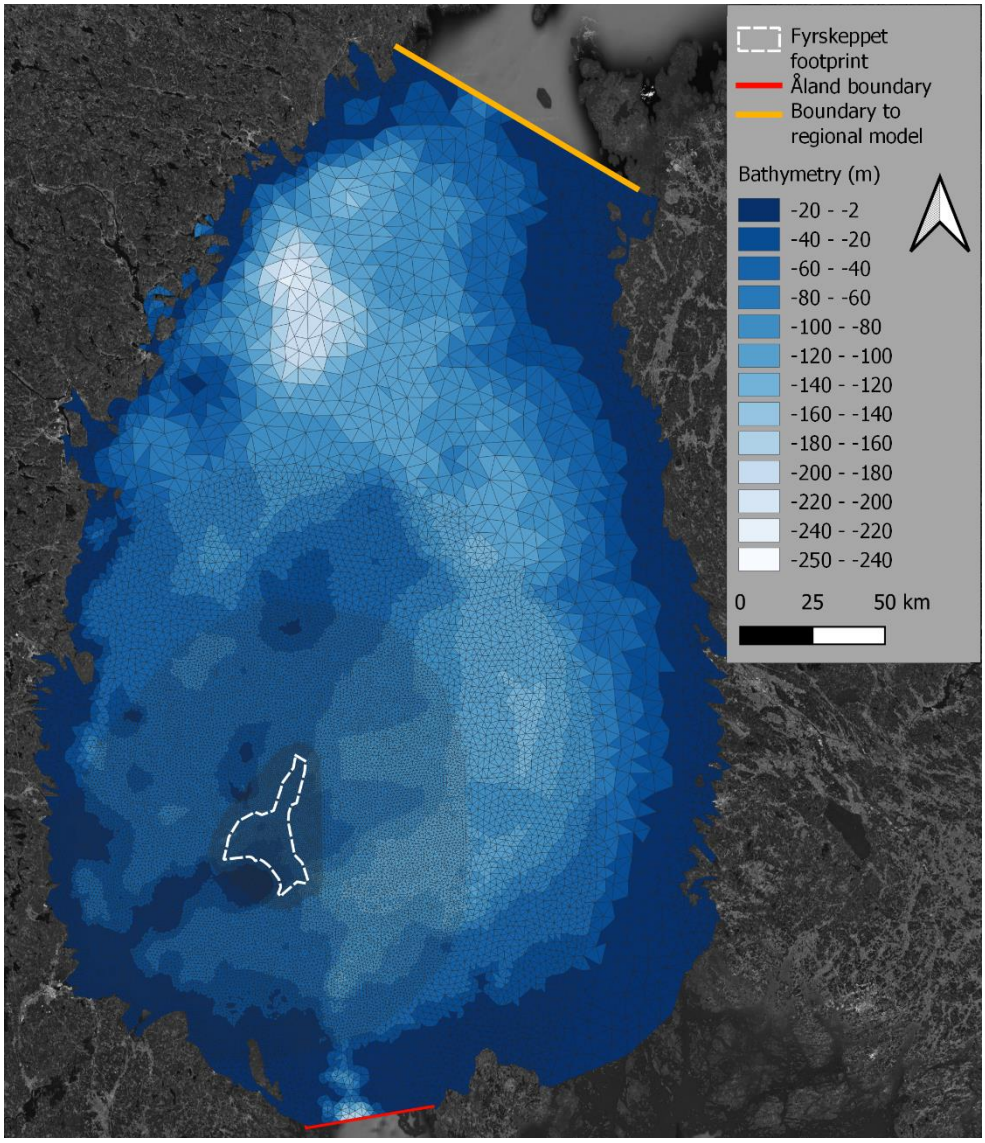

Figure 7.2: Mesh and associated bathymetry of the local model for analysis of hydrodynamic pressures. Map: ESRI.

The local model is constituted of 45104 elements and 23079 nodes, and its vertical resolution is similar to that of the regional model. The local model has a varying horizontal resolution, relatively coarse (25km^2) further than 100km from the Fyrskeppet OWF project area, where direct impacts are expected to be less strong, gradually increasing to 1km^2 within 50km of the project area and 0.25km^2 within the project area, where the impact is expected to be the strongest. It is forced by data from the SMHI model at the Åland boundary and results of the regional model at the northern boundary (red and orange lines in Figure 7.2).

7.2. Boundary data

The regional model at the open boundary towards the Baltic Sea is forced with modelled SMHI data regarding salinity, temperature, and water level. At the surface, ECMWF's ERA5 wind data in the form of wind fields, air pressure, precipitation and evaporation, and sea ice concentration and thickness from the Baltic SMHI model are considered. Heat exchange with the atmosphere has been taken into account via data from ECMWF's ERA5 of net short and longwave radiation, air temperature and humidity at the sea surface. Forcings from the catchment are also considered through the freshwater discharges temperatures from the major rivers listed in chapter 6.7.

To minimize the spin-up period the model is for the first time-step initialized with salinity, temperature and surface elevation from the Baltic Sea SMHI model.

7.3. Model setup and calibration

The regional model is forced at the southern boundary using specified water levels, and salinity and temperature profiles from the Baltic SMHI model. Water levels have been calibrated by adjusting the wind friction coefficients to get a reasonable agreement with observation data.

To account for salinity and temperature stratification, the vertical eddy viscosity is resolved using the k-ε turbulence model. Salinity and temperature profiles have been calibrated against available measurements within the Fyrskeppet OWF project area by adjusting the vertical and horizontal dispersion coefficients, and surface temperatures have been calibrated through the light extinction coefficient determining the depth of the light penetration in the water column.

7.4. Identification of average year

Based on modelled temperature, salinity and currents at Fyrskeppet OWF from SMHI Baltic Sea model, presented in Appendix 2 to Appendix 5, an average year is identified by comparing yearly conditions. Interannual variation is generally low for salinity, temperature and currents, with a general counter-clockwise circulation pattern in the Bothnian Sea and south-eastward to southward currents at Fyrskeppet OWF.

The year 2021 has been chosen as an average year as it follows the general increase in salinity end of spring and the lower surface salinity end of summer. Temperature is highest in late summer with a thermocline going down to 15 meters. Thermocline depth in this area varies between 10-25m, so that 15m is on the lower side and indicates slightly reduced vertical mixing. Comparison between modelled currents by the 2km by 2km and 4km by 4km SMHI models indicate shifted currents from south to south-east in the finer version. The year 2021 experiences currents almost evenly spread around the south-eastward component (southward component for the 4km by 4km), which is also close to the average circulation pattern at Fyrskeppet OWF. The year 2021 was thereby chosen to investigate effects of the wind farm on hydrodynamics.

7.5. Verification

For verification of the model, the period June to October 2022 (June is for warm-up of the model) where project specific data are available is selected.

The model is verified against

1) Observed water levels;
2) Observed current profiles and time series;
3) Observed salinity and temperature profiles, and temperature time series and;
4) Observed wave data.

7.5.1. Water level, time series

The model performs well in representing water level variations for the different monitoring stations with correlation coefficients between 0.97-0.98 and the root mean square error (RMSE) lower than 4cm for all stations.

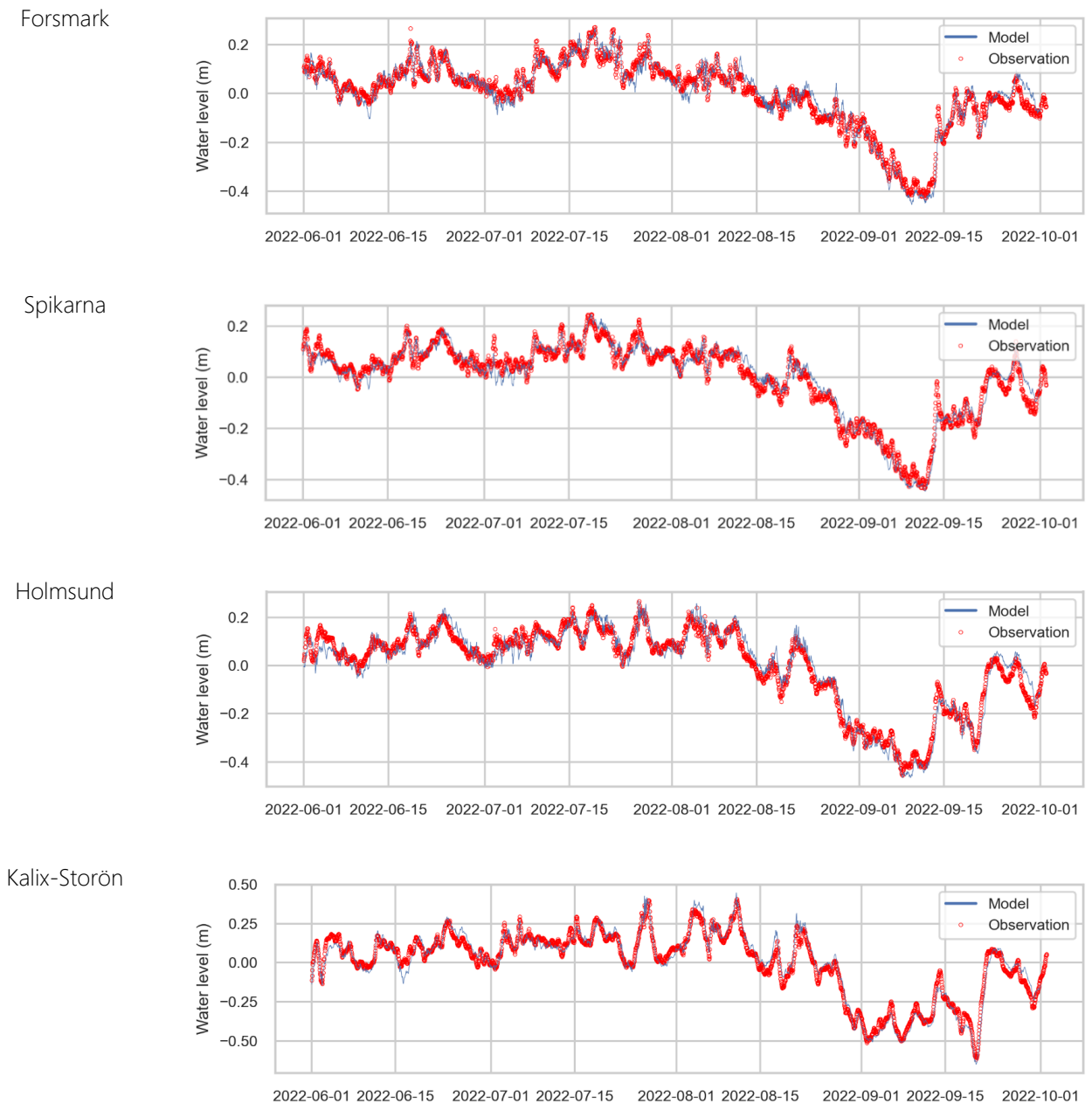

Figure 7.3: Comparison between observed water level in mMSL (red dots) and modelled water level (blue line) for the Forsmark (top row), Spikarna (second row), Holmsund (third row) and Kalix-Storön (bottom row) monitoring stations.

Decreases in water levels are sometimes represented with a slight delay by the model, especially for the Forsmark, Spikarna and Holmsund stations, which could be due to discrepancies in the water level at the Åland boundary taken from SMHI model results. For the Kalix-Storön monitoring station, for which the water levels are more influenced by the wind than by the boundary conditions, the model overestimates some of the peaks, which could be due to

differences between actual and reanalysis wind data from ERA5 used to force the model and to somewhat overestimated wind friction coefficients in the model.

7.5.2. Current, time series

Time series of current speed are shown in Figure 7.4 and show a relatively good agreement between modelled and observed surface currents at -5m (correlation coefficient greater than 0.65 for all stations and RMSE around or lower than 0.05m/s), indicating that the wind driven currents are generally well captured by the model. Representation of the deeper currents at 15m and 25m is somewhat more challenging with correlation around or greater than 0.5 and RMSE around or lower than 0.05m/s for all stations. This could be due to a greater influence of currents driven by salinity and temperature differences and of the boundary conditions, as well as to a coarse representation of the bathymetry in the regional model. Time series of current directions are shown in Figure 7.5 and show that variations in surface current directions at 5m depth are well captured by the model (blue lines and circles). For the deeper currents at 15m and 25m depth, the average current direction is well captured by the model, while some shifts in current directions are not fully captured by the model.

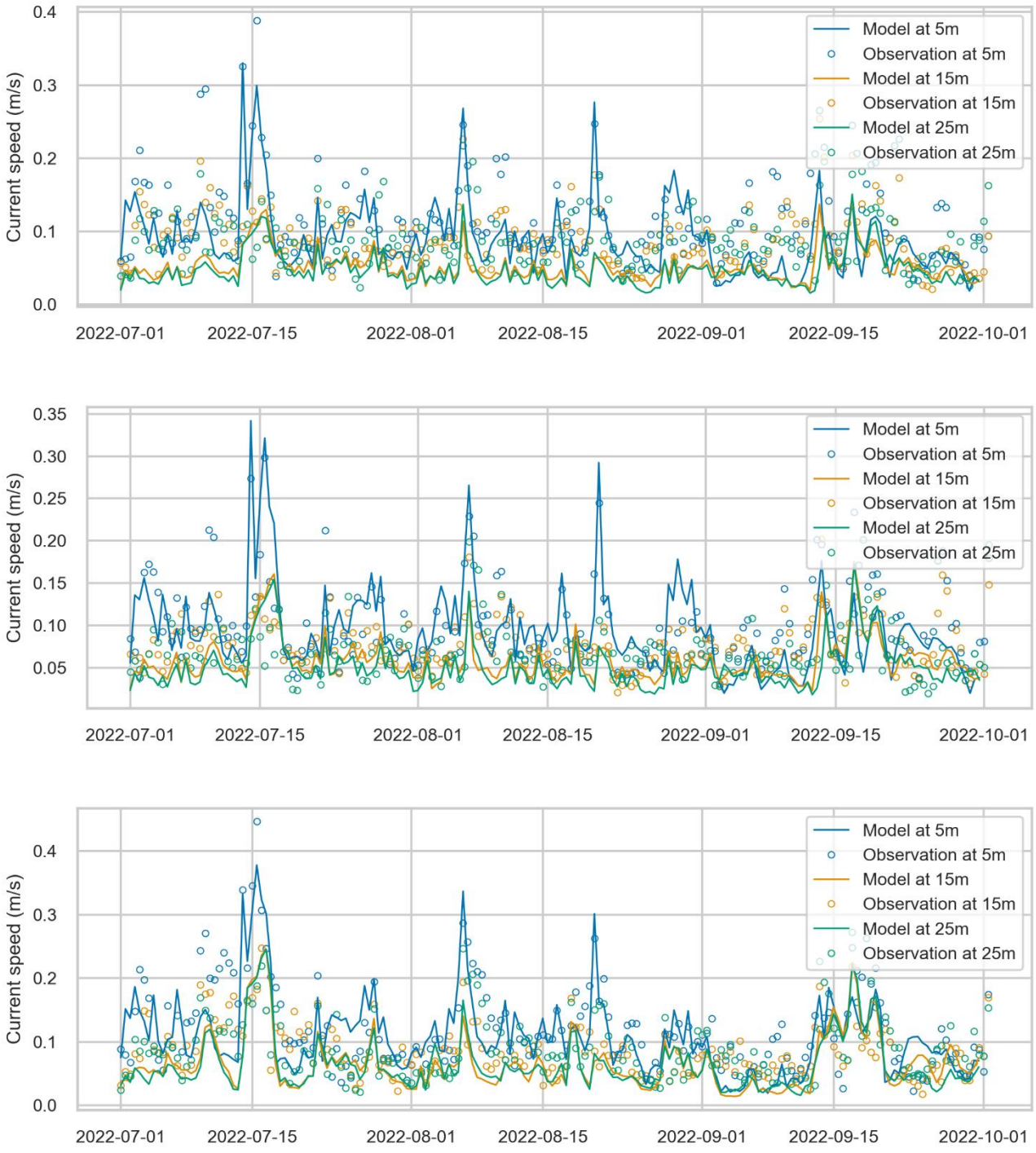

Figure 7.4: Comparison between observed (circles) and modelled (solid lines) current speeds (12-hour average, m/s) at 5-, 15- and 25-meter depths for the monitoring stations FYR1 (top row), FYR2 (second row), and FYR3 (third row).

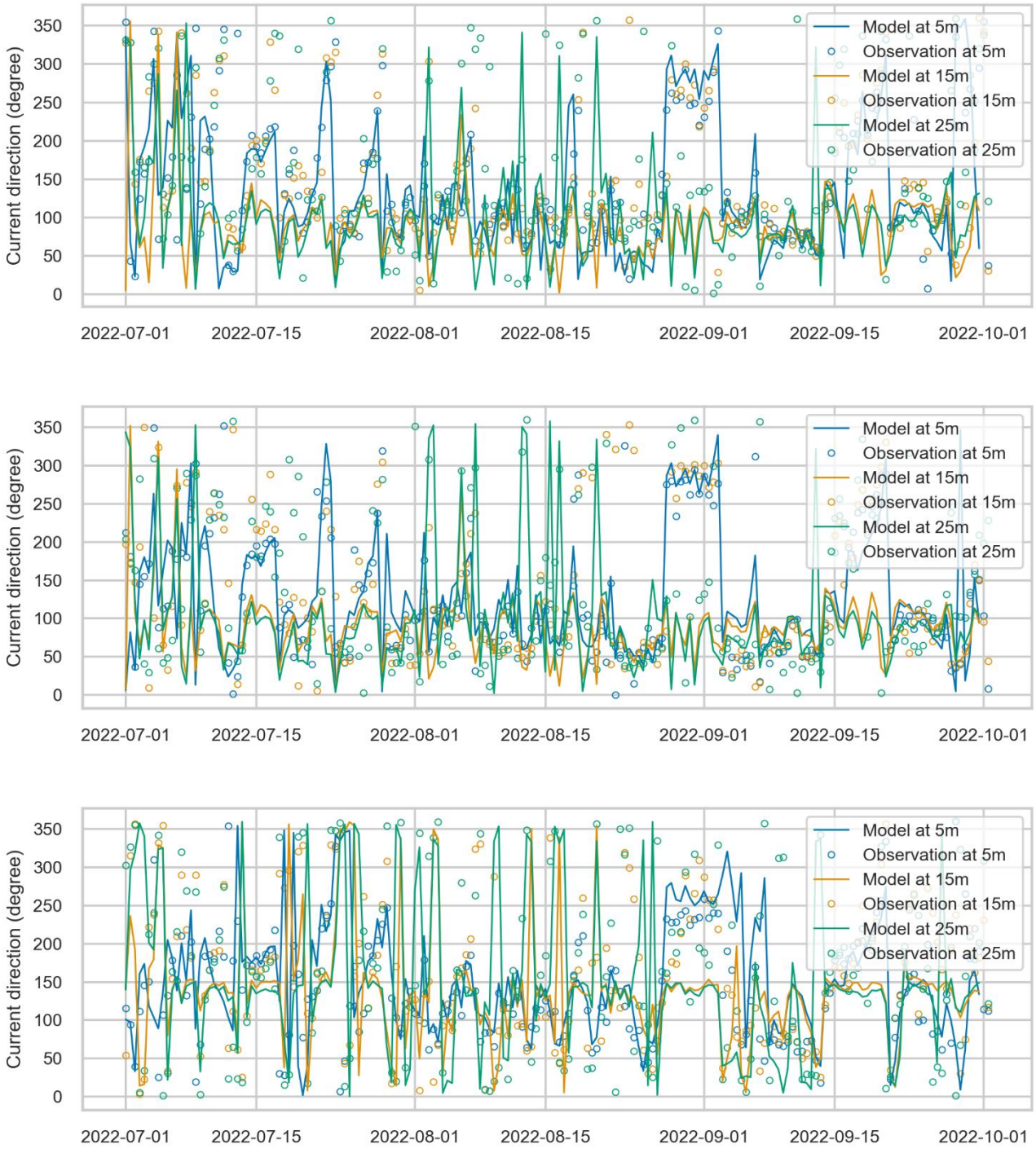

Figure 7.5: Comparison between observed (circles) and modelled (solid lines) current directions (12-hour average, degree) at 5-, 15- and 25-meter depths for the monitoring stations FYR1 (top row), FYR2 (second row), and FYR3 (third row).

7.5.3. Current roses comparison (observations, Mike model and SMHI model)

For FYR1, the current roses (Figure 7.6) show that the average east to southeast current direction is well captured by the present Mike model, with the southern component somewhat overestimated, while the SMIH model overrepresents the east and north-east direction. Averaged current speeds are somewhat underestimated by the Mike model, but less than by the SMHI model. For FYR2, the general eastern direction is captured by both the SMHI and Mike models, with the Mike model shifting currents southwards, while the SMHI model overestimates the northern component. Average current speeds lie within the observation range for both models but are somewhat underestimated by the SMHI model and the southeastern current speeds are somewhat overestimated by the Mike model. For FYR3, the SMHI model captures well the observed distribution of current direction. The dominant direction is also captured by the Mike model, but the southeastern component is overestimated, and the southern component is underestimated.

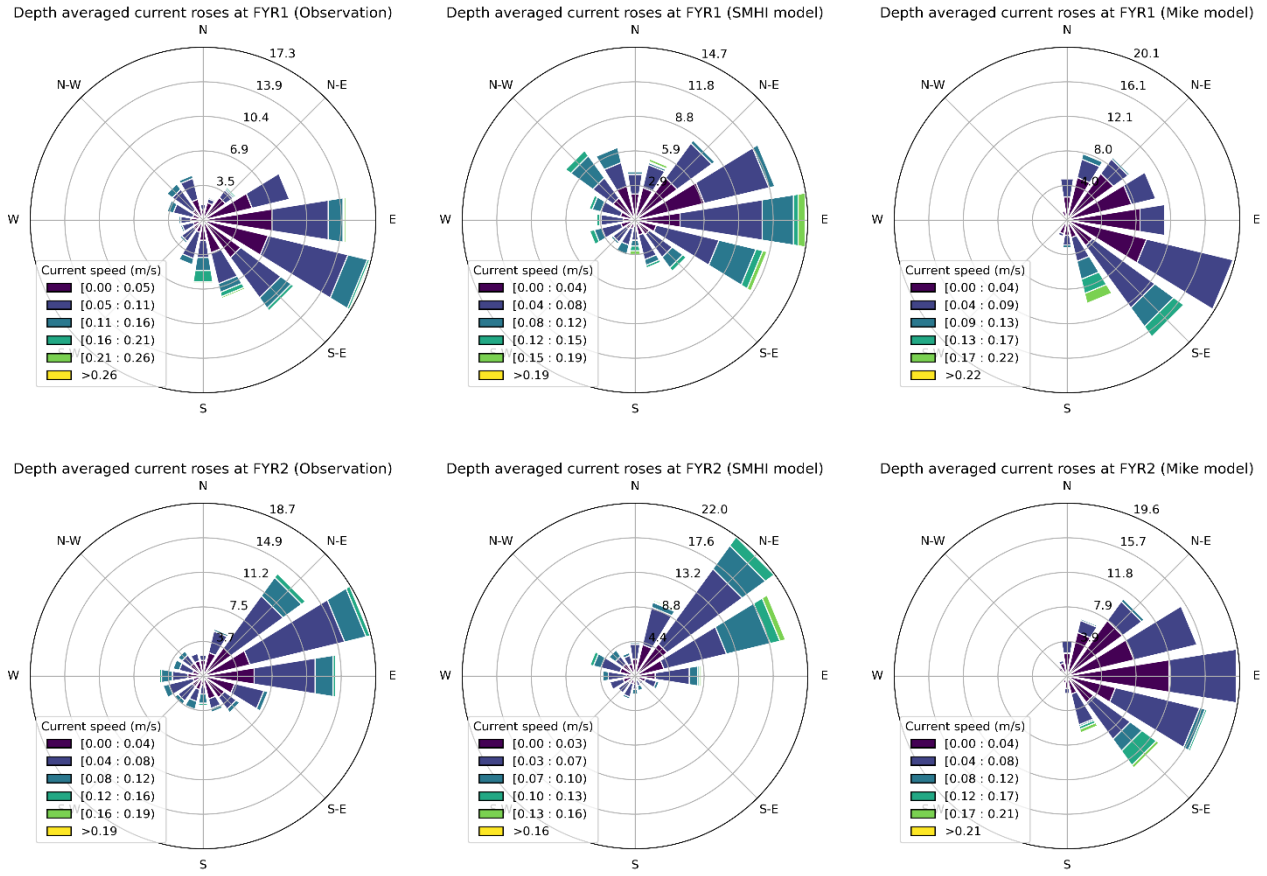

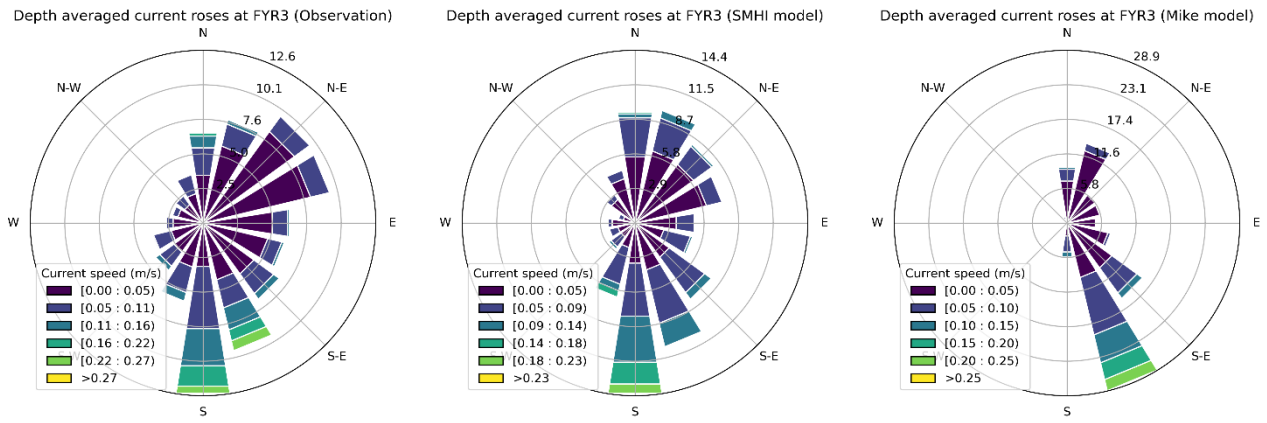

Figure 7.6: Current roses representing the distribution of directions of the depth-averaged current (towards) and associated current speeds for the observed current (first column) and currents modelled by the SMHI (second column) and the Mike (third column) models at Fyr1, Fyr2 and Fyr3.

7.5.4. Current profiles

Current velocity profiles for the stations FYR1, 2 and 3 averaged over the months of July, August and September are presented Figure 7.7. They show a general agreement between modelled and observed current speeds with higher speeds at the surface that decrease with depth down to 10m, increase slightly between 10 and 20m depth, and finally decrease slowly until the bottom.

This pattern is more pronounced in July (and August for FYR3) and well captured by the model and the flatter profiles of September are also well captured by the model, while the model overestimates surface currents in August, which could be due to the wind forcing data.

Current speeds are also somewhat underestimated by the model between 10-30m depth, which can be expected as they represent an average current speed for a given element of the grid. Comparison of modelled current time series, roses and profiles with observation data shows that, despite some discrepancies, the agreement is acceptable, and the model captures the general current dynamic and vertical patterns in the Fyrskeppet OWF project area and performs well against the SMHI model.

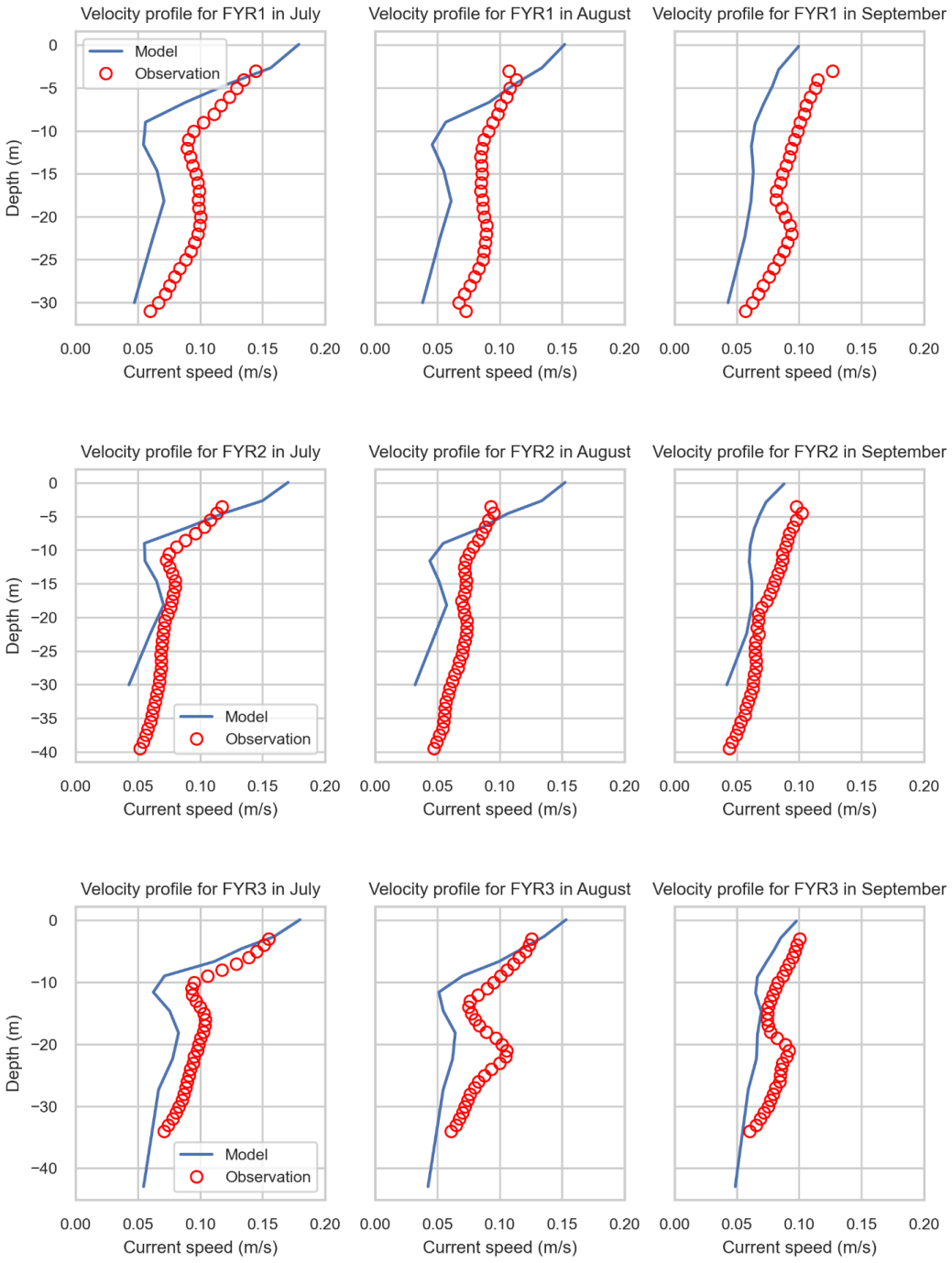

Figure 7.7: Comparison between modelled (blue line) and observed (red dots) monthly averaged current speed profiles in July (first column), August (second column) and September (third column) for the monitoring stations FYR1 (first row), FYR2 (second row) and FYR3 (third row).

7.5.5. Salinity and temperature profiles

Comparison of modelled salinity with observations in different parts of the project area shows that the salinity is well within the range of the observation values. Salinity stratification is somewhat overestimated in June, while it is well captured by the model in August, but with a modelled halocline (zone of maximum salinity gradient) occurring around 15m while the observed one lies around 20m.

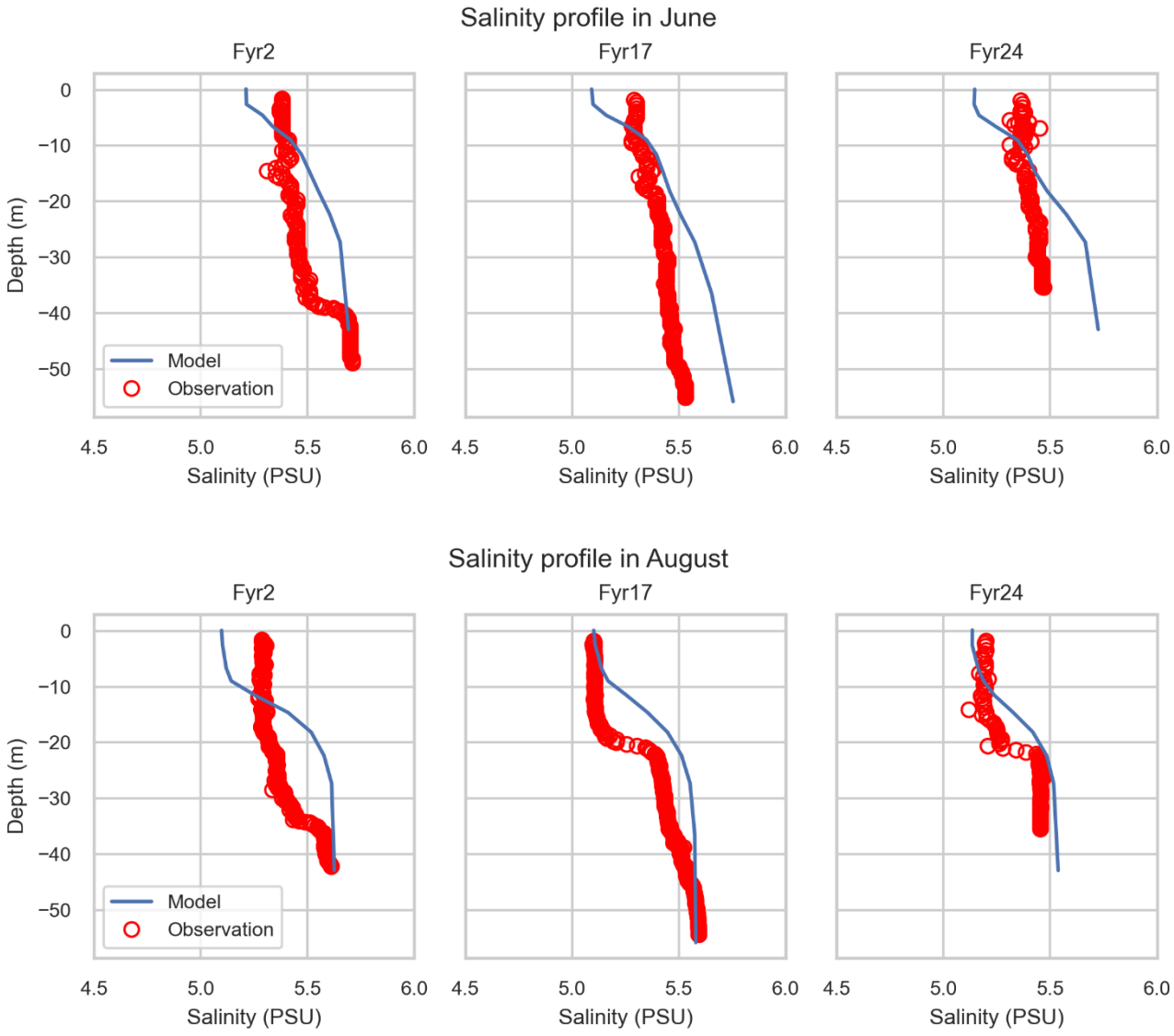

Figure 7.8: Comparison between modelled (blue line) and observed (red dots) salinity profiles at single dates in June (first row) and August (second row) for Fyr2, situated in the northern part, Fyr17, situated in the western part, and Fyr24 situated in the eastern part of the project area (Bladin, Rämö, Lavett, Vinterstare, & Vigouroux, 2022).

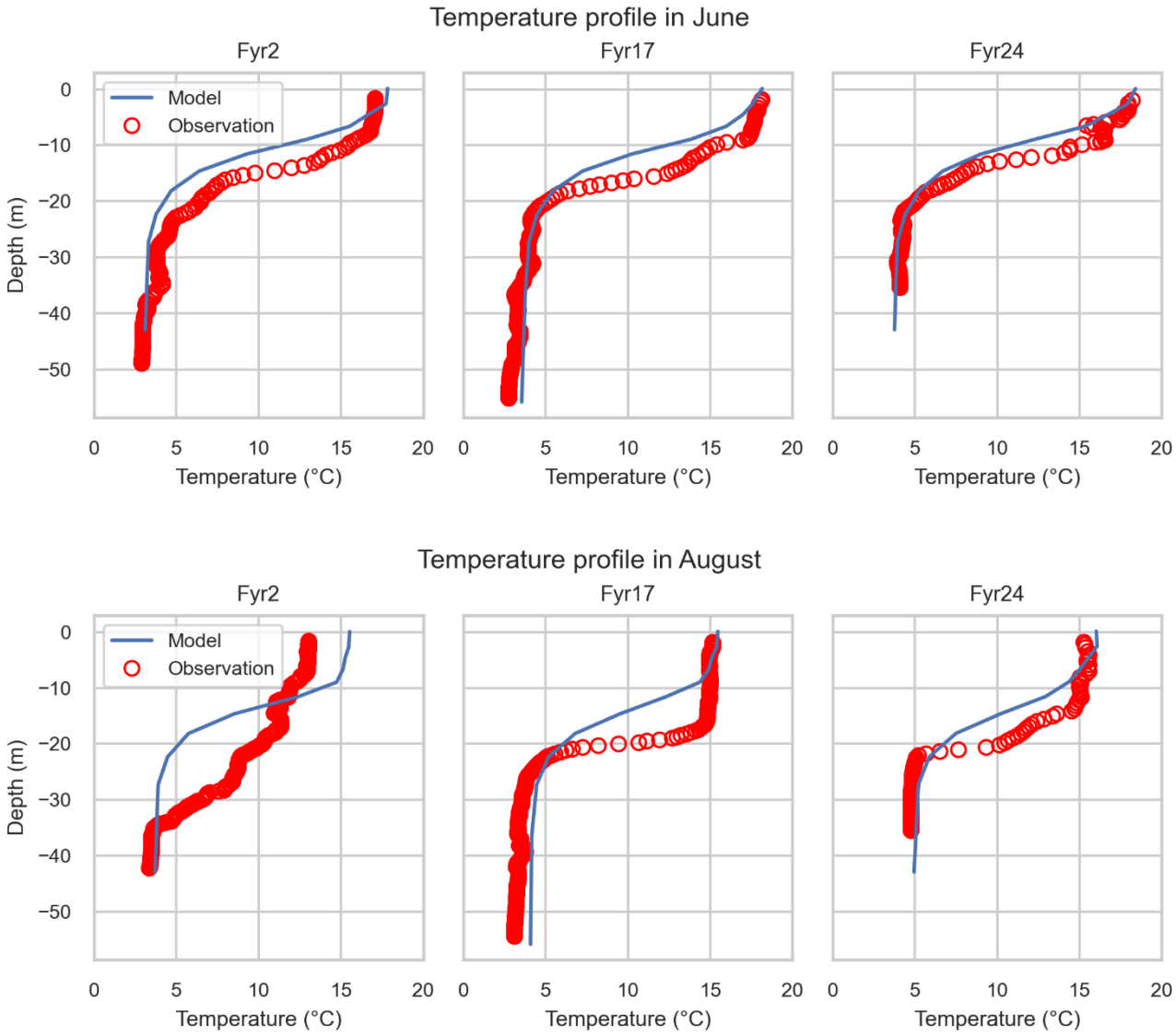

Figure 7.9: Comparison between modelled (blue line) and observed (red dots) temperature profiles at single dates in June (first row) and August (second row) for Fyr2, situated in the northern part, Fyr17, situated in the western part, and Fyr24 situated in the eastern part of the project area (Bladin, Rämö, Lavett, Vinterstare, & Vigouroux, 2022).

Temperature stratification (Figure 7.9) is well represented by the model both in June and August, with very good agreement for both the surface and bottom temperatures at the different stations. The thermocline is also in good agreement in June, while the modelled thermocline lies slightly too high in August. For Fyr2, the shape of the salinity

and temperature profiles could indicate an upwelling, which would depend on variations of bathymetry that are not captured by the coarser regional model. The profiles of current, salinity and temperature thereby indicate a good ability for the model to represent the vertical stratification.

7.5.6. Temperature time series

Modelled surface temperature at Finngrundet shows very good agreement with observation both during the spring and summer periods with a correlation coefficient of 0.99 and a RMSE of 0.86°C. Most of the short-term variations are well captured by the model, while the temperature decreases slightly too quickly during the month of September.

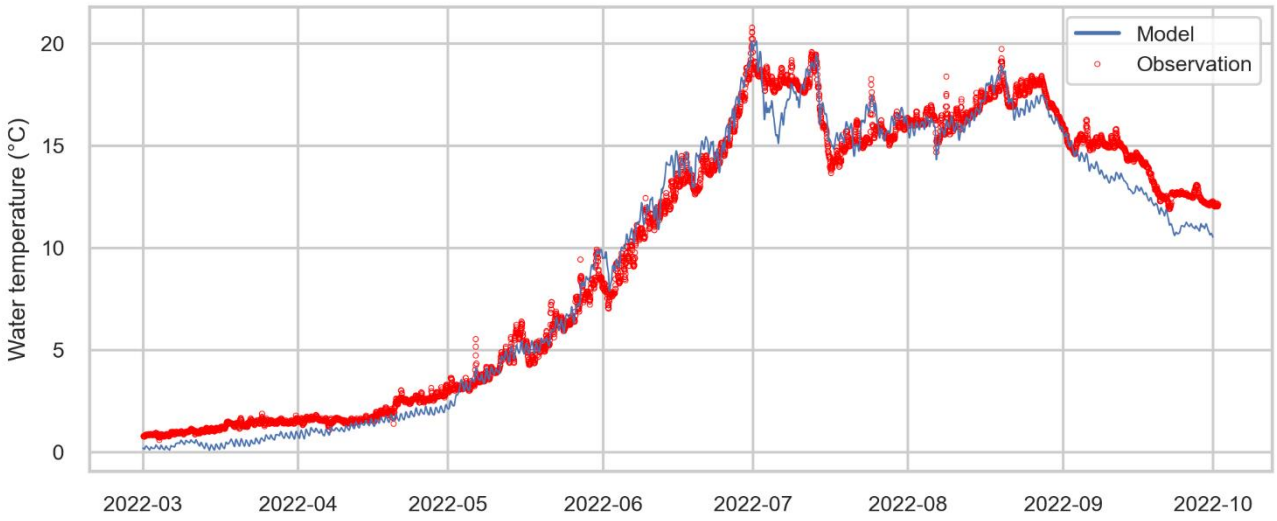

Figure 7.10: Comparison between modelled (blue line) and observed (red circles) surface water temperature time series at Finngrundet.

7.5.7. Waves, time series

Comparison between modelled and observed wave conditions are shown in Figure 7.11 only for Fyr1, since wave conditions are very similar between Fyr1, 2 and 3, and Finngrundet observations (Figure 6.7 and Figure 6.8). The figure shows a very good agreement between model results and observations, with a correlation coefficient of 0.94 and 0.85 and a RMSE of 0.19m and 0.62s for the significant wave height and the peak wave period, respectively. Main variations in mean wave direction are also well captured by the model, with some discrepancies under calmer conditions (low significant wave height). These results show a good ability of the model to describe wave conditions for the Bothnian Sea.

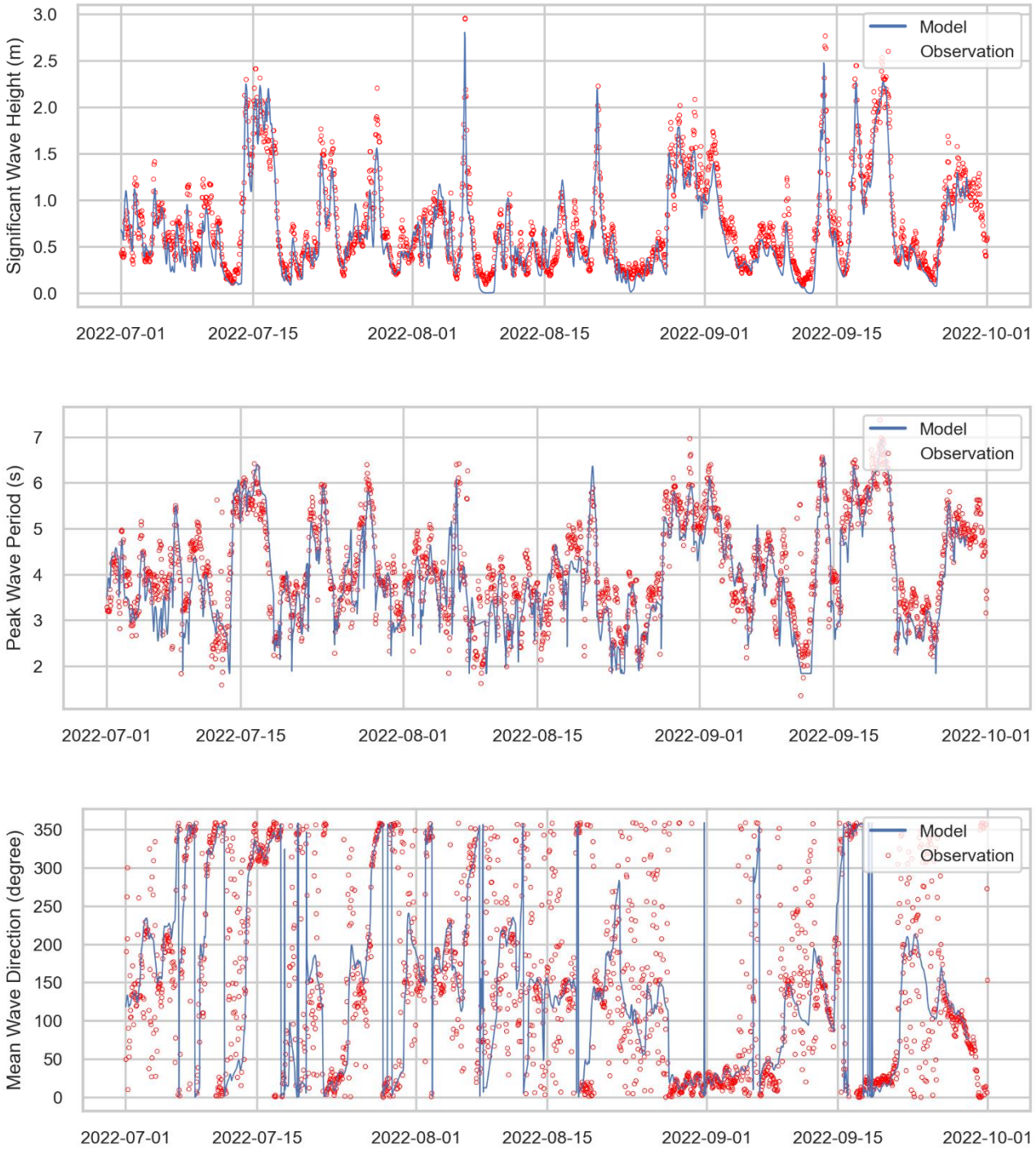

Figure 7.11: Comparison between modelled (blue lines) and observed (red circles) significant wave height (top row), peak wave period (second row) and mean wave direction (third row) for Fyr1

8. Hydrodynamic Pressure

8.1. Model input

To simulate the impact due to the presence of the wind farm the pressure on the hydrodynamics (circulation and stratification patterns) and waves have been modelled by adding the foundation and the reduction in the wind field to the baseline model:

i. Wind turbines: The wind field downstream of the wind farm has been modified with the use of a wake function (Jensen, N.O., 1983) considering the roughness (0.001m), hub height (142.5 m), rotor diameter (245 m) and the thrust coefficient (c_t) for wind speeds of below 5, 5 to 11 and above 15 m/s at each turbine position with cut in at 3 m/ and cut off at 25 m/s. To capture the presence of the turbines the resolution of the wind fields was changed from 0.25° to 0.01° (approx. 0.65 km) and the effect of the wake was imprinted based on a wind direction in steps of 5°.
ii. To be aligned with the wake simulated with WAsP the coefficient κ had to be changed from the recommended 0.04 for offshore wind farms to 0.13.
iii. Substructure: In the hydrodynamic model the blocking from the substructures is described with a simple drag-law to increase the resistance at each position.
iv. Substructure: For the wave model a source term has been introduced at each turbine position.

For illustration of the wind speed and the reduction in the wind speed due to the two cases, the annual average wind speed in 2021 (ECMWF, 2022) and the reductions are presented in Figure 8.1.

At present the annual mean wind speed at Fyskeppet OWF is around 6.8 m/s at 10 mMSL, the predicted reduction from the 187 15MW power rated wind turbines is 0.005 m/s to a maximum distance of 5 km largest northwest and south.

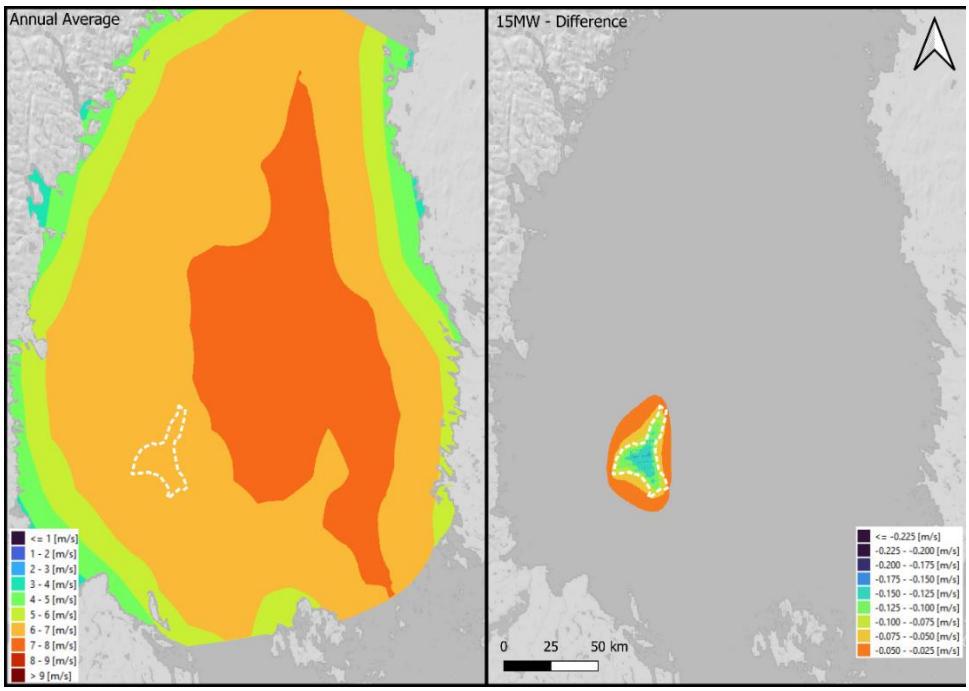

Figure 8.1: Wind. Left: annual average 2021, Right: changes in the due to the 187 turbines.

8.2. Waves

The average significant wave height is 0.8-0.9m over the wind farm and between 0.75 to 1m over the open areas of the Bothnian Sea decreasing to around 0.25m at the coast (Figure 8.2) during the average year 2021. By modifying the wind field and reducing the wind speed, the operation of the wind farm will reduce the average significant wave height at most by 0.02 m close to the foundations. Within the footprint of the wind farm, the impact is generally lower than 0.01 m, while outside the impact is limited to less than 0.005 m.

The significant wave height varies seasonally (Appendix 6) and is highest between October and March (highest average in October of 1.48m), close to average in April, August, and September and lowest between May and July. Propagation of effects due to the operation of the wind farm varies depending on the dominant wind directions, reaching most of the Swedish coast with a mild amplitude in January, spreading from the southern Swedish coast towards the north/northeast in February, April, May, June, and November and being relatively close to the average in March, August, and December, and spreading from the Åland Sea towards the northern Swedish coast in July, September, and October.

The month-to-month impact is aligned with annual average with slightly less impact in the summer time where the average significant wave heigh is around 0.5 m, while a reduction of 0.005-0.01 m spreads around 20 km westward of the wind farm in May and June.

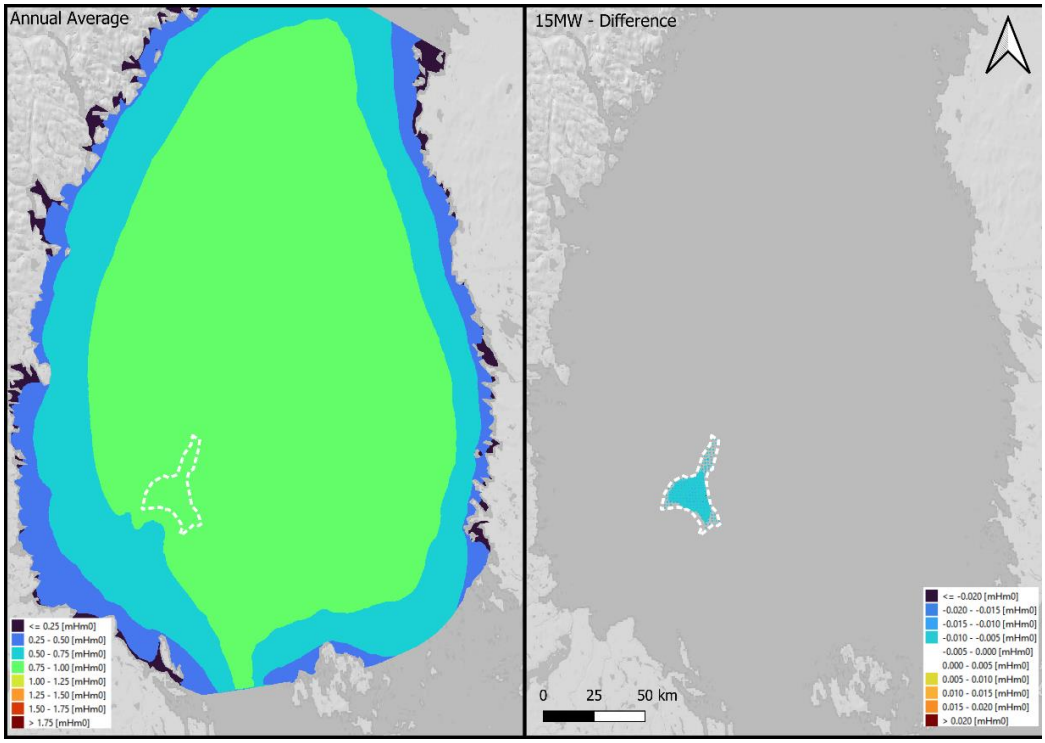

Figure 8.2: Left: Annual (2021) average significant wave height (m). Right: Changes in the annual average significant wave height due to the 187 wind turbines.

The annual maximum wave at the site is around 1.5 m and follows a similar spatial pattern as the significant wave height. Like for the annual significant wave height, the impact is limited. Close to the foundation the reduction is at most 0.03 m and 0.005-0.01 m around and up to 15 km northwest of the wind farm (Figure 8.3).

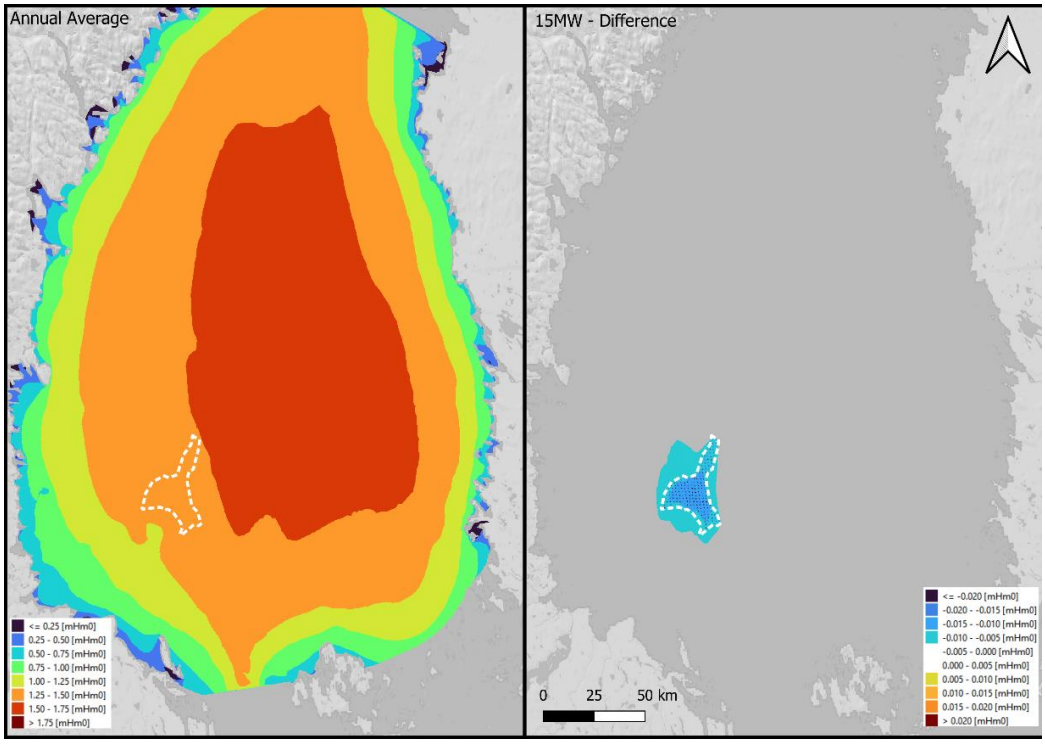

Figure 8.3: Left: Annual (2021) maximum wave height (m). Right: Changes in the maximum annual wave height due to the 187 wind turbines.

Potential effects on longshore sediment are not expected due to the limited magnitude and extent of the reduction in the wave heights. Thereby, the risk for an impact at the coast is low as the reduction in wave height is negligible along the coast, which are moreover mostly formed of archipelagos and fjords with hard bottoms (Schiewer, 2008), indicating limited sediment transport and resuspension.

8.3. Water level

Averaged surface elevation for the year 2021 is very close to 0m, corresponding to the mean sea water level. Surface elevation is somewhat higher in the south and west of the Bothnian Sea (≥ -0.03mMSL) and lower in the north and east coast (≤-0.04mMSL). It averages -0.04m to -0.03m in the open sea, with an area 50km east of Fyrskeppet OWF being experiencing somewhat lower average surface elevation (≤-0.04m; Figure 8.4).

Changes in the average surface elevation due to the operation of the 187 turbines are very small, lower than 1mm everywhere in the Bothnian Sea. Due to the very limited magnitude, the changes are probably dominated by numerical accuracies in the model, but a dipole pattern could be discerned on average for the month of June, shown in Appendix 9.

This dipole pattern can be relevant for changes in currents and temperatures. Limited areas directly west and 30 km north-west of the wind farm experience slightly higher surface elevation (0.2mm), while areas directly north and 30 km east of the wind farm experience slightly lowered surface elevation (1mm). These changes are well within the range of

natural variability and direct impacts on sea-level are negligible but can be linked with changes in currents and stratification, discussed in the following sections. Areas with higher surface elevation, towards which surface currents that transport warmer and less salty water converge, create downwelling zones, while areas with lower surface elevation, from which surface currents diverge, create upwelling zones transporting colder and saltier water from the deeper water (Christiansen, Daewel, Djath, & Schrum, 2022). However, investigation of monthly changes in temperature and water level did not show this pattern (e.g., comparing changes in temperature and water level in June, Appendix 8 and Appendix 9).

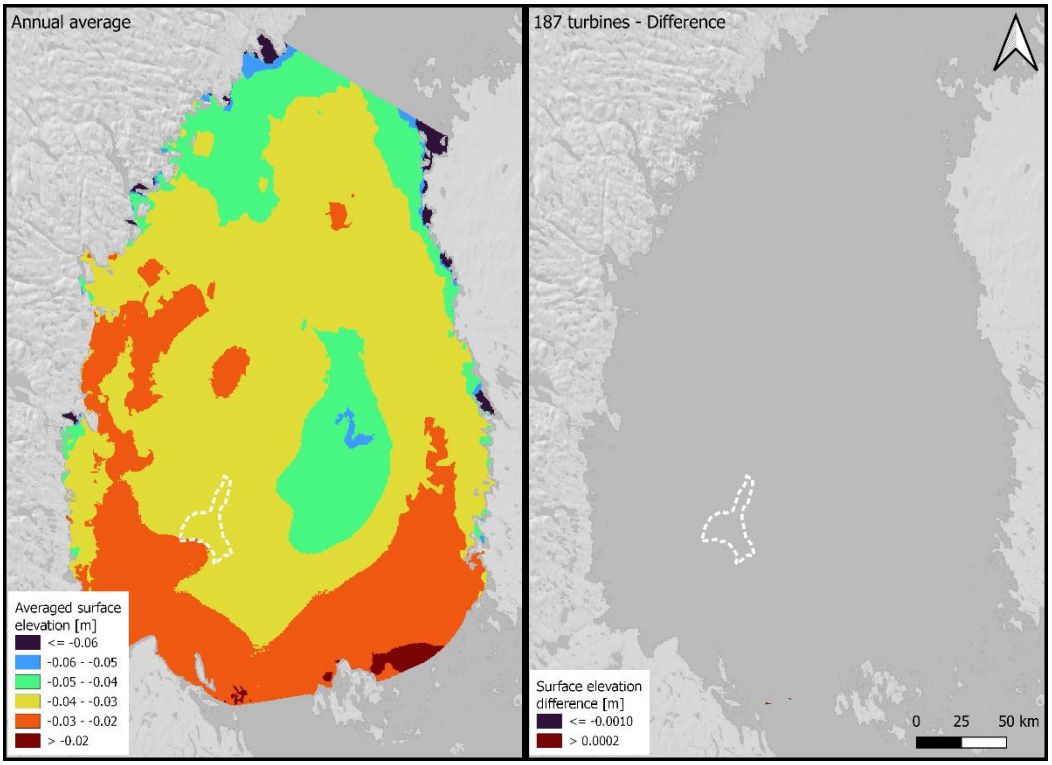

Figure 8.4: Left: Annual (2021) average water level (m). Right: Changes in average surface elevation due to the 187 wind turbines.

8.4. Current

Current speeds under average conditions of the year 2021 are generally low in the Bothnian Sea due to the absence of tides in the Baltic Sea. Average surface currents between 0 and -10m (Figure 8.5) range from 0.05 to 0.1 m/s for most of the Bothnian Sea, except for a few areas around the eastern coast, Finngrundet and the boundaries to the Åland Sea and to the Bothnian Bay experiencing somewhat greater currents (greater than 0.1 m/s) and the western coast experiencing currents lower than 0.05 m/s.

Annual average current speeds decrease with depth, in accordance with the current profiles (Figure 7.7), with current speeds between -10m and -20m ranging between 0.05 to 0.1 m/s, except in the western parts where current speeds are generally lower than 0.05 m/s, and very few areas with current speeds greater than 0.1 m/s. Average current speeds between -20m and -30m are lower than 0.05 m/s for most of the sea area, except along the east coast where they lie somewhat over 0.05 m/s.

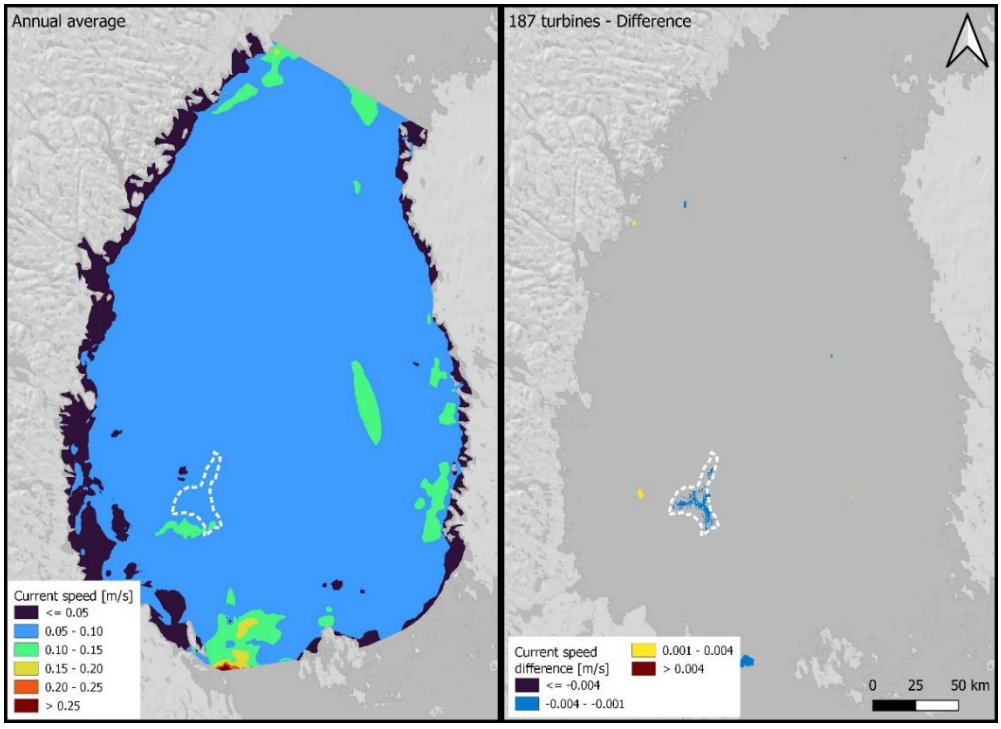

Figure 8.5: Left: Annual (2021) average current speed from 0 to -10 m. Right: Change in current speeds due to the 187 wind turbines.

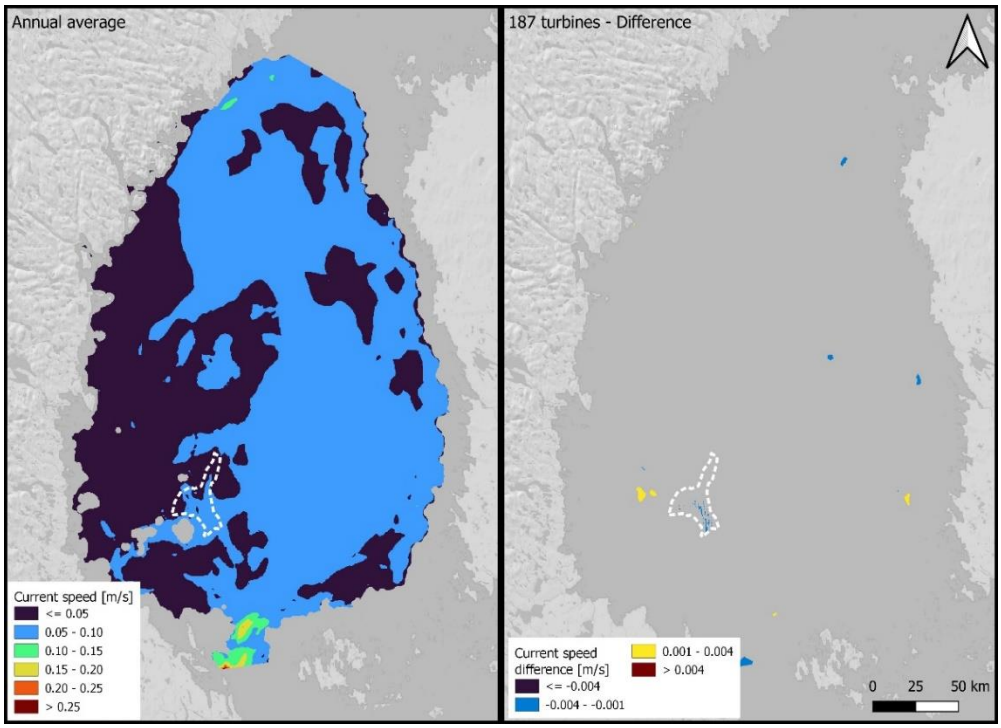

Figure 8.6: Left: Annual (2021) average current speed from -10 to -20 m (bottom in grey). Right: Change in current speeds due to the 187 wind turbines.

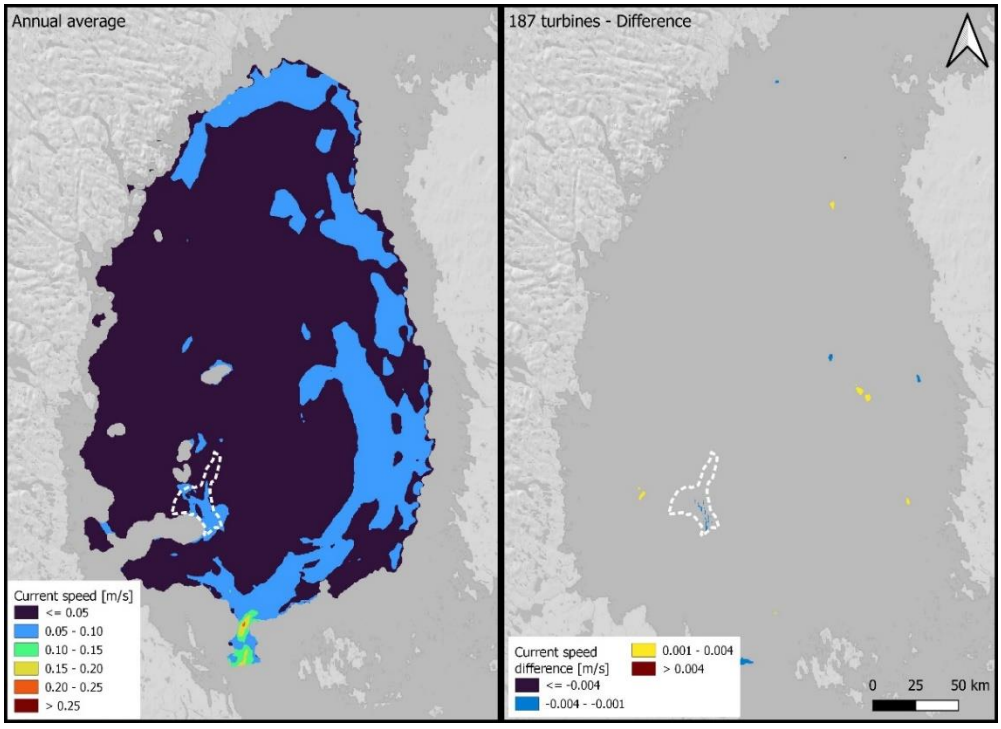

Figure 8.7: Left: Annual (2021) average current speed from -20 to -30 m (bottom in grey). Right: Changes in current speeds due to the 187 wind turbines.

The 187 turbines wind farm yields a decrease of the average surface current speeds within the wind farm of 0.001-0.003 m/s in all vertical layers, which is more pronounced in extent for the surface (0-10 m) layer and corresponds 1-6 %. This decrease can be explained by the presence of turbine foundations modifying the water flow (discussed in section 8.7). An increase in current speed of 0.001-0.003 m/s is observed 20 km west of the wind farm, is likely due to the modification of the flow from the foundations that in turn increases the flow at other locations. This slight increase is very limited in extent and somewhat more pronounced in the 10-20 m layer. No change in current speeds is observed at the Finngrundet area, directly south of the wind farm.

8.5. Temperature

Annual average surface temperature (0-10m) for the year 2021 is generally somewhat higher in the southern and open sea parts (ranging between 7°C and 8.2°C) and lower at the coast and northern parts (ranging between 5.8°C to 7°C).

Due to the temperature stratification in summer, with warmer temperatures at the surface, yearly averaged temperatures decrease with depth. The thermocline generally lies between -5 to -25m in the summer. Between 10m and 20m depth, most of the sea area range between 5°C and 6°C, and some areas east of the wind farm and near the Åland boundary have average temperature above 6°C. Between 20m and 30m depth, the average temperature lies between 4°C and 5°C over most of the sea area, except in shallower areas around the Swedish coastline.

Temperature conditions present strong seasonal variations (see Appendix 7 and Appendix 8), with average temperature in January in the 10-20m layer varying between 3°C in most of the open sea to over 4°C in the western parts. Temperatures are lower in February and March, ranging between 1°C to 3°C, and increase in April to over 2°C,

except around the eastern coast. Temperature increase relatively strongly between April and August to reach around 12°C (maximum temperature of 16°C) in the 10-20m layer for most of the sea, expect for some areas in the west and east. Temperatures start to decrease in the easter areas during September, while they increase slightly in the western areas, and decrease strongly from October to December to average between 3-4°C in the west and 4-5.3°C in the east of the Bothnian Sea.

Increase in yearly average temperature of just under 0.1°C due to the operation of the 187 turbines are only observed in a very limited area west of the wind farm, in the 10-20 m layer (Figure 8.8 to Figure 8.10). No change greater than 0.1 °C is observed in the Bothnian Sea, indicating a negligible impact on yearly temperatures in comparison to the natural variability.

Impacts on monthly temperatures have been analysed in Appendix 7 for the layer 10-20 meter, where largest impacts on temperature can be seen. Impacts of more than 0.3°C can be seen only during the summer months (June – September), during which a thermocline is present. Impacts are generally seen in the vicinity of the wind farm, but some changes are also observed closer to the boundary and north-east of the wind farm, which could be due to propagation of effects or of numerical accuracies.

Close to the wind farm, temperature changes are located on the western. Impacts on temperature are also illustated through monthly vertical profiles for points where a change in monthly temperature is observed in Appendix 8.

Difference in profiles are only seen during the summer months and only affect the thermocline layer, with both surface and bottom water temperatures remaining unchanged. For example in June, the thermocline is slightly located slightly higher for point 4, corresponding to a somewhat reduction of the water temperature in the 10-20 m layer, while it is somewhat lower for point 3, corresponding to a slight increase of the water temperature. If these changes were due to the changes in water level from difference in wind speeds, point 3 (with higher temperature) would be in an area of increased water levels and point 4 (slighly lower temperature) would be in an area of decreased water level, however the opposite is seen (Appendix 9). Thereby, temperature changes area more likely to be caused by differences in currents from the foundations, discussed section 8.7. Overall, increases and decreases are within the range -0.6 to 0.5 °C over limited areas, which is small in comparison of natural variability.

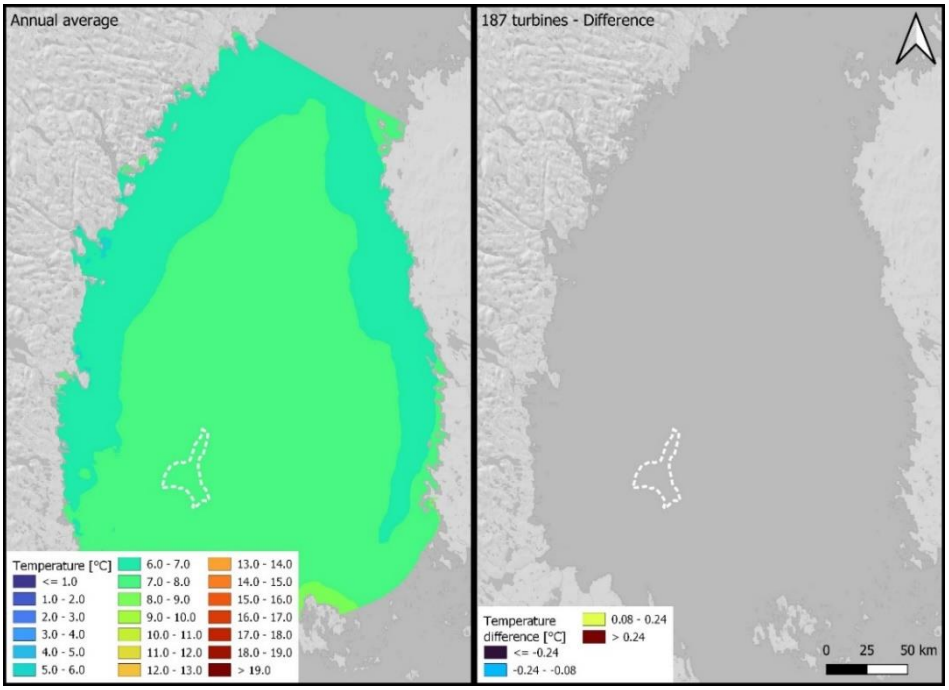

Figure 8.8: Left: Annual (2021) average temperature (°C) from 0 to -10 m. Right: Changes in temperature due to the 187 wind turbines.

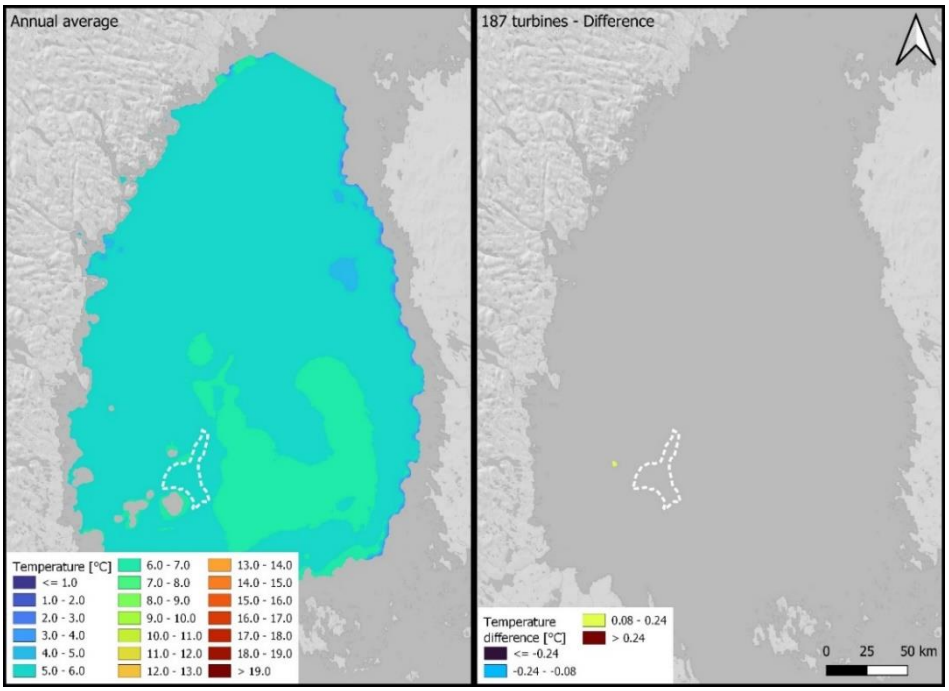

Figure 8.9: Left: Annual (2021) average temperature (°C) from -10 to -20 m (bottom in grey). Right: Changes in temperature due to the 187 wind turbines.

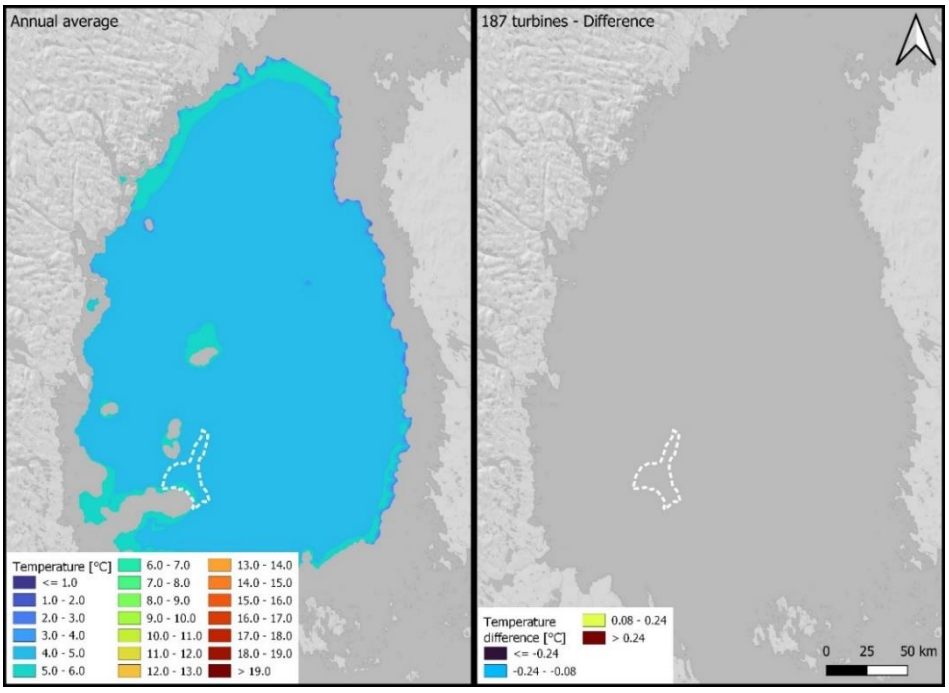

Figure 8.10: Left: Annual (2021) average temperature (°C) from -20 to -30 m (bottom in grey). Right: Changes in temperature due to the 187 wind turbines.

8.6. Salinity

Average salinity in the surface layer (0-10m) range from 3.4PSU to 5.6 PSU and are highest at the centre of the Bothnian Sea, east of the wind farm, and at the boundary with the Åland Sea, and lowest at the coast (due to river discharges) and at the northern boundary due to important river discharges in the Bothnian Bay (Figure 8.11). Salinity generally increases with depth and are higher in the layer -10m to -20m, somewhat above 5.5PSU (maximum salinity of 5.7PSU) in the eastern part of the Bothnian Sea and between 5PSU and 5.5PSU in the north and western parts of the sea. In the layer -20m to -30m, the salinity is generally above 5.5PSU (maximum salinity of 5.9PSU) except in the western part of the Bothnian Sea, closer to the coast, where it is between 5PSU and 5.5PSU. Thereby, the salinity experiences low vertical gradients, with a maximum increase by less than 0.5PSU between the surface and the -20m to -30m layers, and low horizontal gradient with variations by less than 0.5PSU in the open Bothnian Sea.

No change in average salinity due to the operation of the 187 turbines wind farm of more than 0.05 PSU is observed in the Bothnian Sea (Figure 8.11 to Figure 8.13). A change of 0.05 PSU corresponds to 1% of the natural salinity and is negligible in comparison to the natural variability. Thereby, the operation of the wind farm is expected to have negligible impacts on the salinity field.

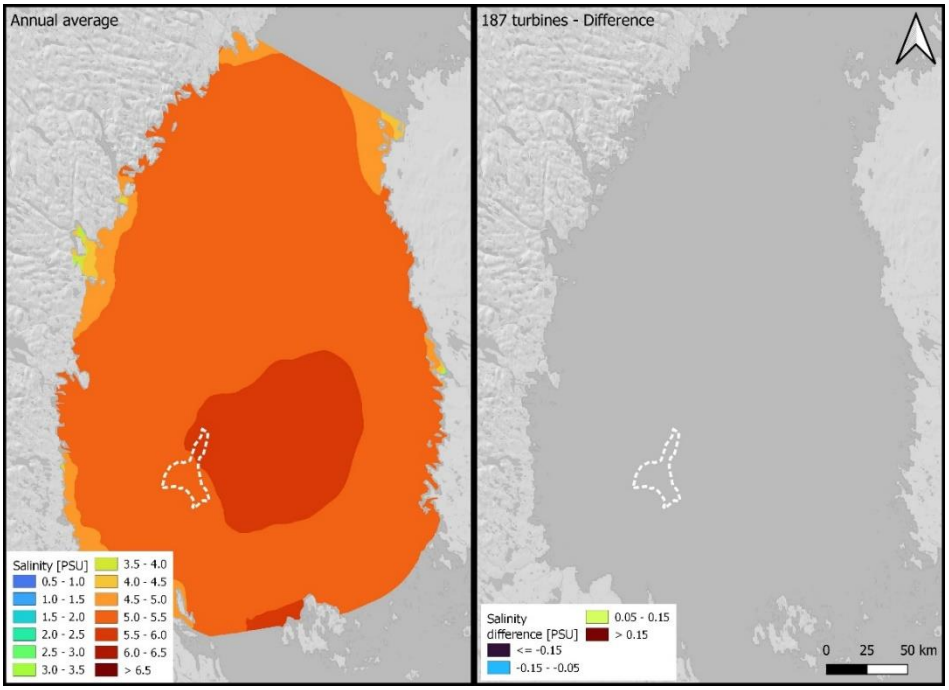

Figure 8.11: Left: Annual (2021) average salinity (PSU) from 0 to -10 m. Right: Changes in salinity due to the 187 wind turbines.

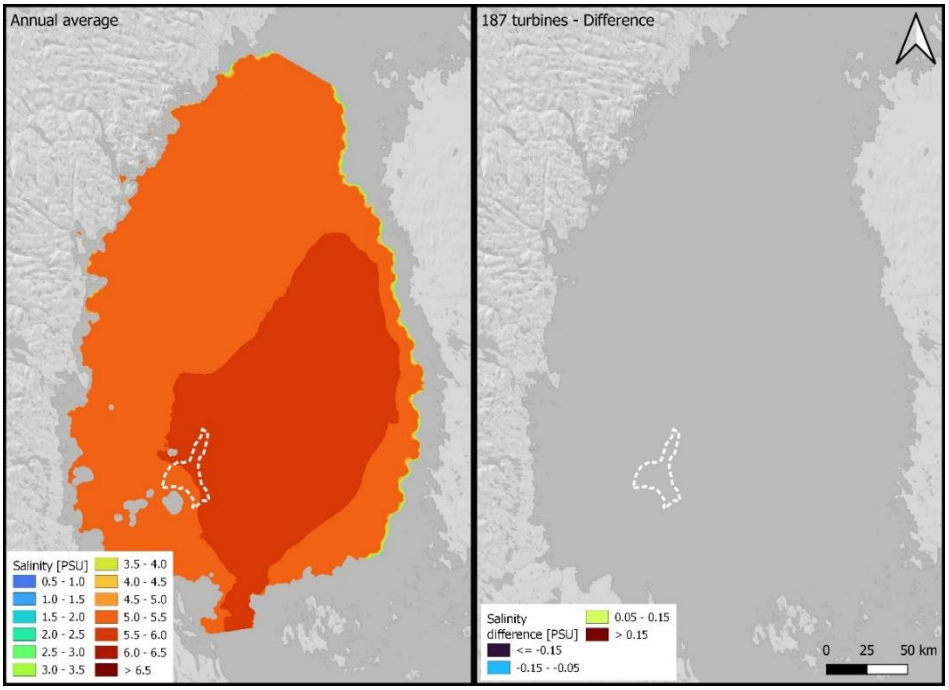

Figure 8.12: Left: Annual (2021) average salinity (PSU) from -10 to -20 m (bottom in grey). Right: Changes in salinity due to the 187 wind turbines.

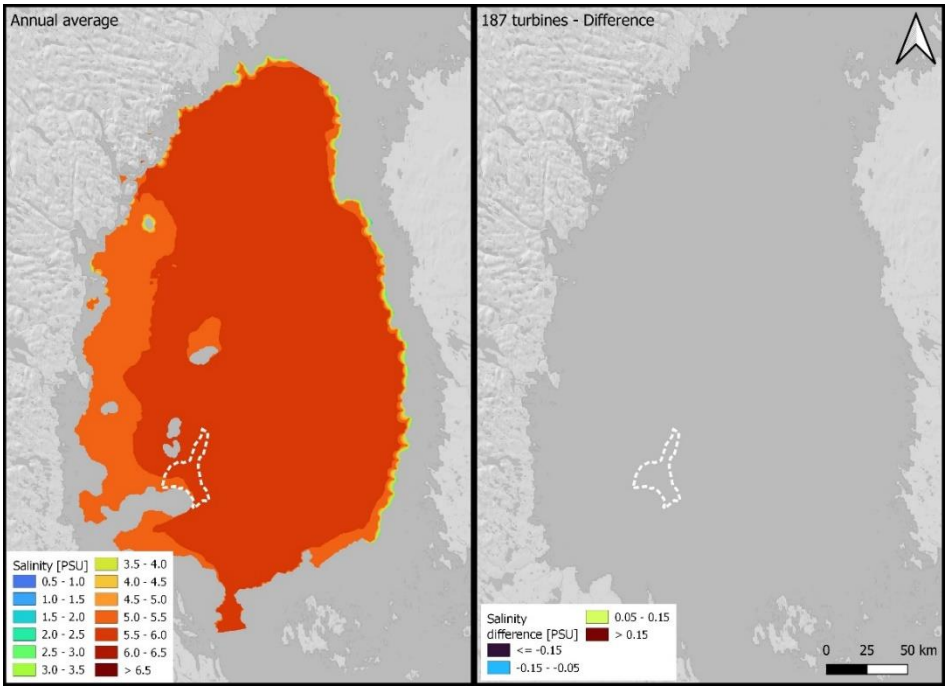

Figure 8.13: Left: Annual (2021) average salinity (PSU) from -20 to -30 m (bottom in grey). Right: Changes in salinity due to 187 wind turbines.

8.7. Blocking, water exchange

Figure 8.14 to Figure 8.16 show the annual average currents under baseline conditions for the year 2021 and the difference in currents due 187 wind turbines for the 0-10m, 10-20m and 20-30m layers, zoomed in around the wind farm.

Current speed reductions of at most 0.002 m/s can be observed in the wind farm for all layers, more pronounced for the surface layer (0-10 m). In the surface layer, the reduction is generally between 0.001 to 0.002 m/s and at most 0.003 m/s, while surface currents are around 0.07 m/s, corresponding to a reduction of the current of at most 4%. In the 10-20 m layer, the reduction is lower than 0.001 m/s and at most 0.03, and currents are around 0.05 m/s (minimum of 0.04 m/s), corresponding to a reduction of the current of at most 7%. In the 20-30 m layer, the reduction is lower than 0.002 m/s, and currents are around 0.05 m/s (minimum of 0.03 m/s), corresponding to a reduction of the current of at most 7%. Thereby a blocking from the structure can be observed but is limited in magnitude. To compensate this blocking and reduced water flow through the Fyrskeppet OWF, an increase of currents can be observed on the east, west and north side of the wind farm generally lower than 0.001 m/s and at most 0.0023 m/s in the 10-20 m layer, corresponding to a maximum increase of 6%.

Overall, the impact of the 187 turbine fundaments on hydrodynamic conditions (currents, temperature, and salinity) are very limited. Current patterns are somewhat modified at the wind farm and up to a 20 km around due to the foundations. These change in current could explain the changes in temperature as the latter do not correlate with changes in water levels, but as seen in the previous section, the impact on temperature and salinity is very limited. No modification of the current is seen in the Finngrundet area, south of the wind farm.

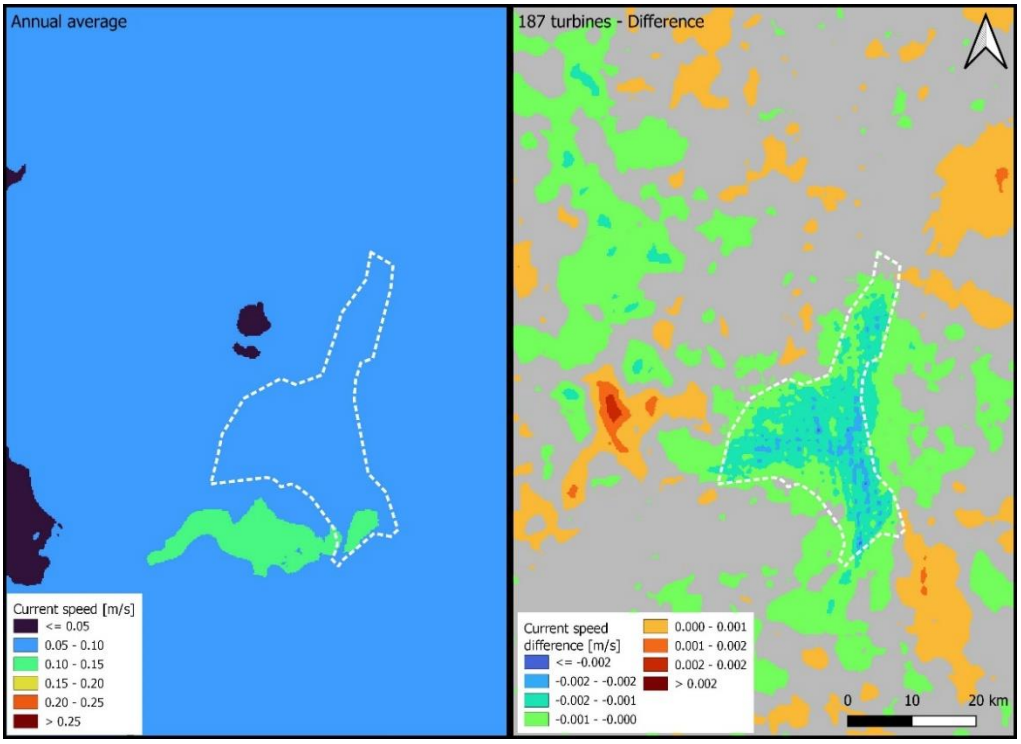

Figure 8.14: Left: Annual average current speed (m/s) from 0 to -10 m. Right: Changes in current speeds due to the 187 turbines.

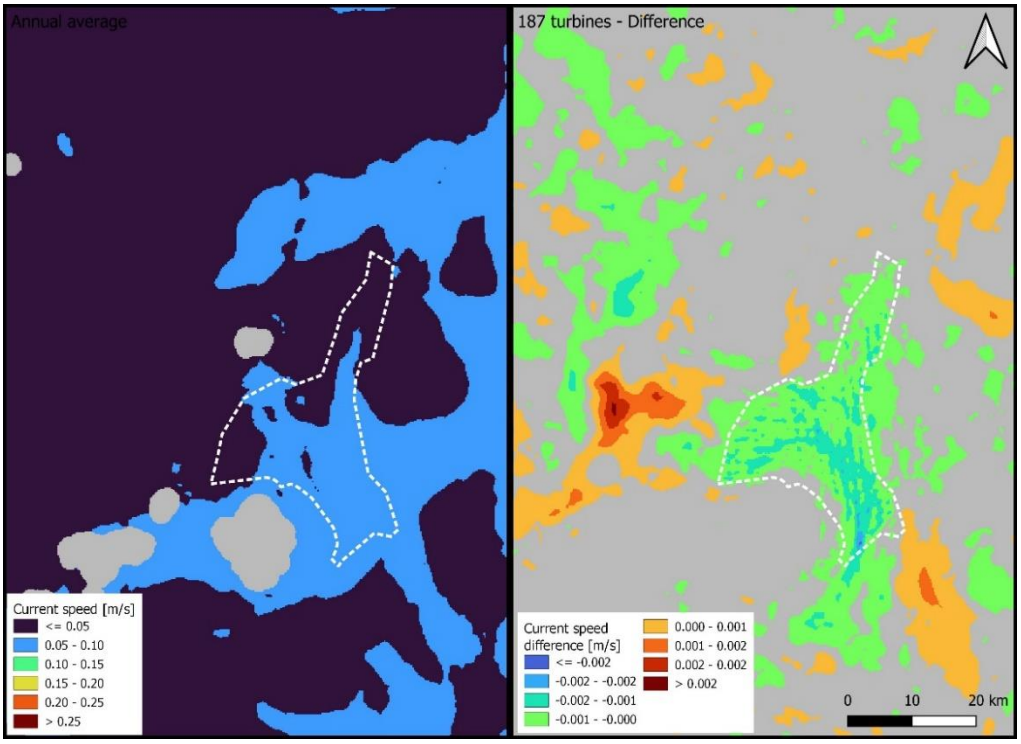

Figure 8.15: Left: Average current speed (m/s) from -10 to -20 m (bottom in grey). Right: Changes in current speeds due to the 187 turbines

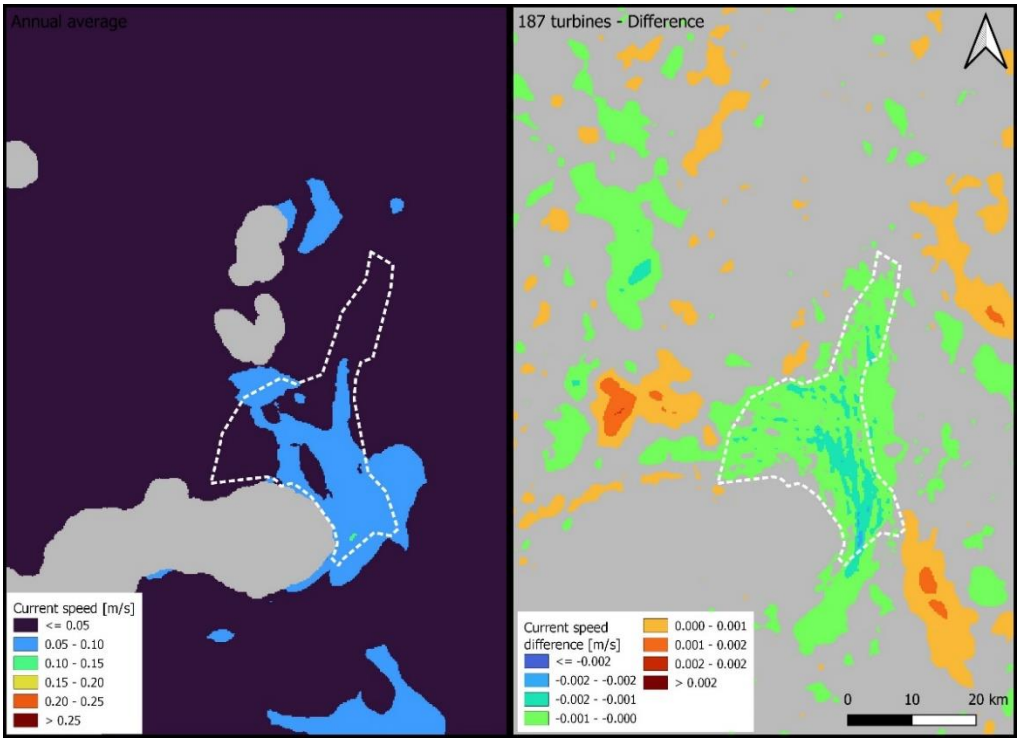

Figure 8.16: Average current speed (m/s) from -20 to -30 m (bottom in grey). Right: Changes in current speeds due to the 187 turbines

9. References

Bladin, K., Rämö, R., Lavett, E., Vinterstare, J., & Vigouroux, G. (2022). *Fältundersökningar inom Fyrskeppet 2022*. AquaBiota Report 2022:30.

Christiansen, N., Daewel, U., Djath, B., & Schrum, C. (2022). Emergence of large-scale hydrodynamic structures due to atmospheric offshore wind farm wakes. *Frontiers in Marine Science*, 64.

Copernicus. (2022, 10). *Baltic Sea Physics Analysis and Forecast, 2x2km*. Retrieved from https://resources.marine.copernicus.eu/product-detail/BALTICSEA_ANALYSISFORECAST_PHY_003_006/INFORMATION

Copernicus. (2022, 10). *Baltic Sea Physics Reanalysis 4x4km*. Retrieved from Copernicus: https://resources.marine.copernicus.eu/product-detail/BALTICSEA_REANALYSIS_PHY_003_011/INFORMATION

ECMWF, C. C. (2022, 12 01). *Climate Data Store*. (ECMWF) Retrieved from https://cds.climate.copernicus.eu/cdsapp#!/dataset/reanalysis-era5-single-levels?tab=form

EMODnet. (2021, 03 15). *Bathymetry*. Retrieved from portal.emodnet-bathymetry.eu/#: portal.emodnet-bathymetry.eu/#

Jensen, N.O. (1983). *A note on wind generator interaction.* DTU.

Schiewer, U. (2008). The Baltic Coastal Zones. In U. Schiewer, *Ecology of Baltic coastal waters* (pp. 23-33). Springer.

Appendix 1: Current speeds and direction for the SMHI monitoring stations

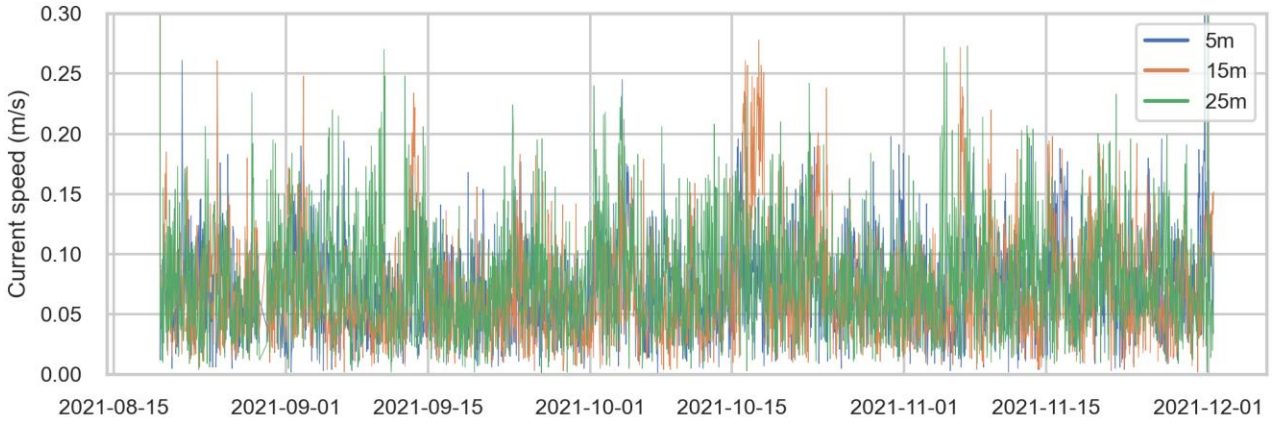

Figure 9.1: Current speed at 5, 15 and 25m depth at Norrbyn Boj monitoring station

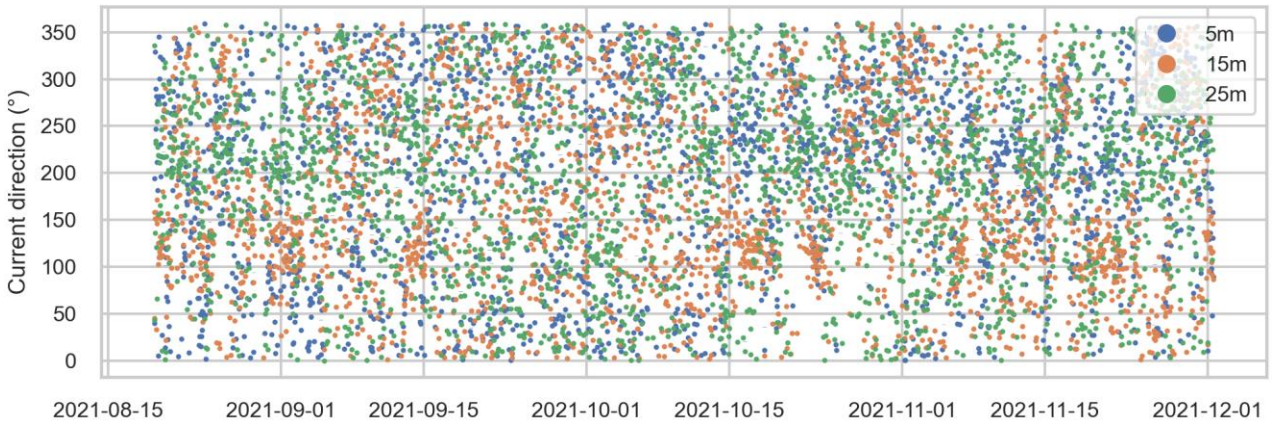

Figure 9.2: Current direction at 5, 15 and 25m depth at Norrbyn Boj monitoring station

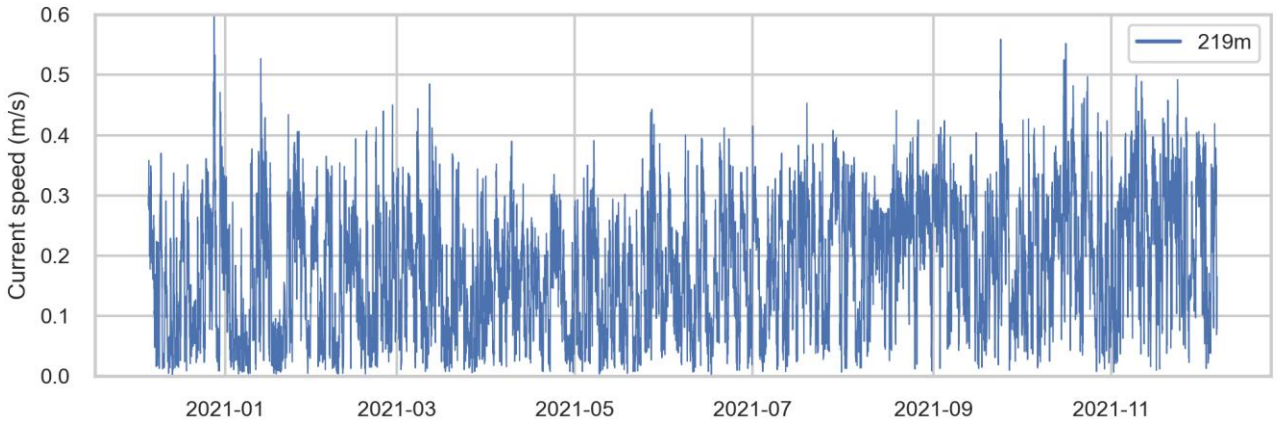

Figure 9.3: Current speed at 219m depth at Understen BS monitoring station

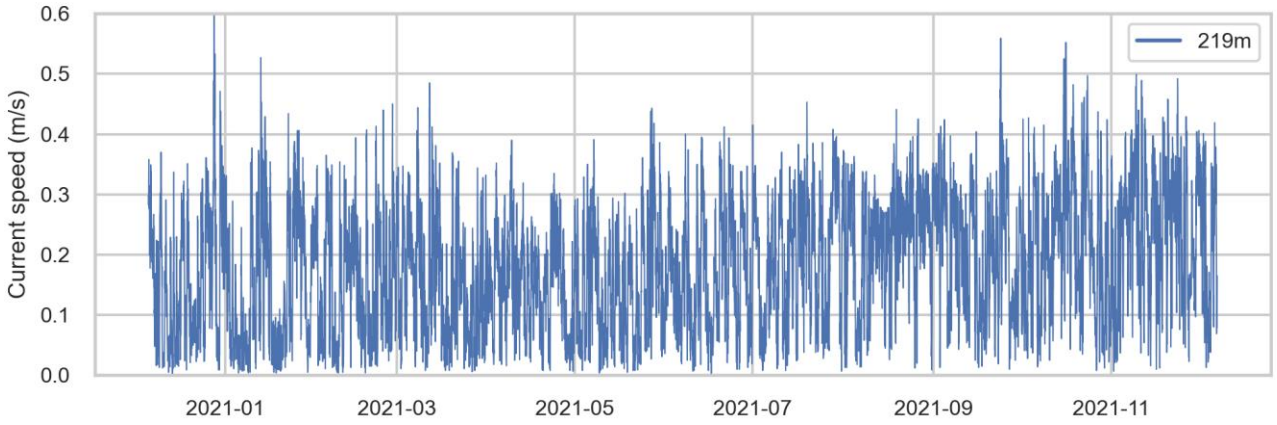

Figure 9.4: Current direction at 219m depth at Understen BS monitoring station

Appendix 2: Fyrskeppet OWF, Temperature profiles (SMHI, modelled 4x4km)

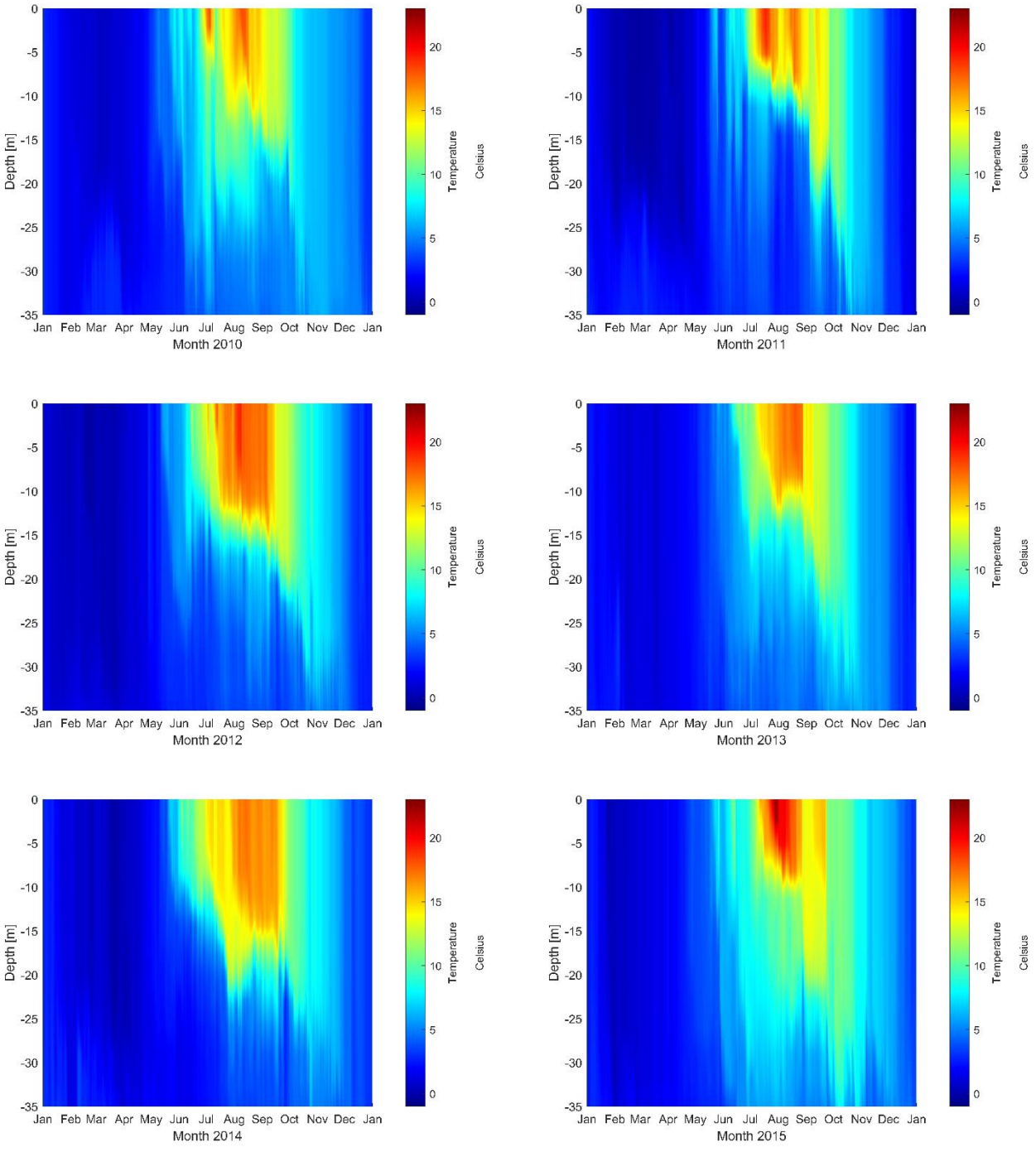

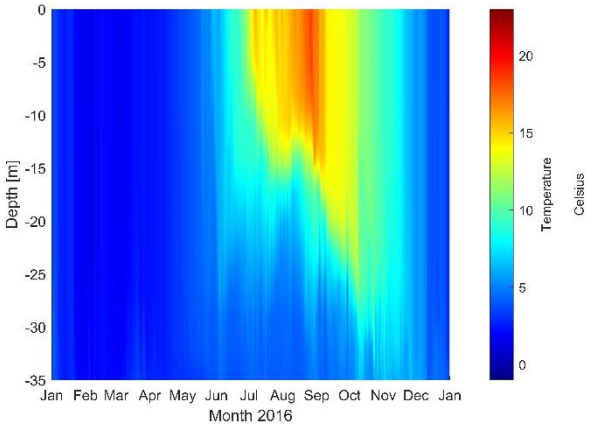
Depth [m]
0
-5
-10
-15
-20
-25
-30
-35
Jan Feb Mar Apr May Jun Jul Aug Sep Oct Nov Dec Jan
Month 2016
Temperature
Celsius
20
15
10
5
0

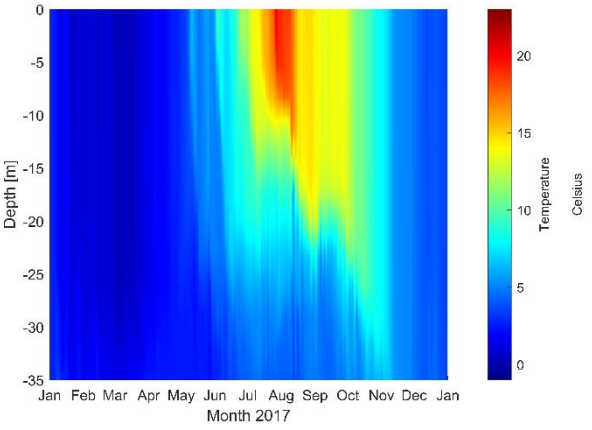
Depth [m]
0
-5
-10
-15
-20
-25
-30
-35
Jan Feb Mar Apr May Jun Jul Aug Sep Oct Nov Dec Jan
Month 2017
Temperature
Celsius
20
15
10
5
0

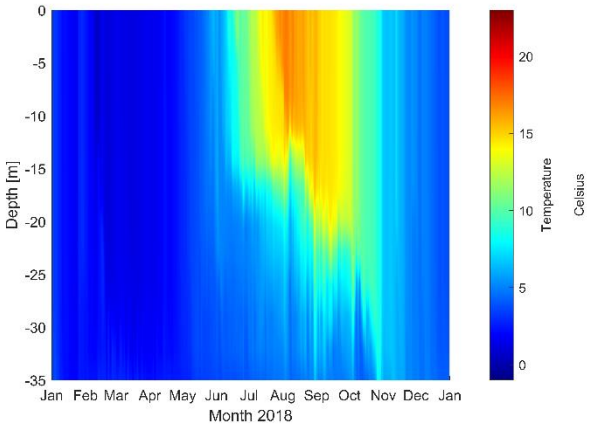
Depth [m]
0
-5
-10
-15
-20
-25
-30
-35
Jan Feb Mar Apr May Jun Jul Aug Sep Oct Nov Dec Jan
Month 2018
Temperature
Celsius
20
15
10
5
0

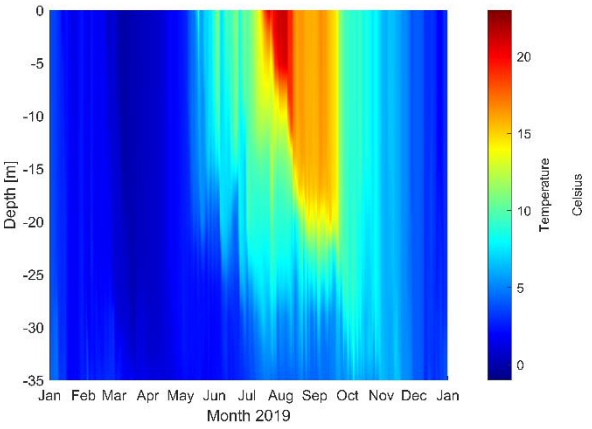
Depth [m]
0
-5
-10
-15
-20
-25
-30
-35
Jan Feb Mar Apr May Jun Jul Aug Sep Oct Nov Dec Jan
Month 2019
Temperature
Celsius
20
15
10
5
0

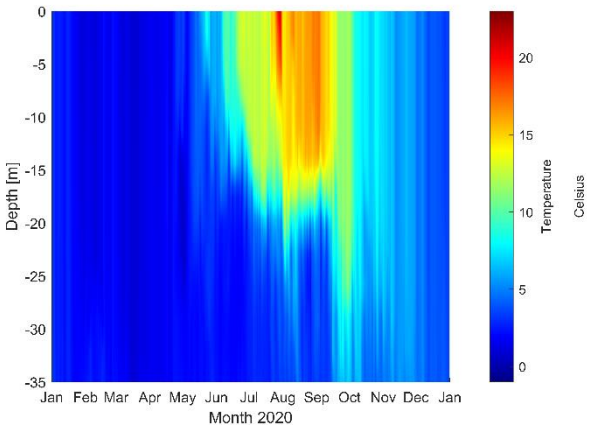
Depth [m]
0
-5
-10
-15
-20
-25
-30
-35
Jan Feb Mar Apr May Jun Jul Aug Sep Oct Nov Dec Jan
Month 2020
Temperature
Celsius
20
15
10
5
0

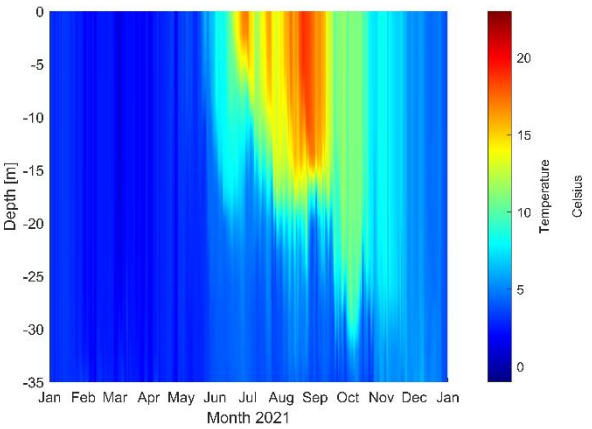
Depth [m]
0
-5
-10
-15
-20
-25
-30
-35
Jan Feb Mar Apr May Jun Jul Aug Sep Oct Nov Dec Jan
Month 2021
Temperature
Celsius
20
15
10
5
0

Appendix 3 Fyrskeppet OWF, Salinity profiles (SMHI, modelled 4x4km)

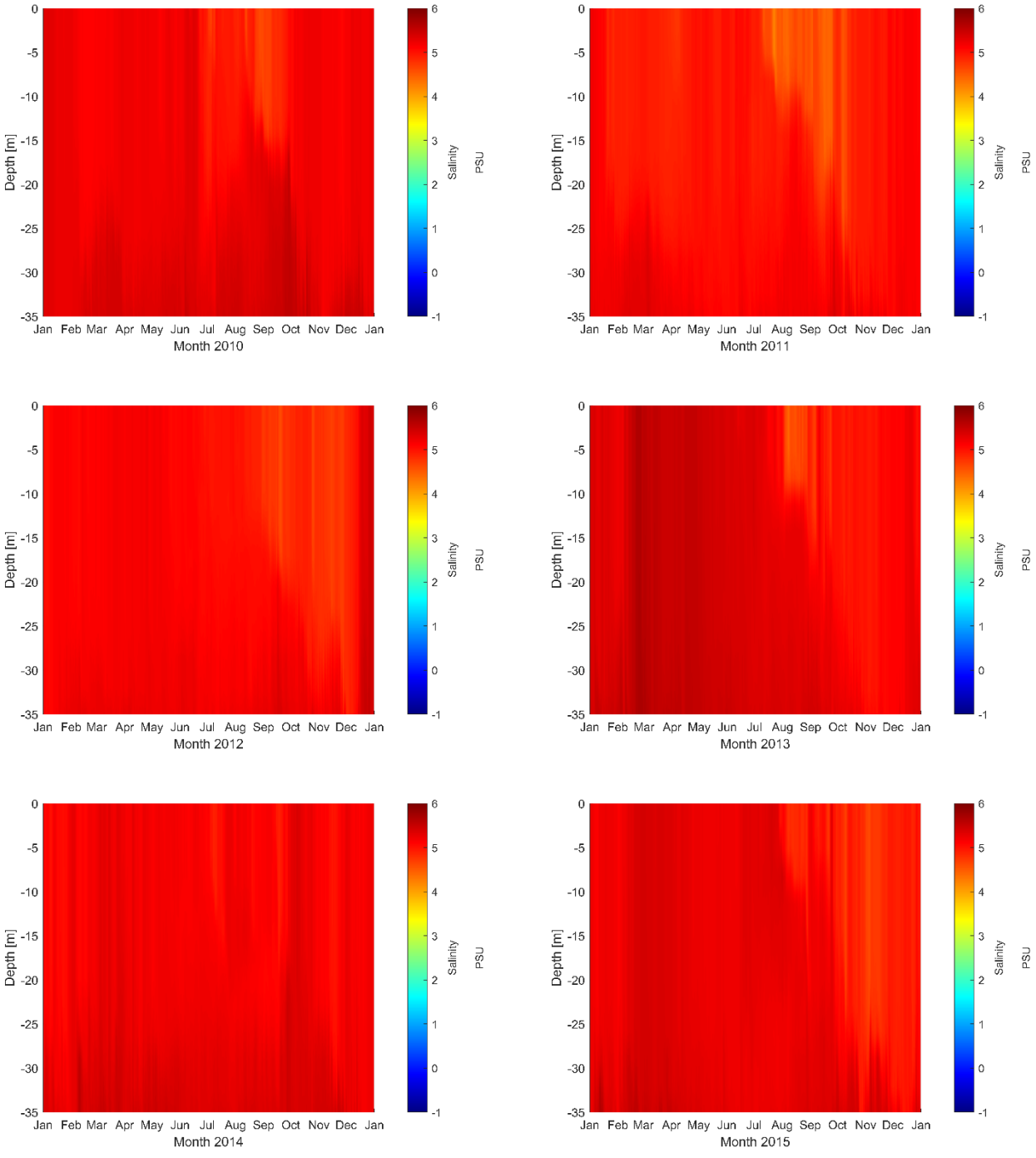

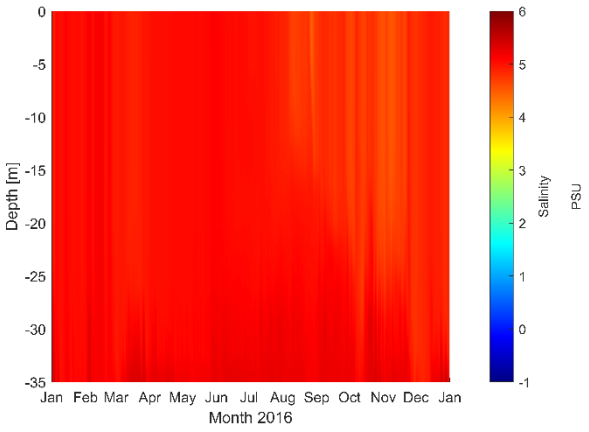
Depth [m]
0
-5
-10
-15
-20
-25
-30
-35
Jan Feb Mar Apr May Jun Jul Aug Sep Oct Nov Dec Jan
Month 2016
Salinity
PSU
6
5
4
3
2
1
0
-1

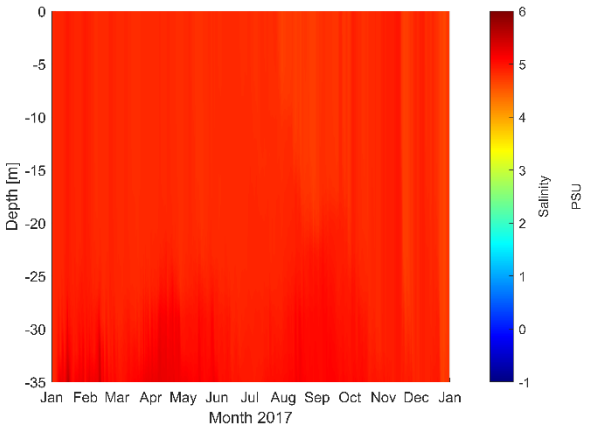
Depth [m]
0
-5
-10
-15
-20
-25
-30
-35
Jan Feb Mar Apr May Jun Jul Aug Sep Oct Nov Dec Jan
Month 2017
Salinity
PSU
6
5
4
3
2
1
0
-1

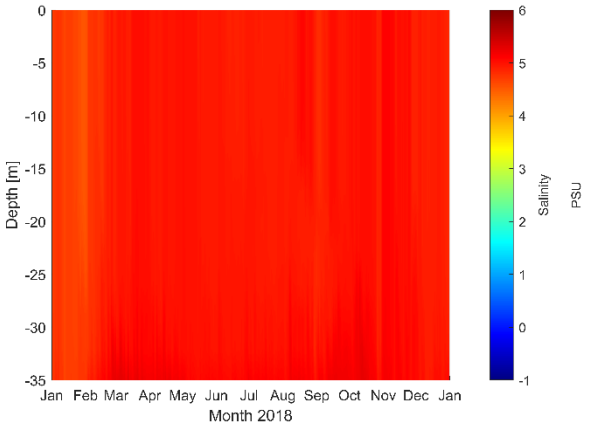
Depth [m]
0
-5
-10
-15
-20
-25
-30
-35
Jan Feb Mar Apr May Jun Jul Aug Sep Oct Nov Dec Jan
Month 2018
Salinity
PSU
6
5
4
3
2
1
0
-1

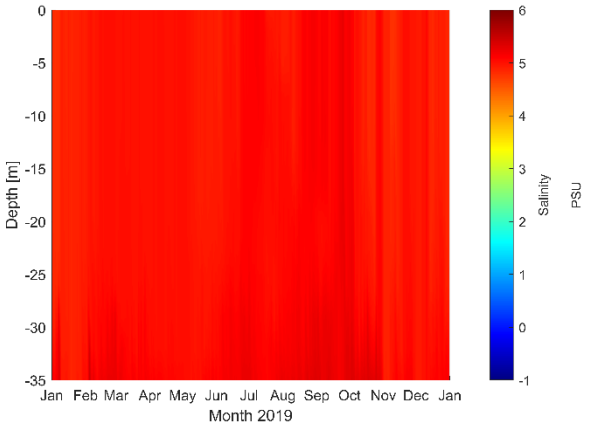
Depth [m]
0
-5
-10
-15
-20
-25
-30
-35
Jan Feb Mar Apr May Jun Jul Aug Sep Oct Nov Dec Jan
Month 2019
Salinity
PSU
6
5
4
3
2
1
0
-1

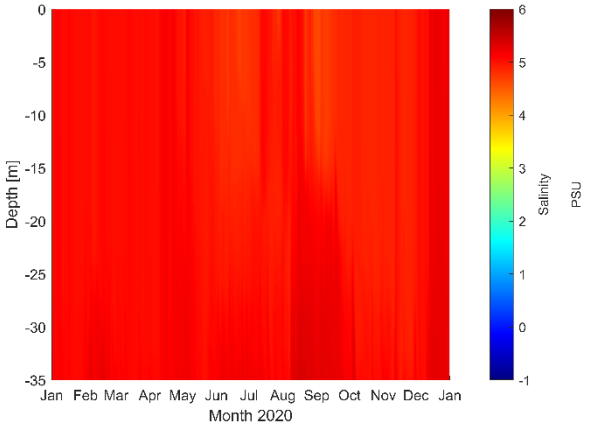
Depth [m]
0
-5
-10
-15
-20
-25
-30
-35
Jan Feb Mar Apr May Jun Jul Aug Sep Oct Nov Dec Jan
Month 2020
Salinity
PSU
6
5
4
3
2
1
0
-1

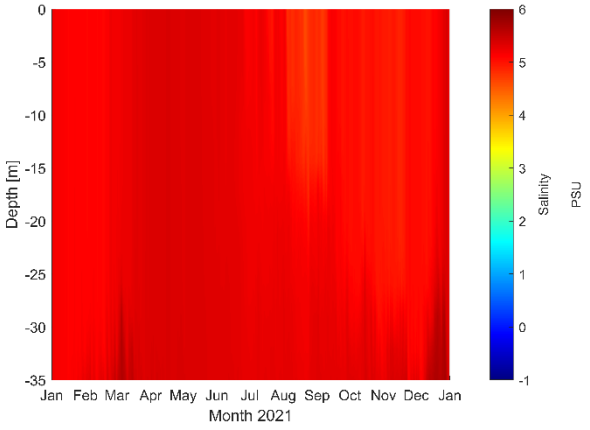
Depth [m]
0
-5
-10
-15
-20
-25
-30
-35
Jan Feb Mar Apr May Jun Jul Aug Sep Oct Nov Dec Jan
Month 2021
Salinity
PSU
6
5
4
3
2
1
0
-1

Appendix 4 Fyrskeppet OWF, Current roses (SMHI, modelled 4x4km)

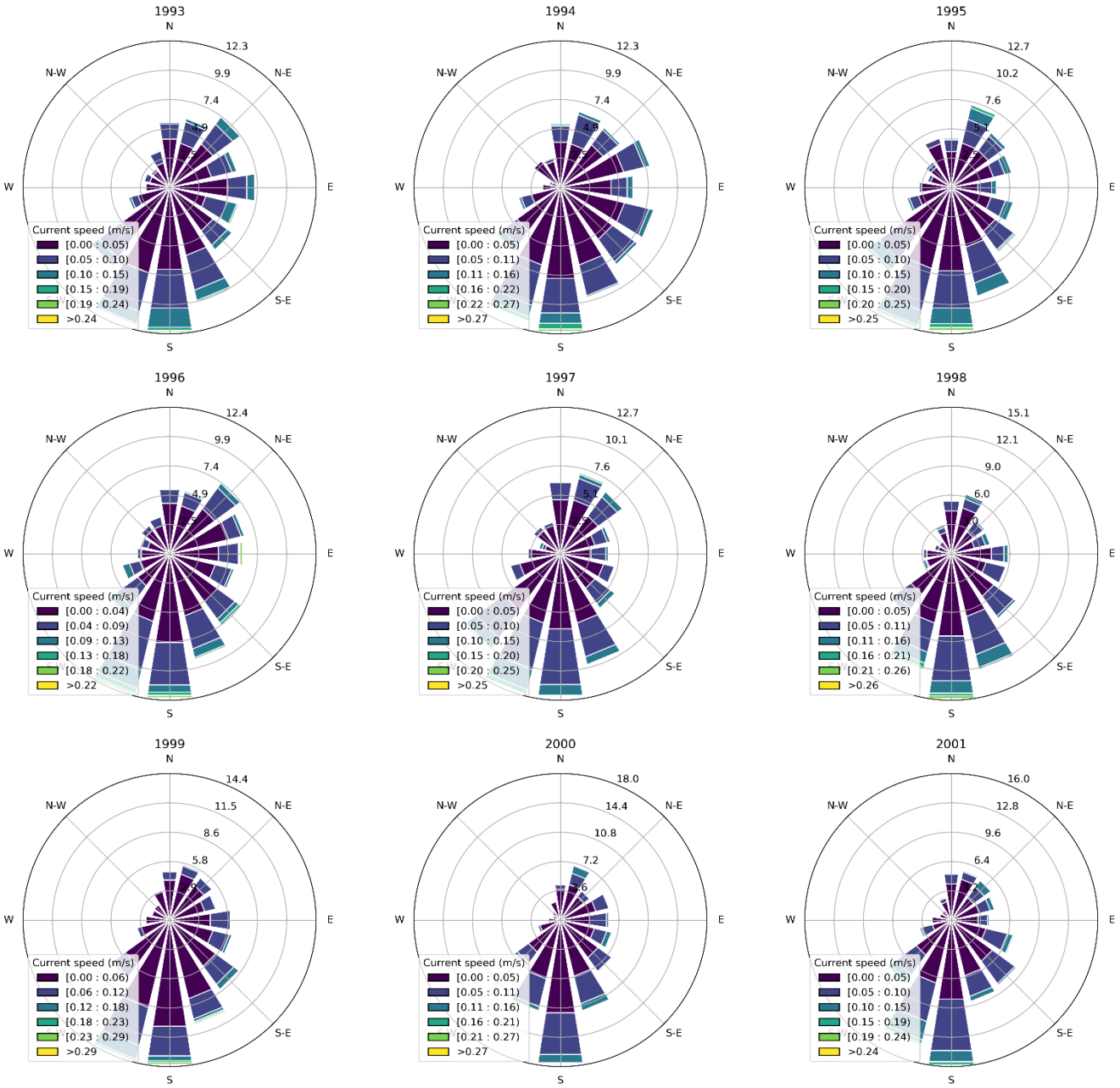

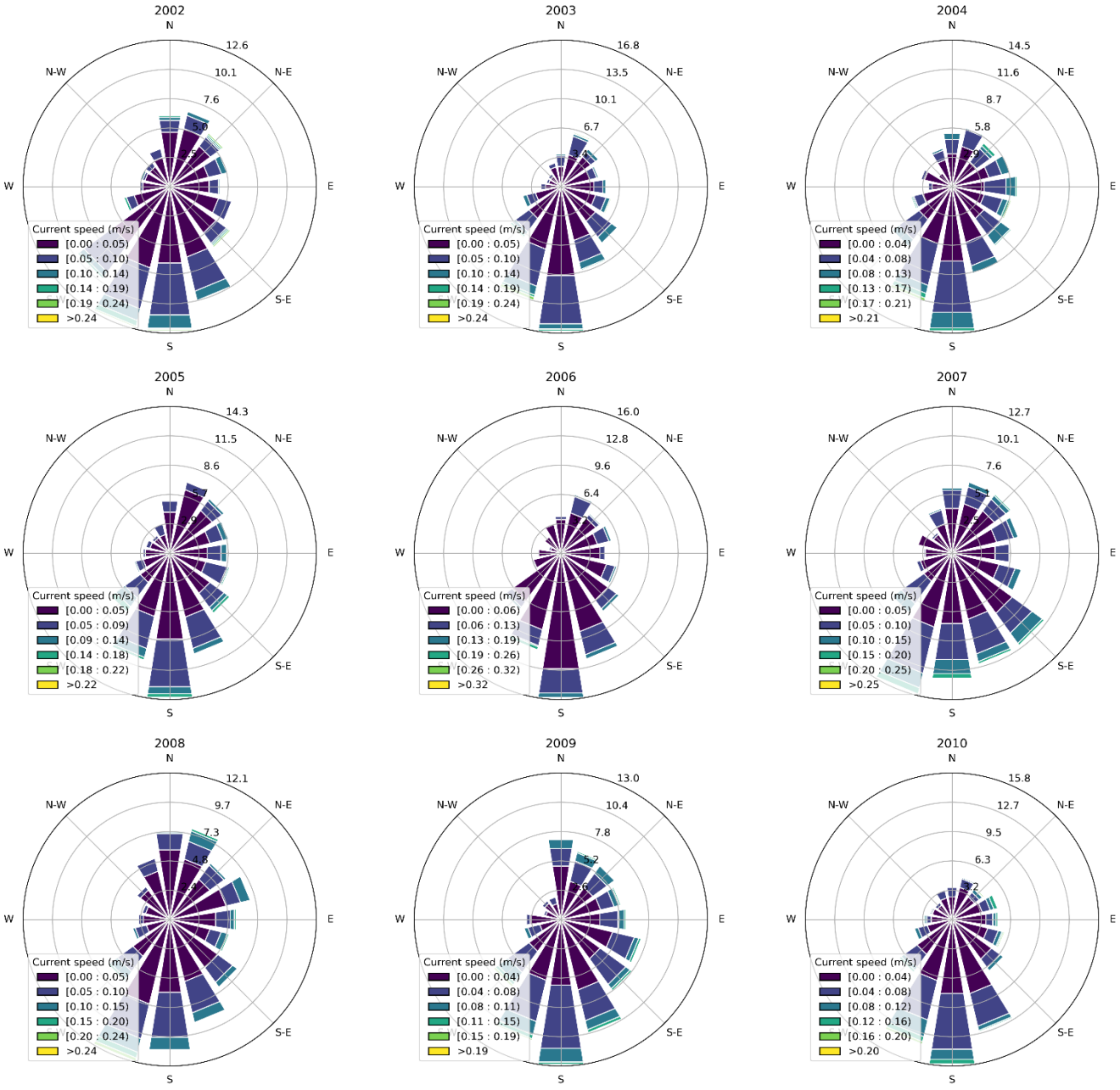
2002
N
N-E
E
S-E
S
W
N-W
12.6
10.1
7.6
5.0
Current speed (m/s)
[0.00 : 0.05)
[0.05 : 0.10)
[0.10 : 0.14)
[0.14 : 0.19)
[0.19 : 0.24)
>0.24
2003
16.8
13.5
10.1
6.7
3.4
Current speed (m/s)
[0.00 : 0.05)
[0.05 : 0.10)
[0.10 : 0.14)
[0.14 : 0.19)
[0.19 : 0.24)
>0.24
2004
14.5
11.6
8.7
5.8
Current speed (m/s)
[0.00 : 0.04)
[0.04 : 0.08)
[0.08 : 0.13)
[0.13 : 0.17)
[0.17 : 0.21)
>0.21
2005
14.3
11.5
8.6
Current speed (m/s)
[0.00 : 0.05)
[0.05 : 0.09)
[0.09 : 0.14)
[0.14 : 0.18)
[0.18 : 0.22)
>0.22
2006
16.0
12.8
9.6
6.4
Current speed (m/s)
[0.00 : 0.06)
[0.06 : 0.13)
[0.13 : 0.19)
[0.19 : 0.26)
[0.26 : 0.32)
>0.32
2007
12.7
10.1
7.6
Current speed (m/s)
[0.00 : 0.05)
[0.05 : 0.10)
[0.10 : 0.15)
[0.15 : 0.20)
[0.20 : 0.25)
>0.25
2008
12.1
9.7
7.3
4.8
Current speed (m/s)
[0.00 : 0.05)
[0.05 : 0.10)
[0.10 : 0.15)
[0.15 : 0.20)
[0.20 : 0.24)
>0.24
2009
13.0
10.4
7.8
5.2
Current speed (m/s)
[0.00 : 0.04)
[0.04 : 0.08)
[0.08 : 0.11)
[0.11 : 0.15)
[0.15 : 0.19)
>0.19
2010
15.8
12.7
9.5
6.3
Current speed (m/s)
[0.00 : 0.04)
[0.04 : 0.08)
[0.08 : 0.12)
[0.12 : 0.16)
[0.16 : 0.20)
>0.20

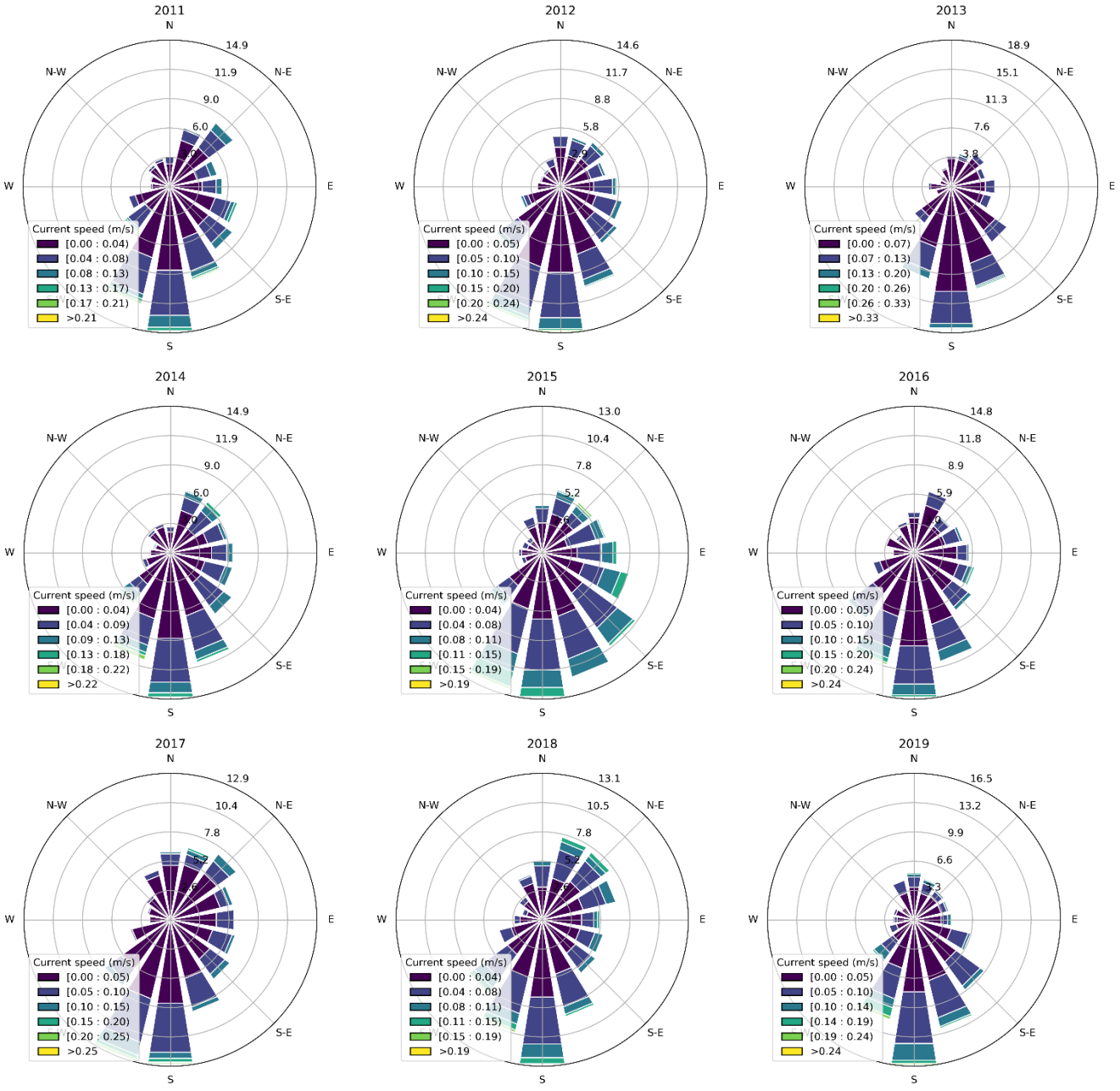
2011
N
N-E
E
S-E
S
W
N-W
14.9
11.9
9.0
6.0
Current speed (m/s)
[0.00 : 0.04)
[0.04 : 0.08)
[0.08 : 0.13)
[0.13 : 0.17)
[0.17 : 0.21)
>0.21
2012
14.6
11.7
8.8
5.8
Current speed (m/s)
[0.00 : 0.05)
[0.05 : 0.10)
[0.10 : 0.15)
[0.15 : 0.20)
[0.20 : 0.24)
>0.24
2013
18.9
15.1
11.3
7.6
3.8
Current speed (m/s)
[0.00 : 0.07)
[0.07 : 0.13)
[0.13 : 0.20)
[0.20 : 0.26)
[0.26 : 0.33)
>0.33
2014
14.9
11.9
9.0
6.0
Current speed (m/s)
[0.00 : 0.04)
[0.04 : 0.09)
[0.09 : 0.13)
[0.13 : 0.18)
[0.18 : 0.22)
>0.22
2015
13.0
10.4
7.8
5.2
Current speed (m/s)
[0.00 : 0.04)
[0.04 : 0.08)
[0.08 : 0.11)
[0.11 : 0.15)
[0.15 : 0.19)
>0.19
2016
14.8
11.8
8.9
5.9
Current speed (m/s)
[0.00 : 0.05)
[0.05 : 0.10)
[0.10 : 0.15)
[0.15 : 0.20)
[0.20 : 0.24)
>0.24
2017
12.9
10.4
7.8
5.2
Current speed (m/s)
[0.00 : 0.05)
[0.05 : 0.10)
[0.10 : 0.15)
[0.15 : 0.20)
[0.20 : 0.25)
>0.25
2018
13.1
10.5
7.8
5.2
Current speed (m/s)
[0.00 : 0.04)
[0.04 : 0.08)
[0.08 : 0.11)
[0.11 : 0.15)
[0.15 : 0.19)
>0.19
2019
16.5
13.2
9.9
6.6
Current speed (m/s)
[0.00 : 0.05)
[0.05 : 0.10)
[0.10 : 0.14)
[0.14 : 0.19)
[0.19 : 0.24)
>0.24

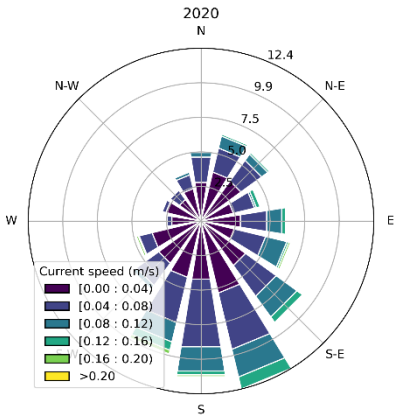
2020
N
N-E
E
S-E
S
W
N-W
12.4
9.9
7.5
Current speed (m/s)
[0.00 : 0.04)
[0.04 : 0.08)
[0.08 : 0.12)
[0.12 : 0.16)
[0.16 : 0.20)
>0.20

Appendix 5 Fyrskeppet OWF, Current roses (SMHI, modelled 2x2km)

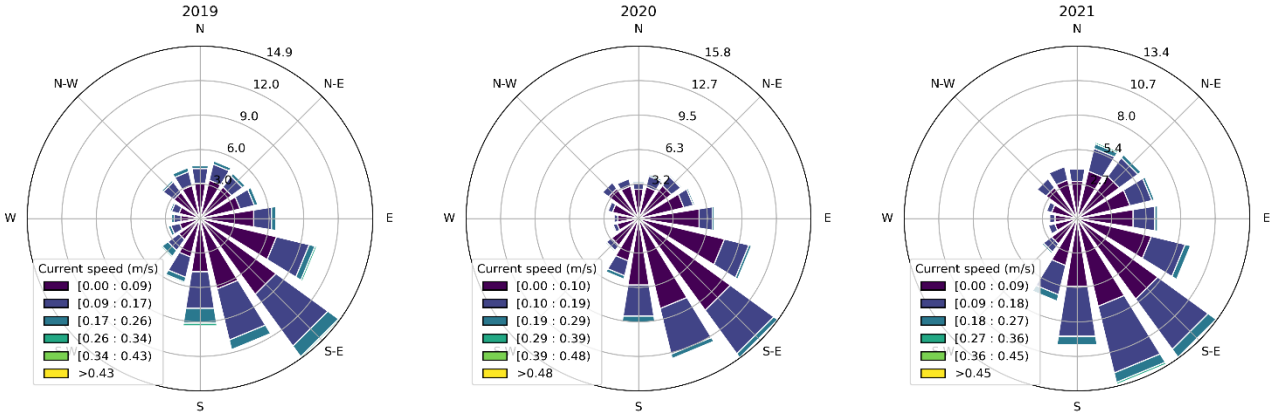

Appendix 6 Fyrskeppet OWF, Significant wave height – Monthly average

January, 2021

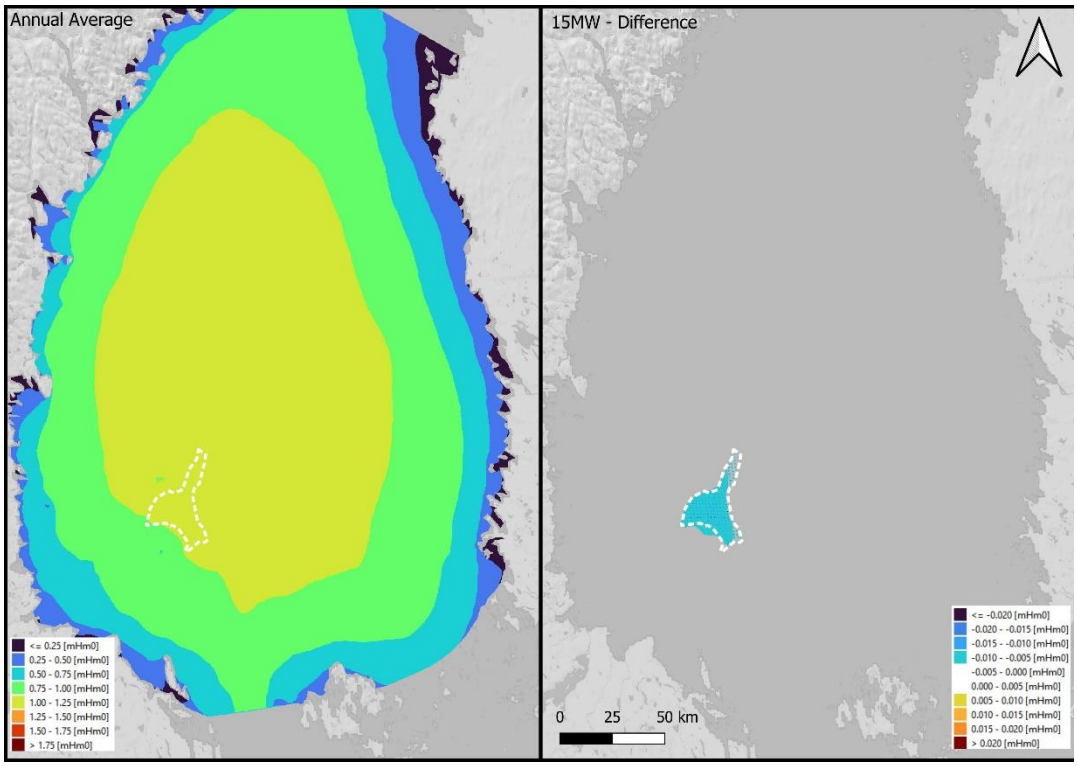

February, 2021

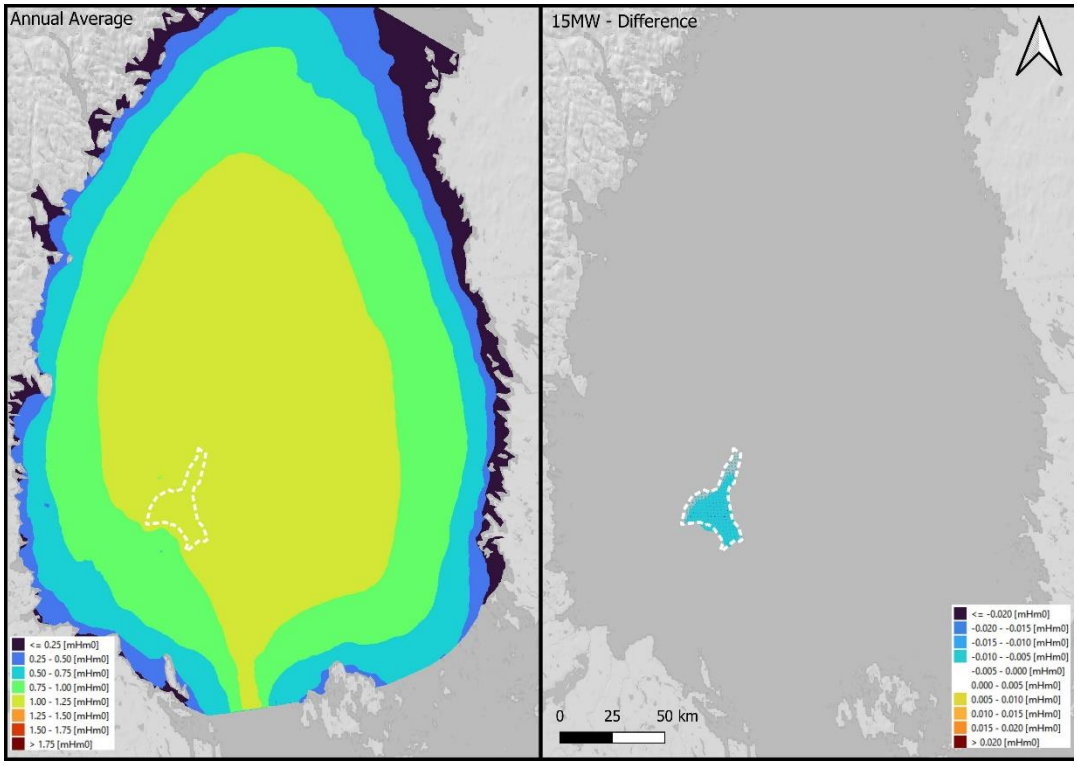

March 2021

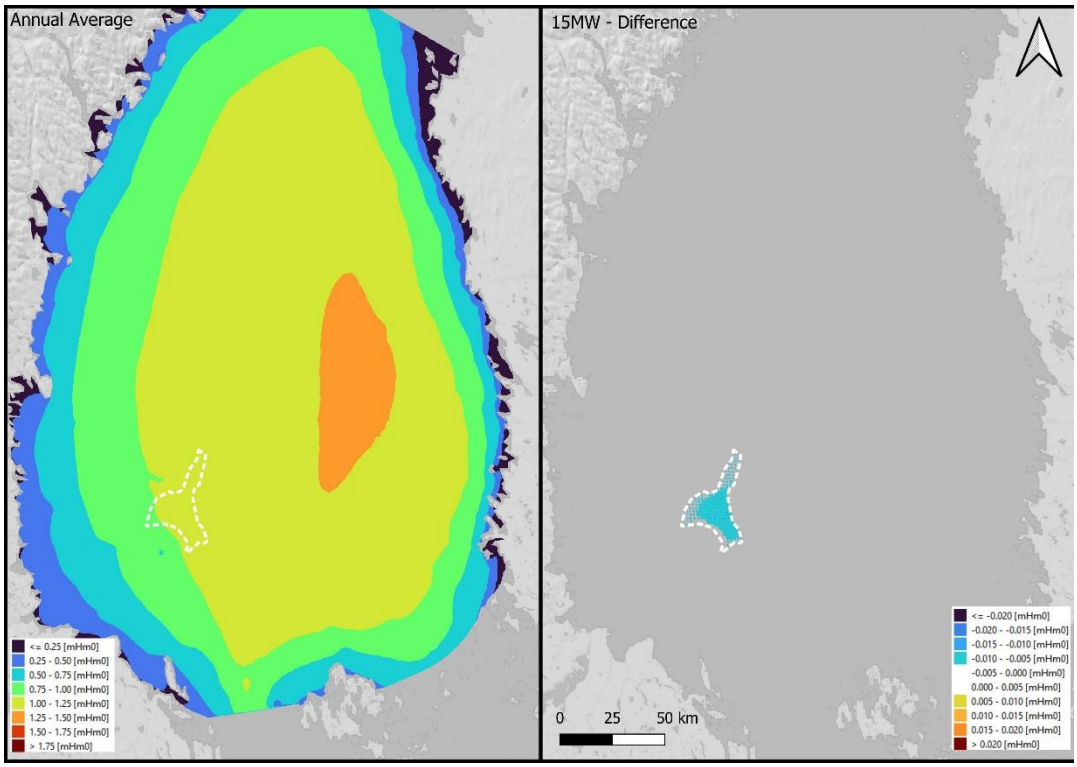

April 2021

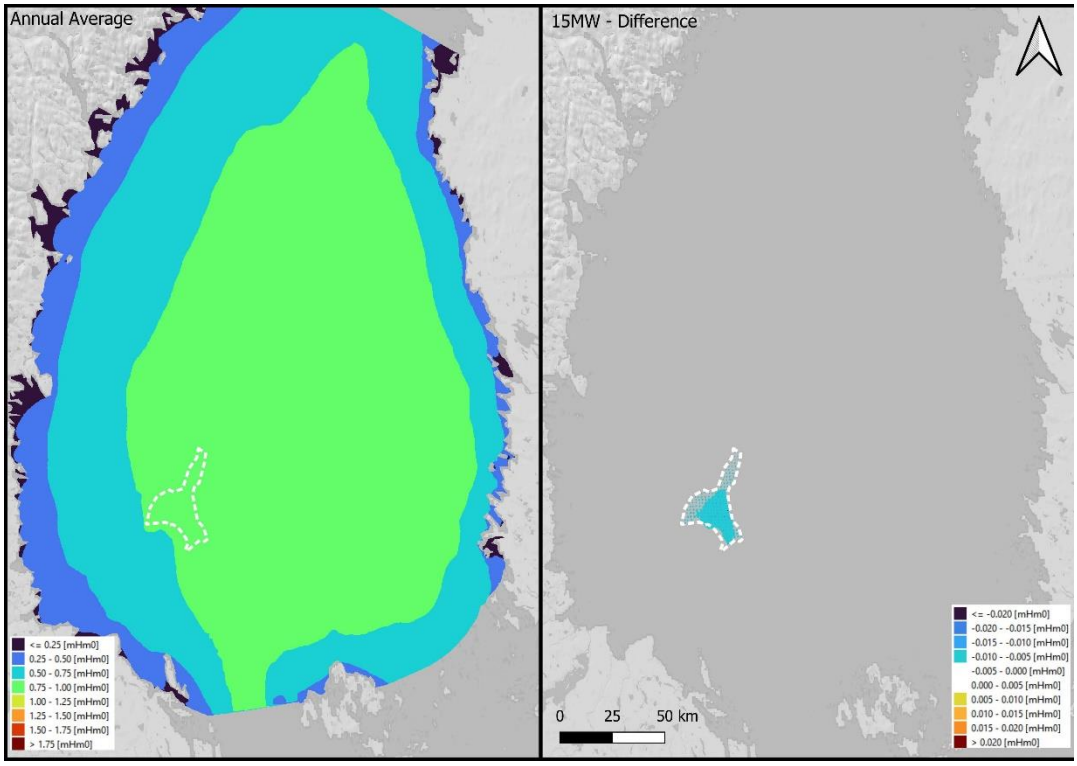

May 2021

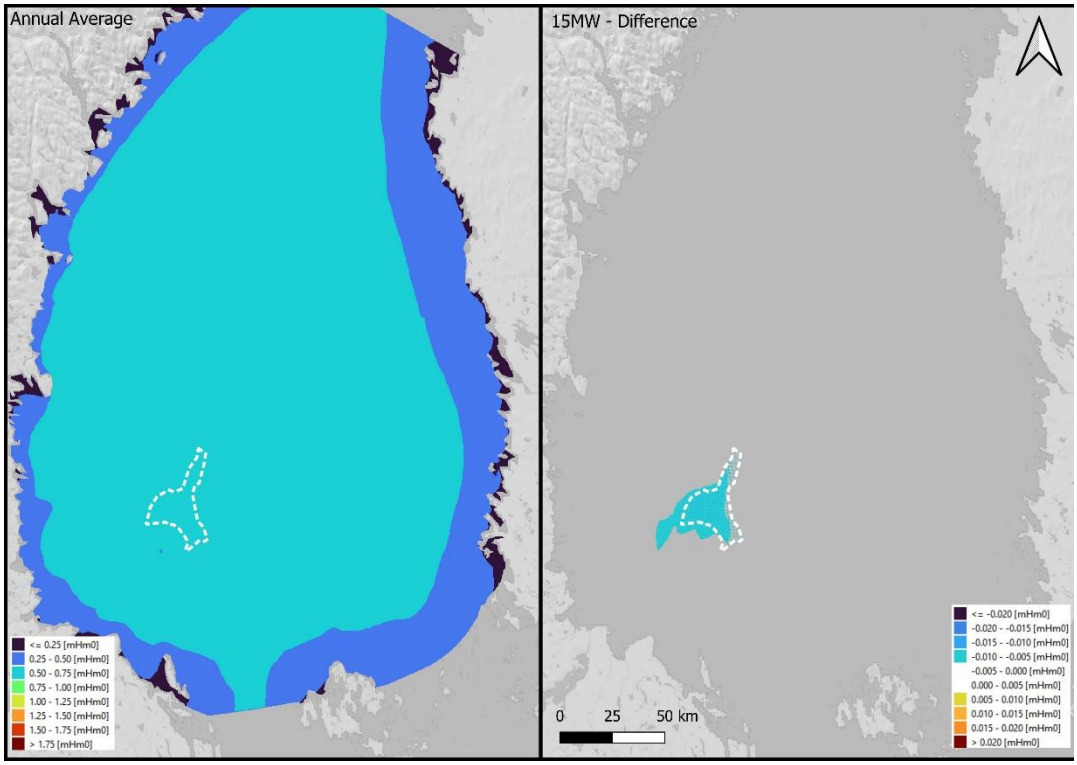

June 2021

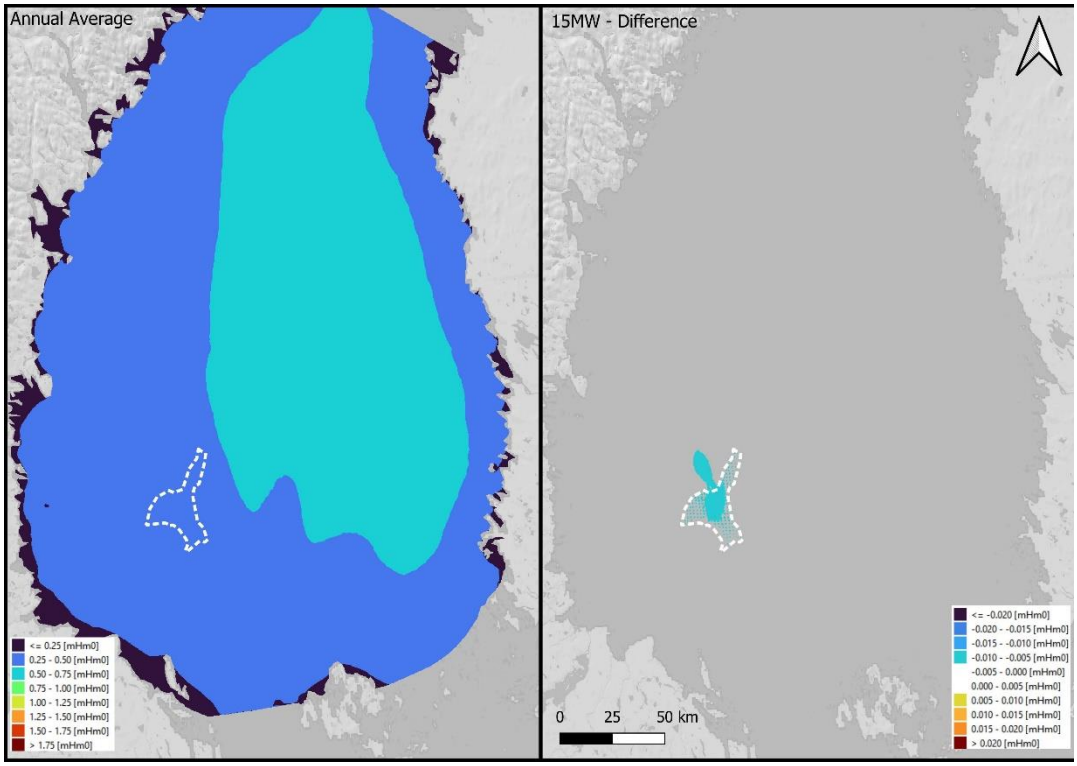

July 2021

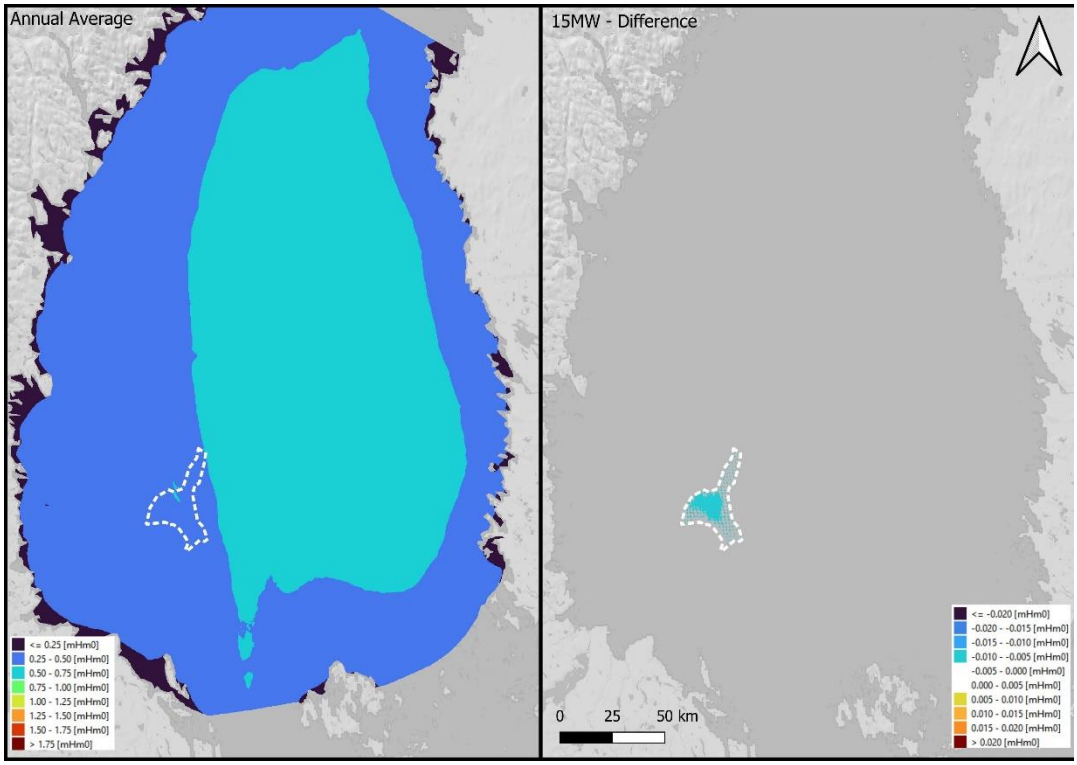

Aug. 2021

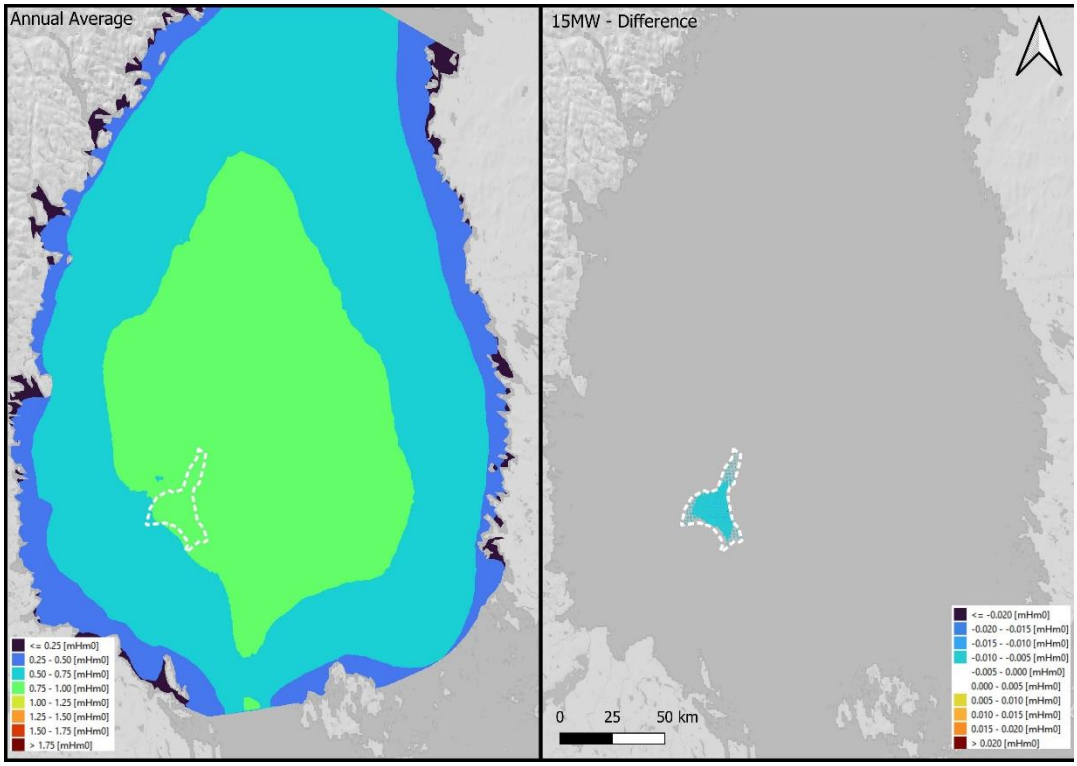

Sep. 2021

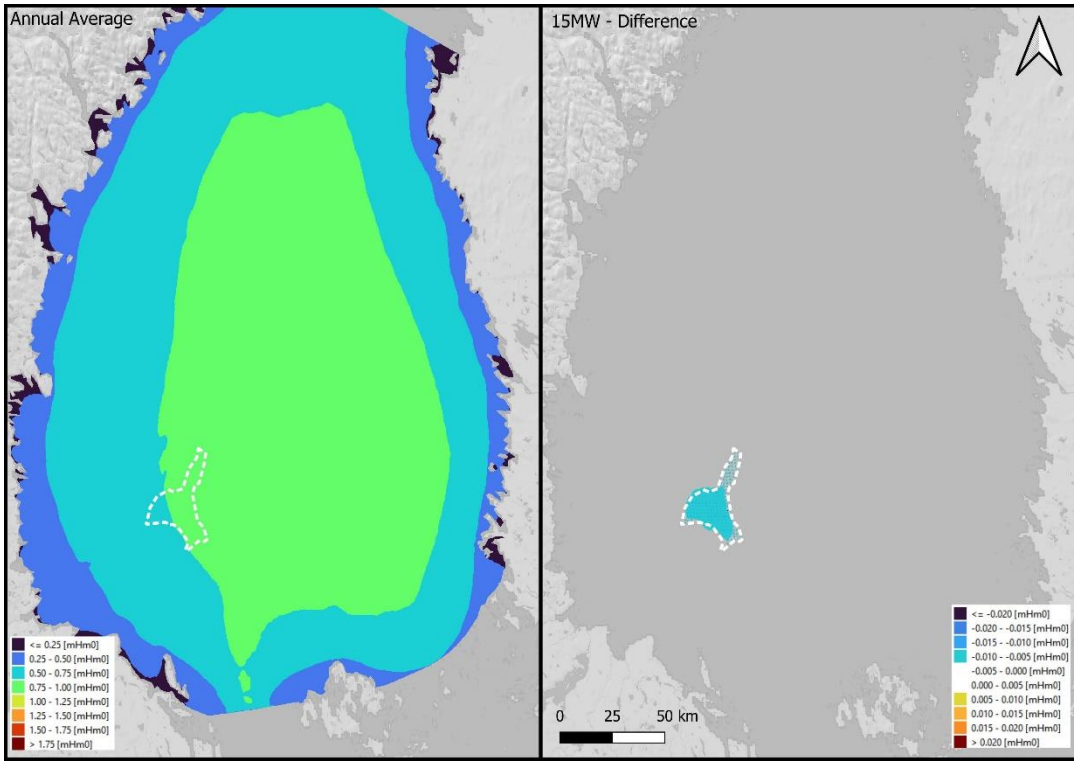

Oct. 2021

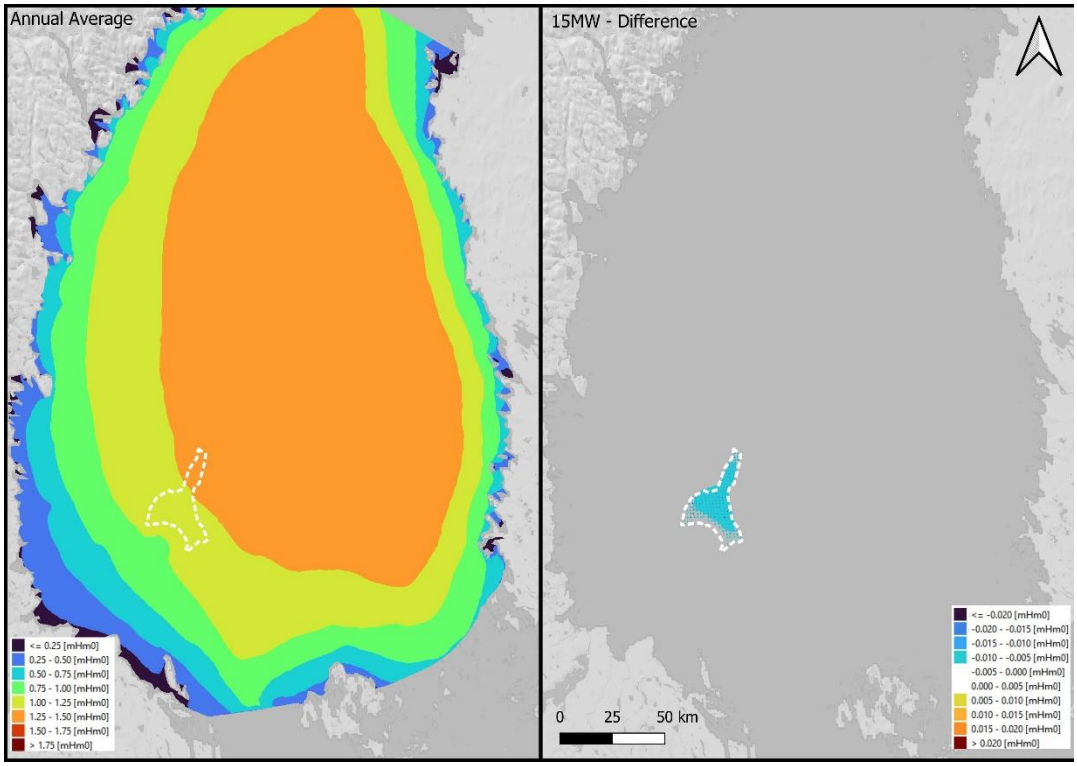

Nov. 2021

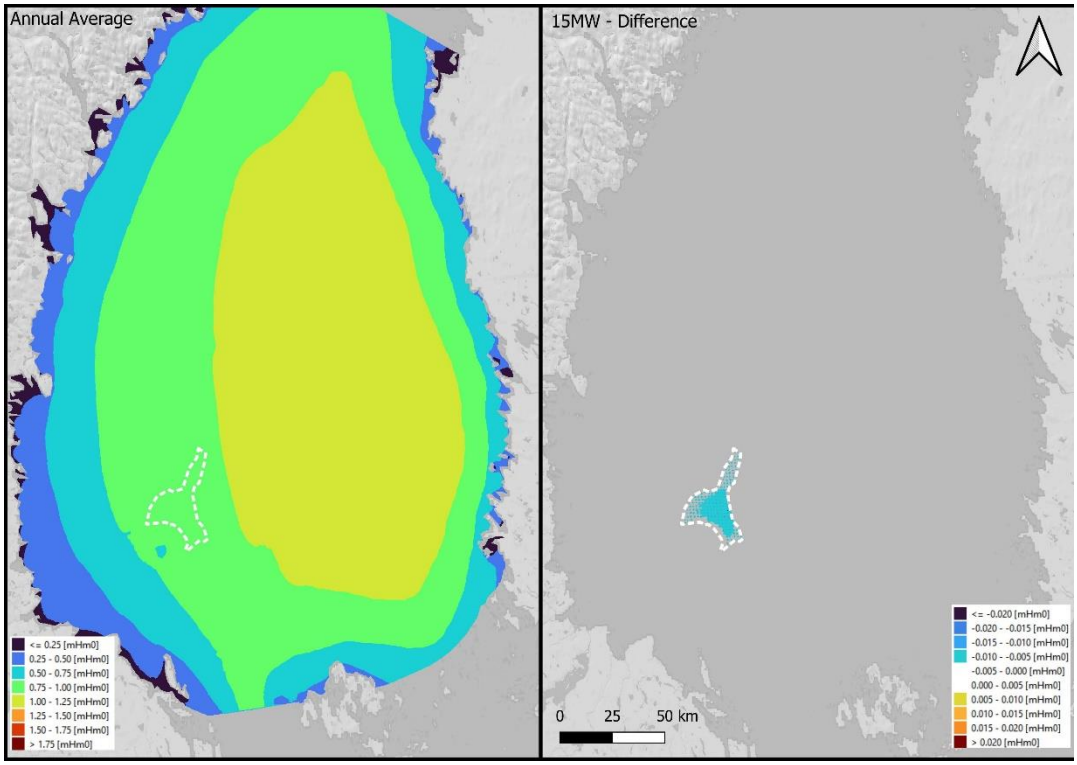

Dec. 2021

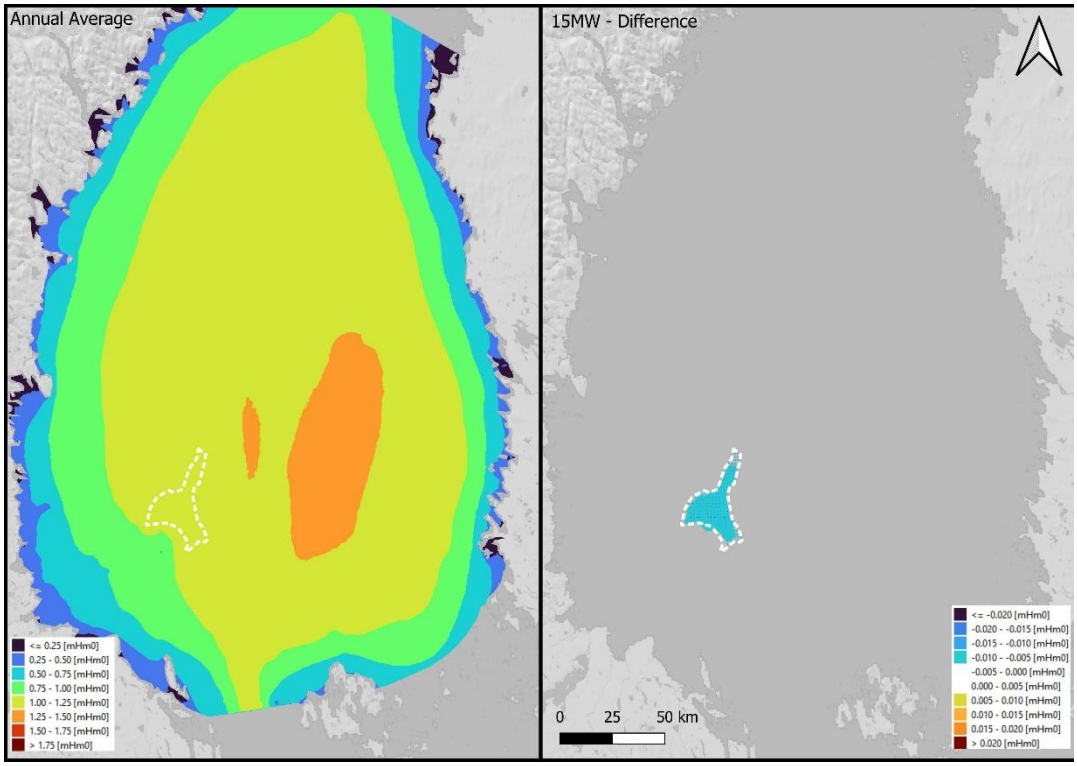

Appendix 7 Fyrskeppet OWF, Temperature -10 to -20 m – Monthly average

January, 2021

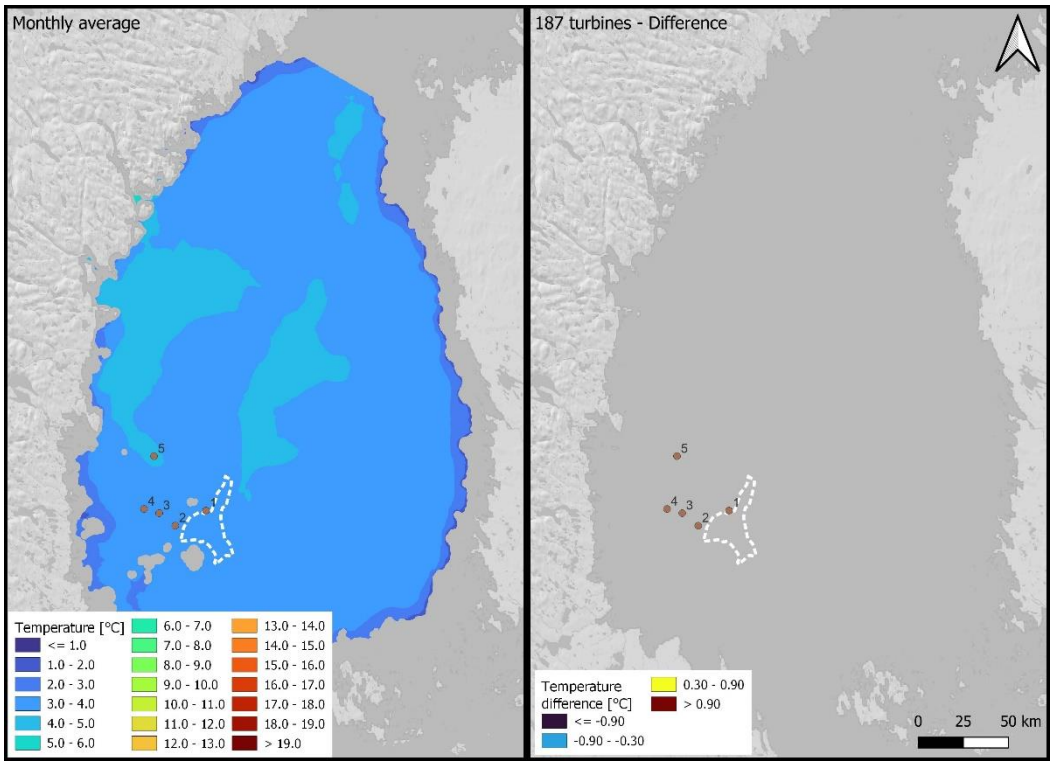

February, 2021

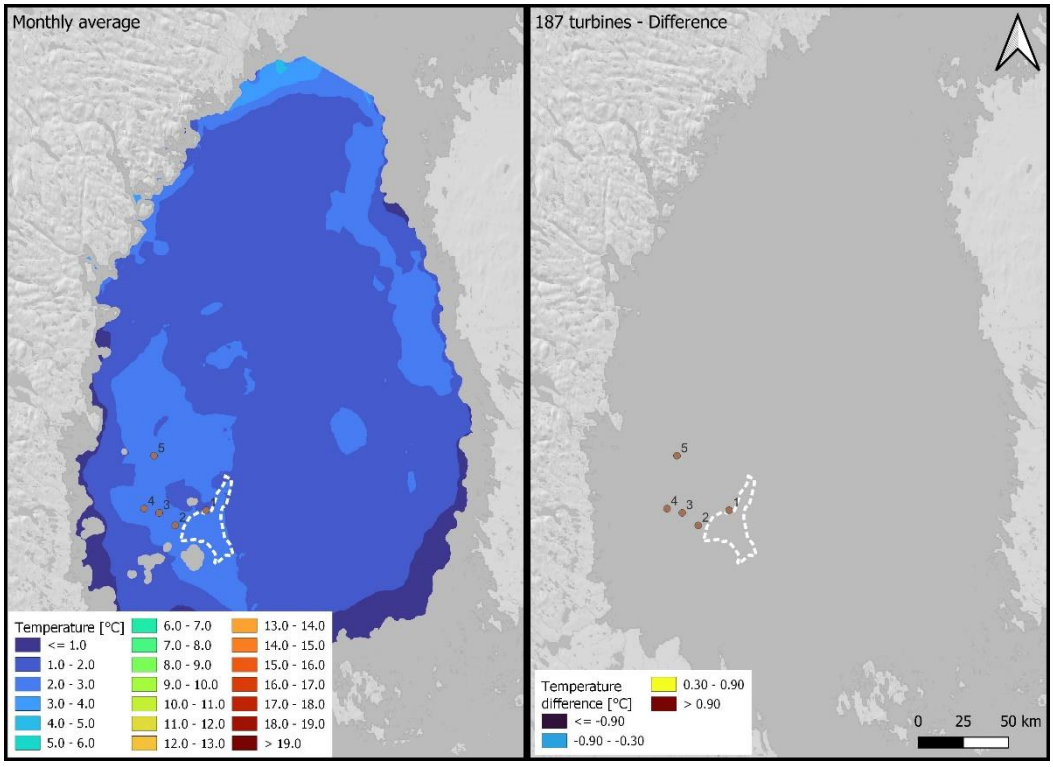

March 2021

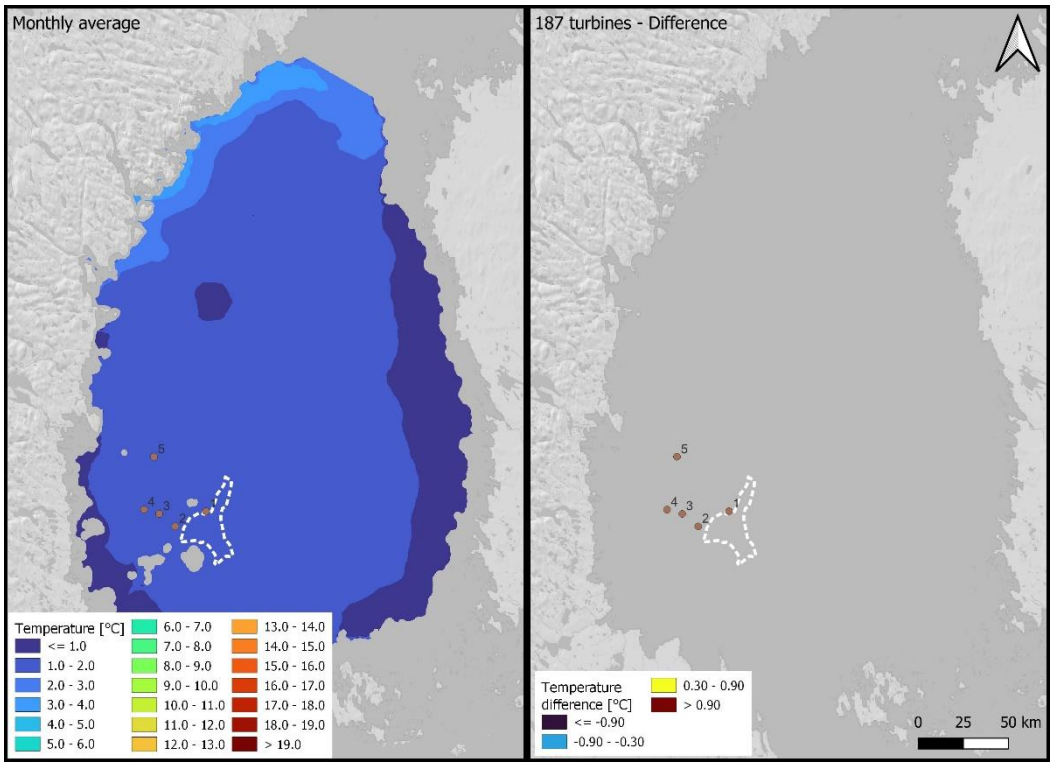

April 2021

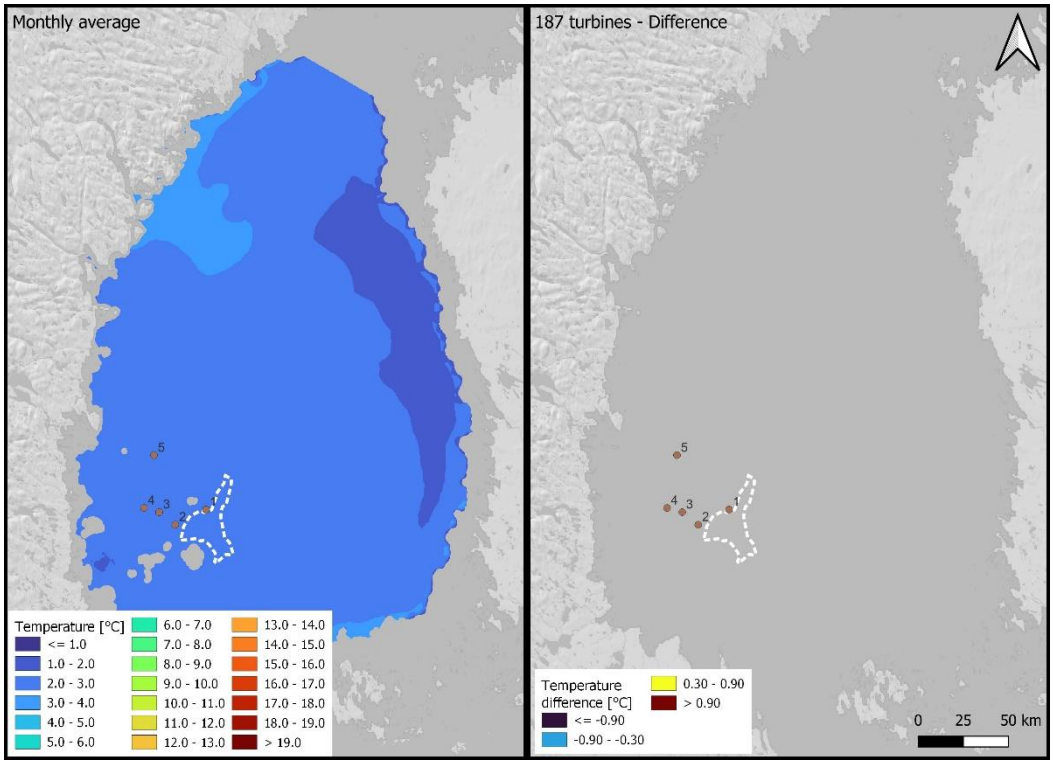

May 2021

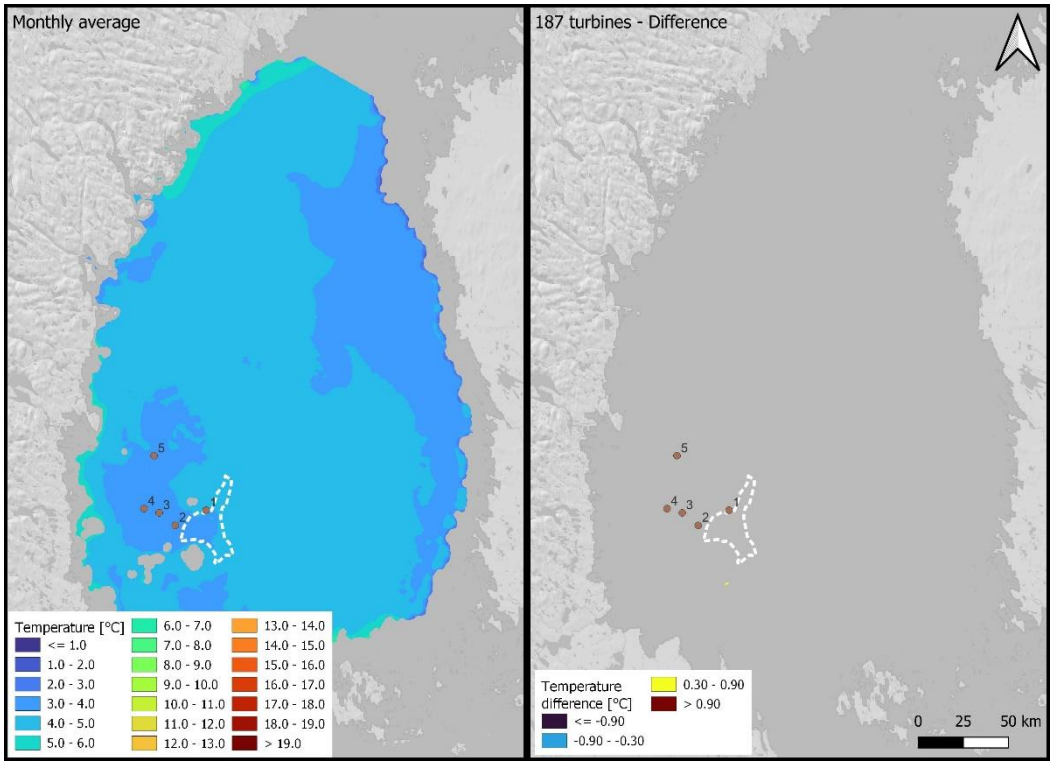

June 2021

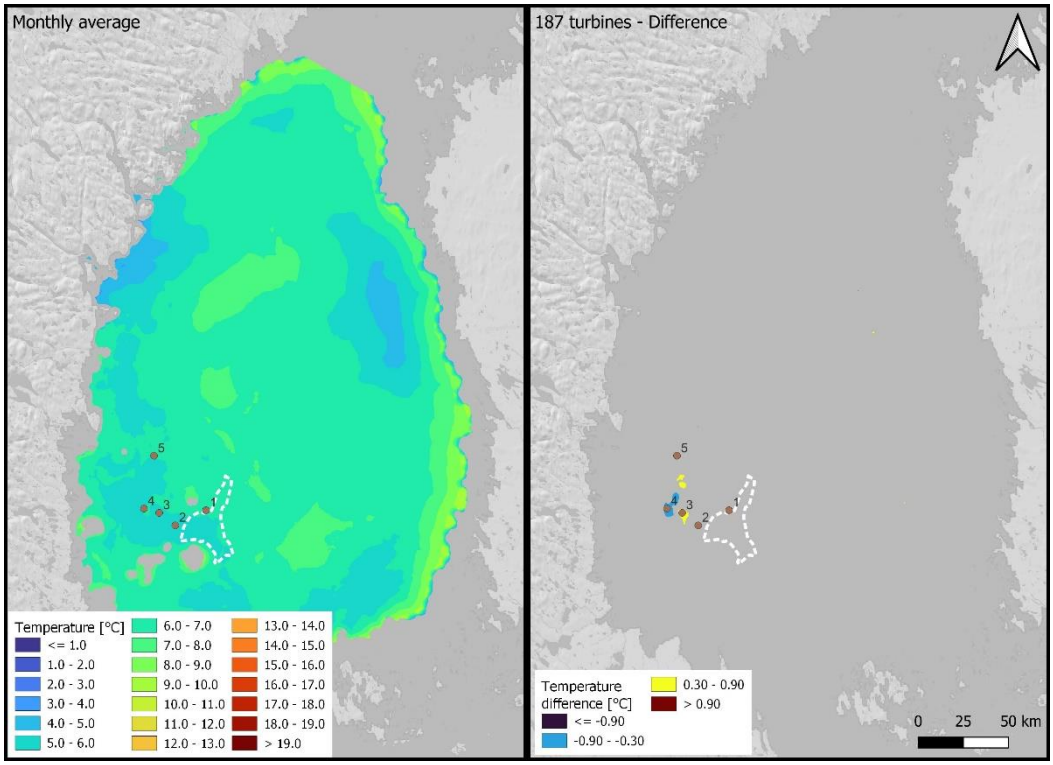

July 2021

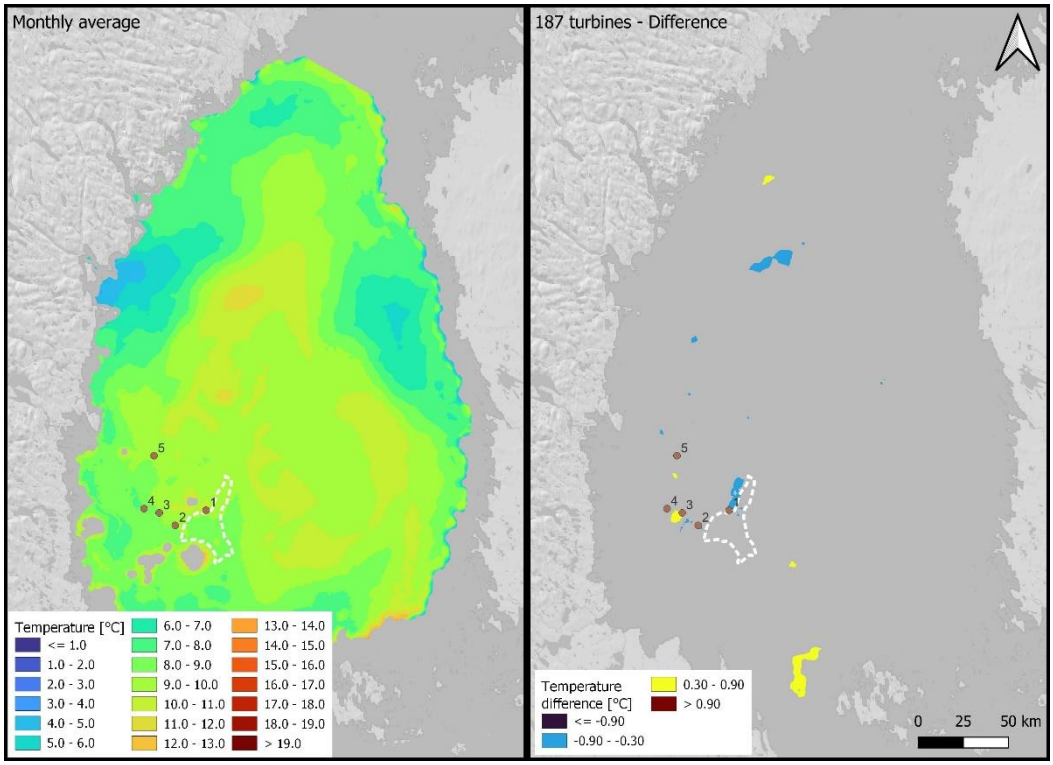

Aug. 2021

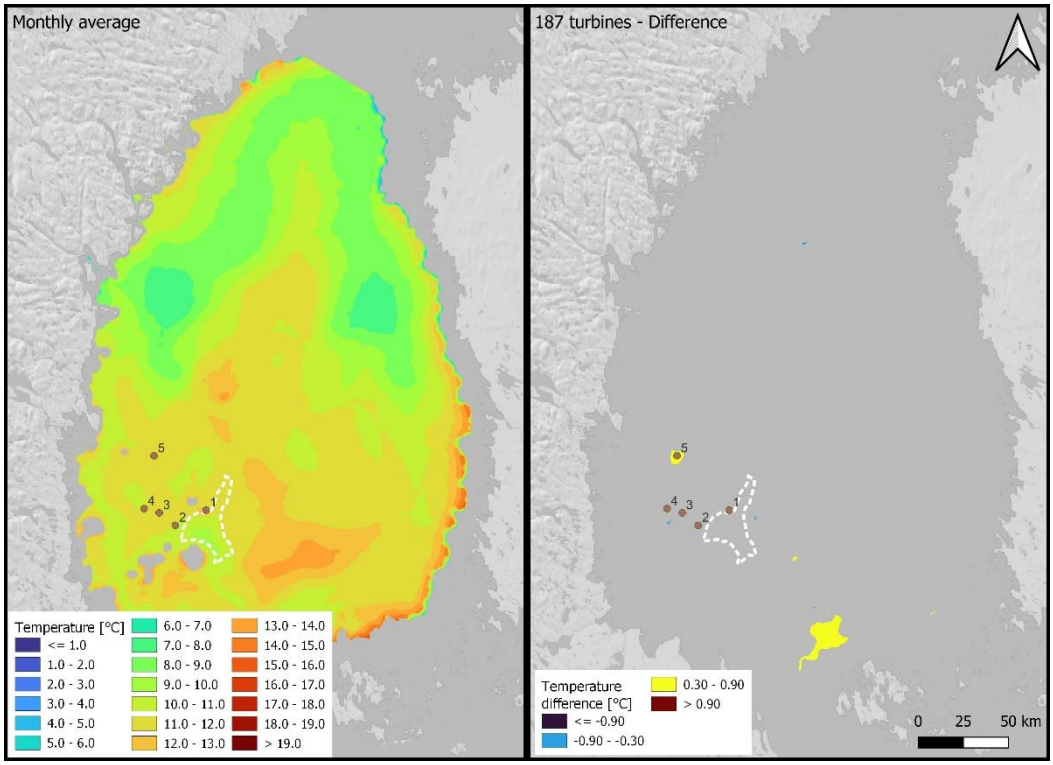

Sep. 2021

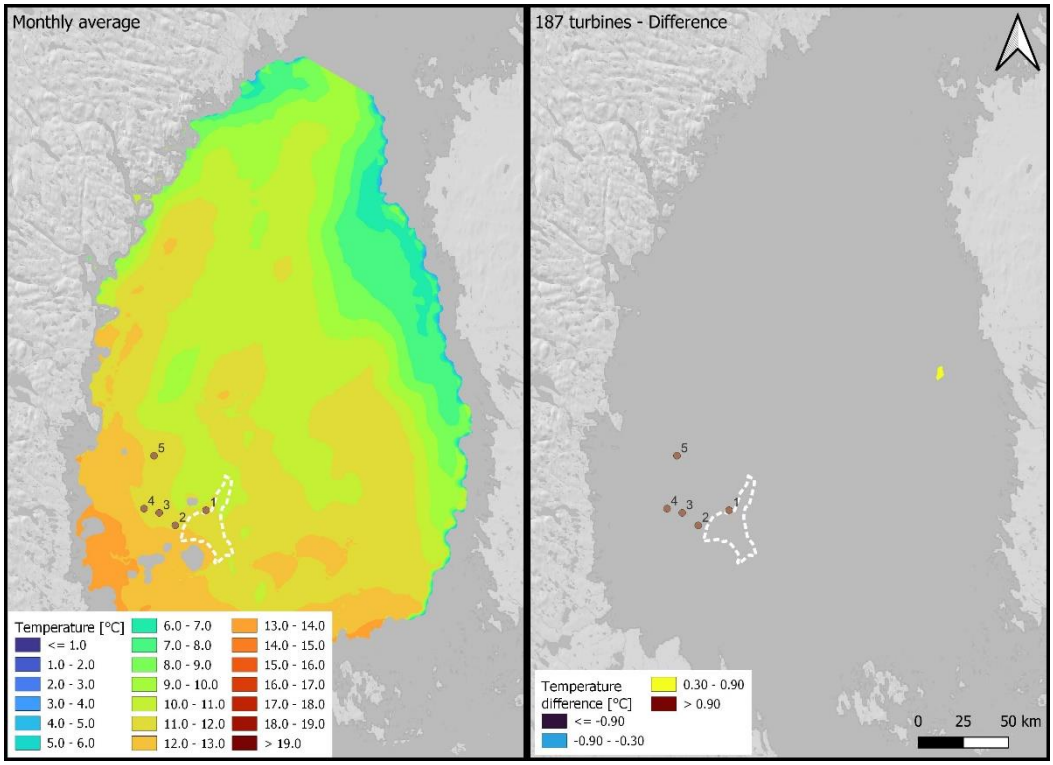

Oct. 2021

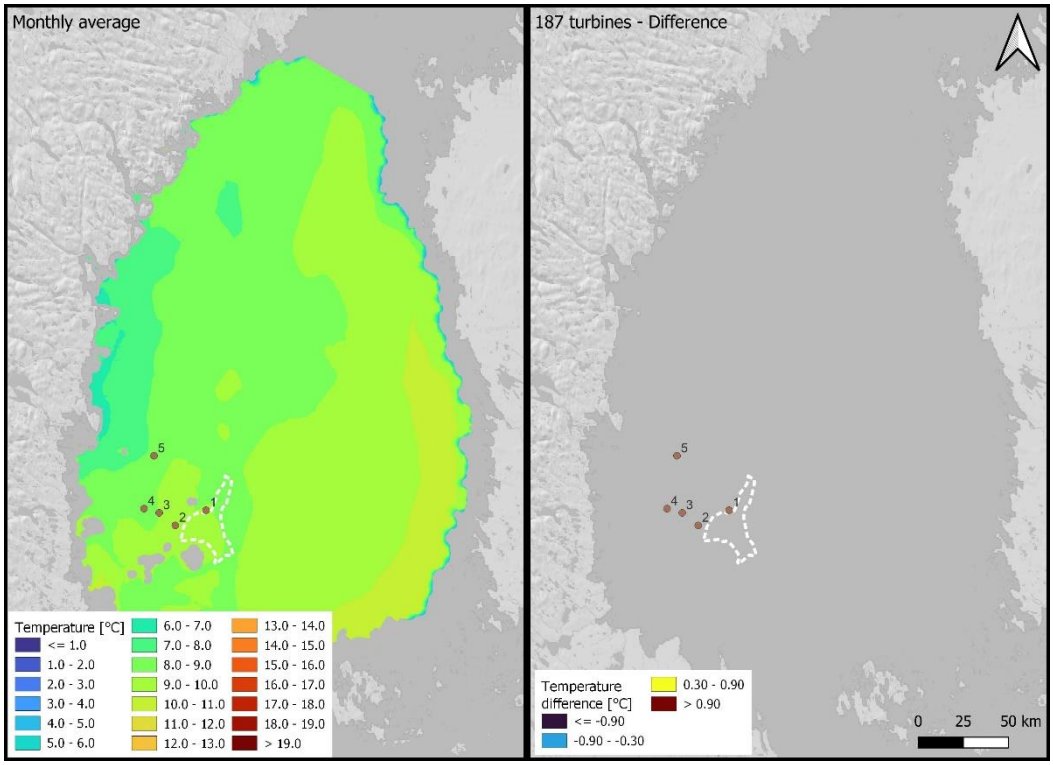

Nov. 2021

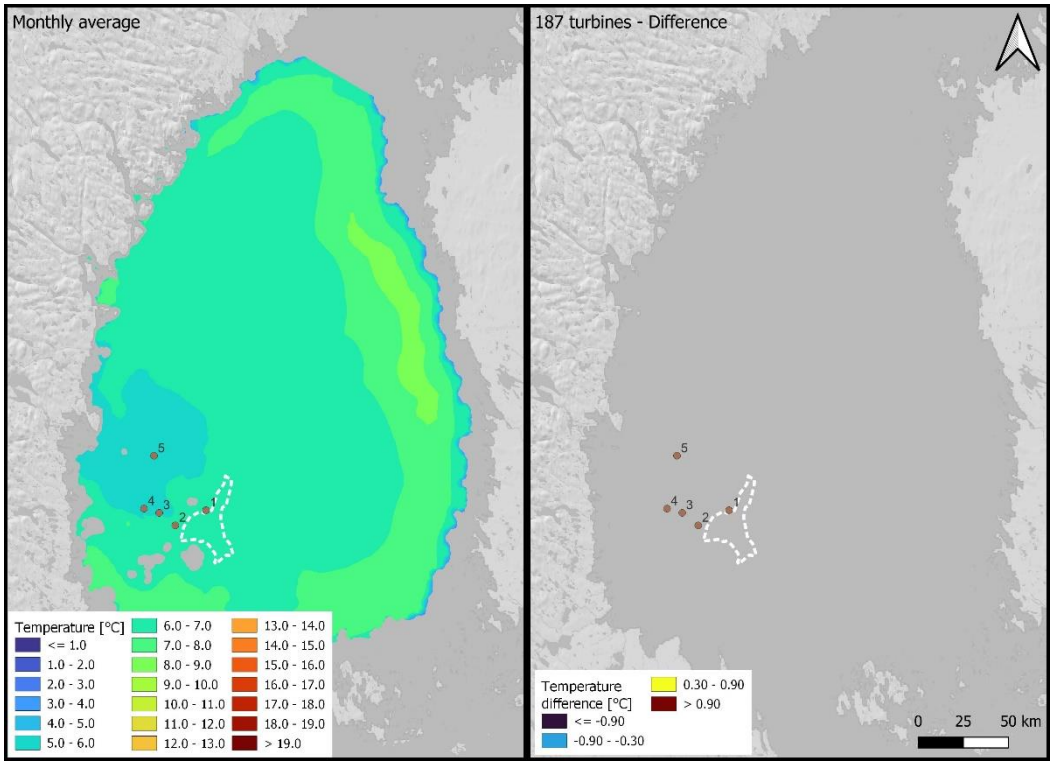

Dec. 2021

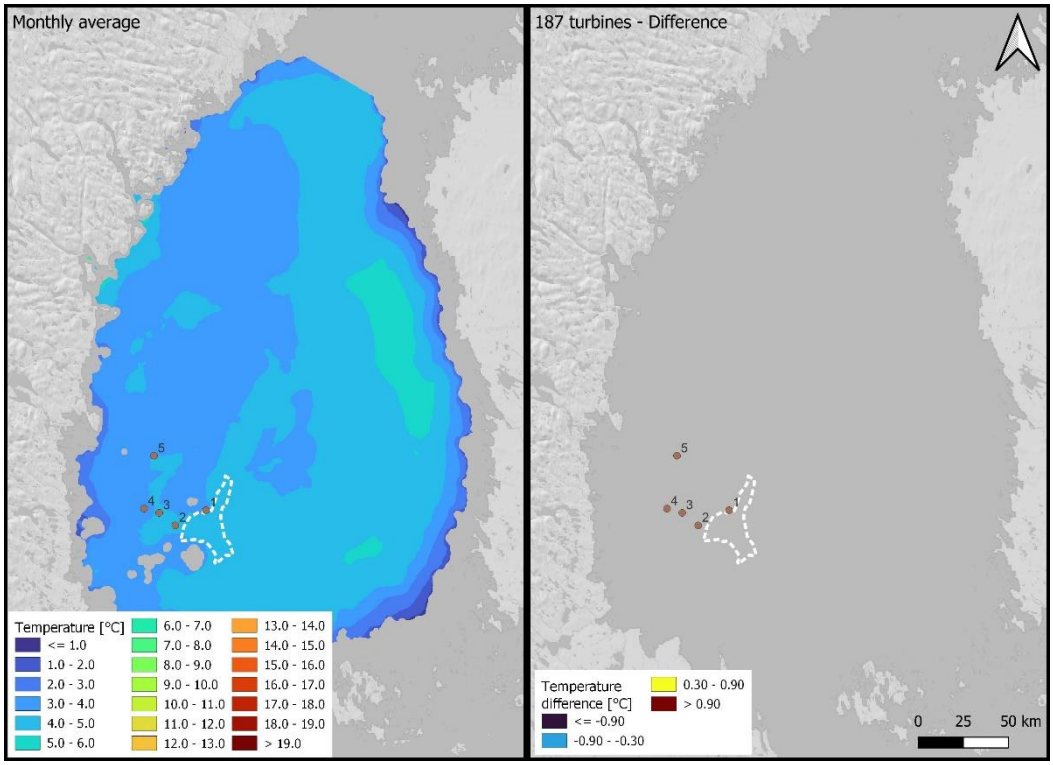

Appendix 8 Fyrskeppet OWF, Temperature profiles

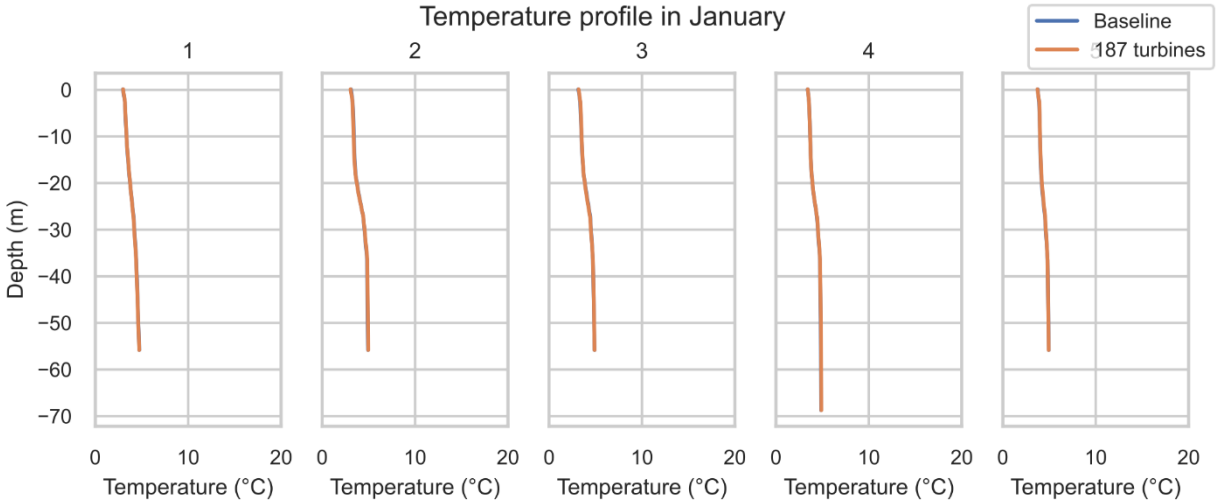

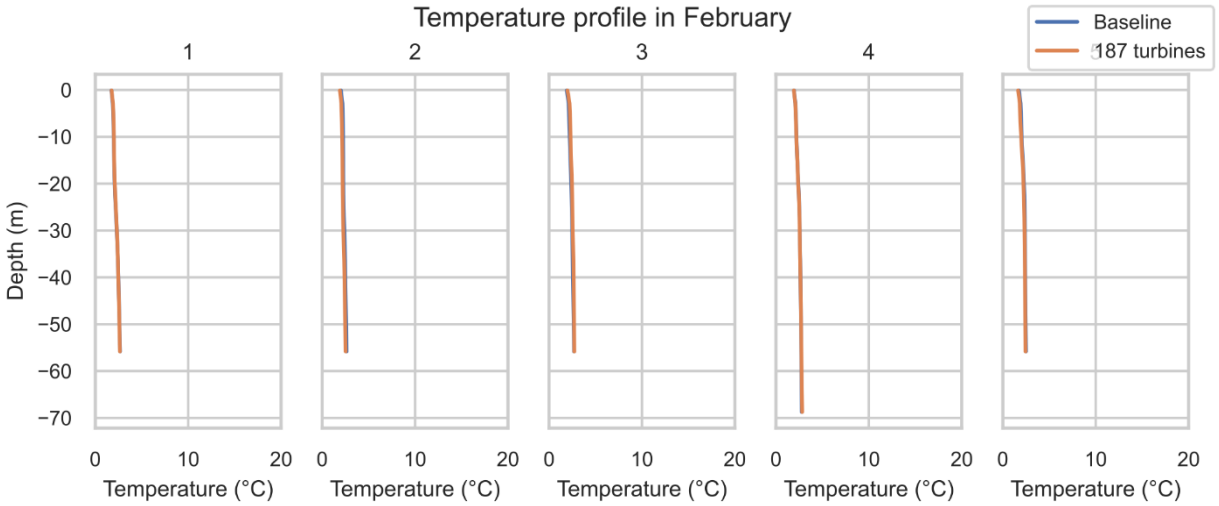

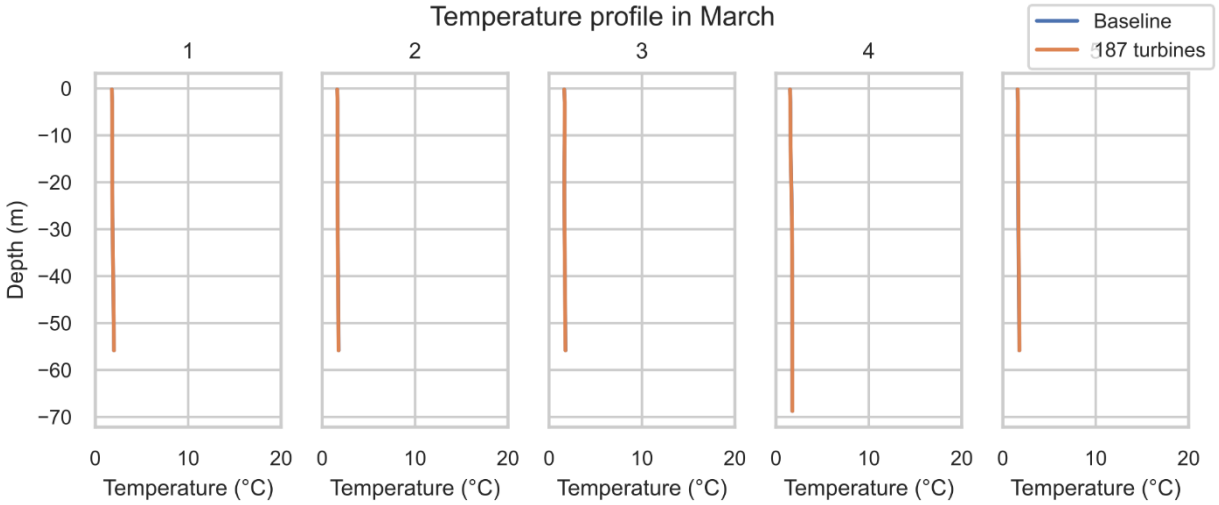
Temperature profile in March
Baseline
187 turbines
1
2
3
4
Depth (m)
0
−10
−20
−30
−40
−50
−60
−70
0
10
20
Temperature (°C)

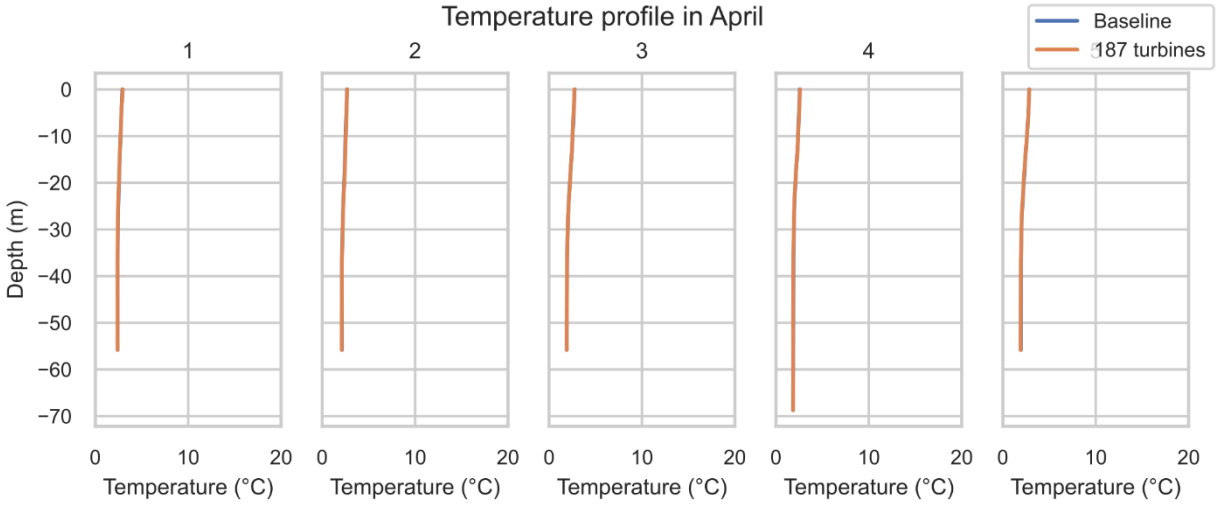
Temperature profile in April
Baseline
187 turbines
1
2
3
4
Depth (m)
0
−10
−20
−30
−40
−50
−60
−70
0
10
20
Temperature (°C)

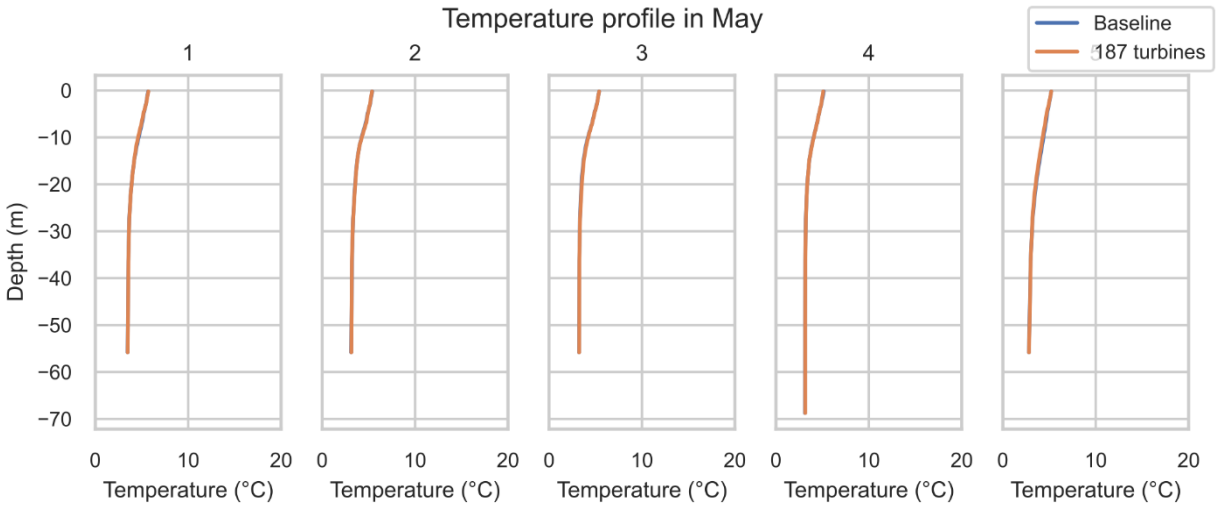
Temperature profile in May
Baseline
187 turbines
1
2
3
4
Depth (m)
0
−10
−20
−30
−40
−50
−60
−70
0
10
20
Temperature (°C)

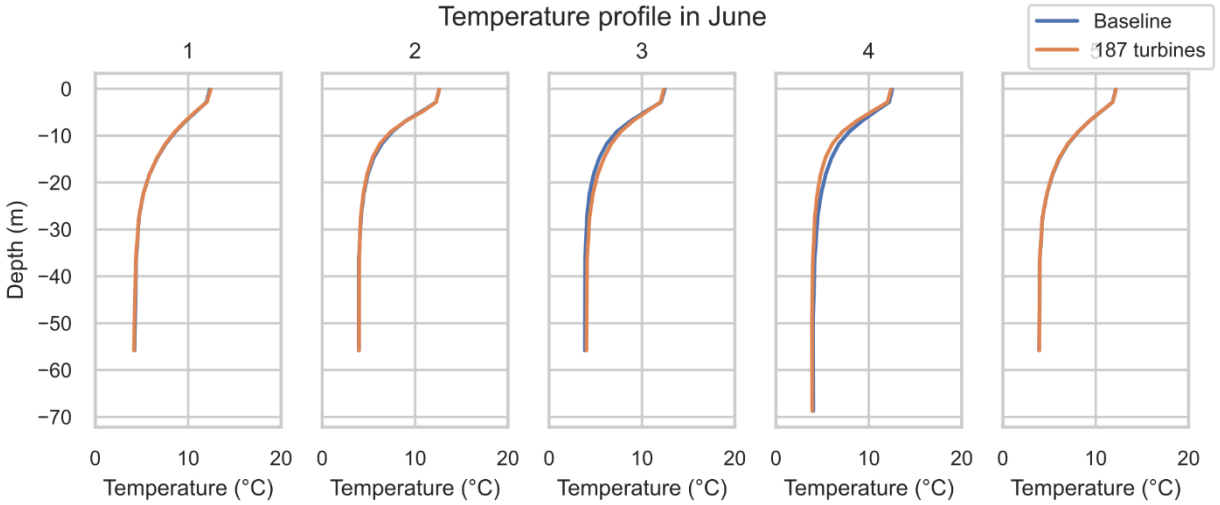
Temperature profile in June
Baseline
187 turbines
1
2
3
4
Depth (m)
0
−10
−20
−30
−40
−50
−60
−70
0
10
20
Temperature (°C)

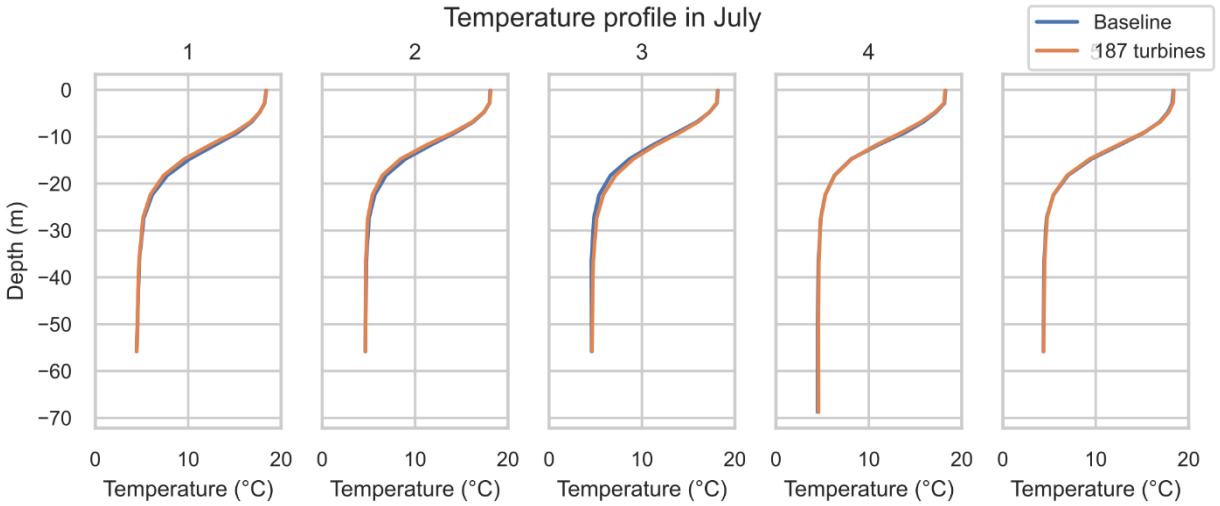
Temperature profile in July
Baseline
187 turbines
1
2
3
4
Depth (m)
0
−10
−20
−30
−40
−50
−60
−70
0
10
20
Temperature (°C)

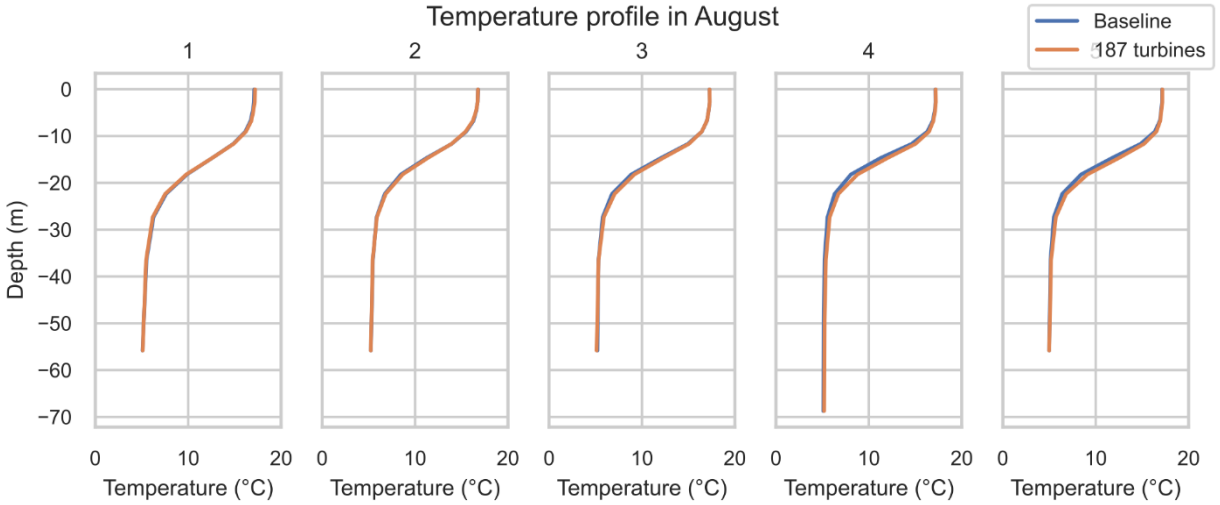
Temperature profile in August
Baseline
187 turbines
1
2
3
4
Depth (m)
0
−10
−20
−30
−40
−50
−60
−70
0
10
20
Temperature (°C)

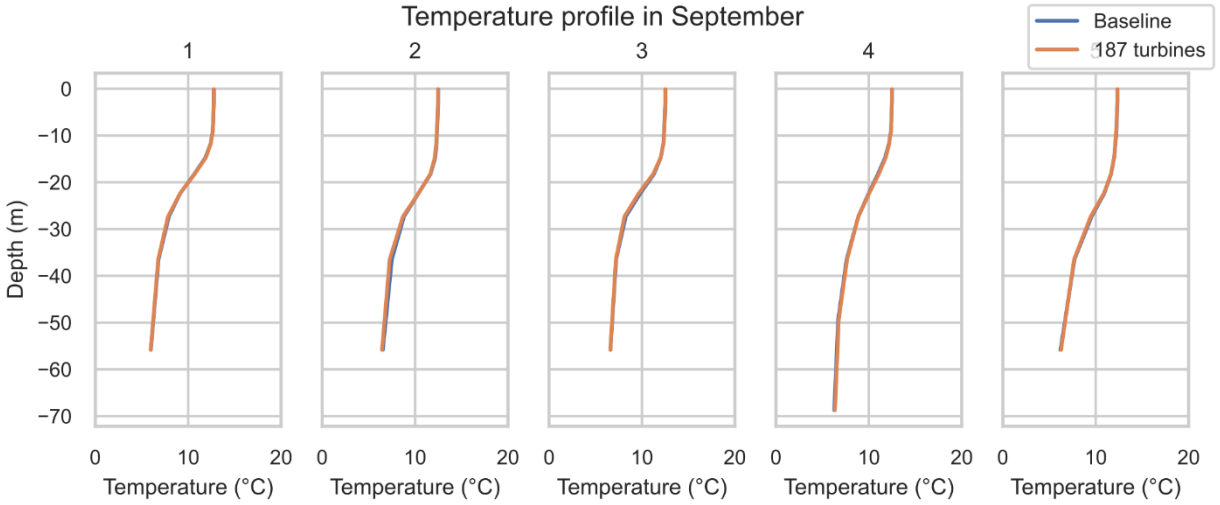
Temperature profile in September
Baseline
187 turbines
1
2
3
4
Depth (m)
0
−10
−20
−30
−40
−50
−60
−70
0
10
20
Temperature (°C)

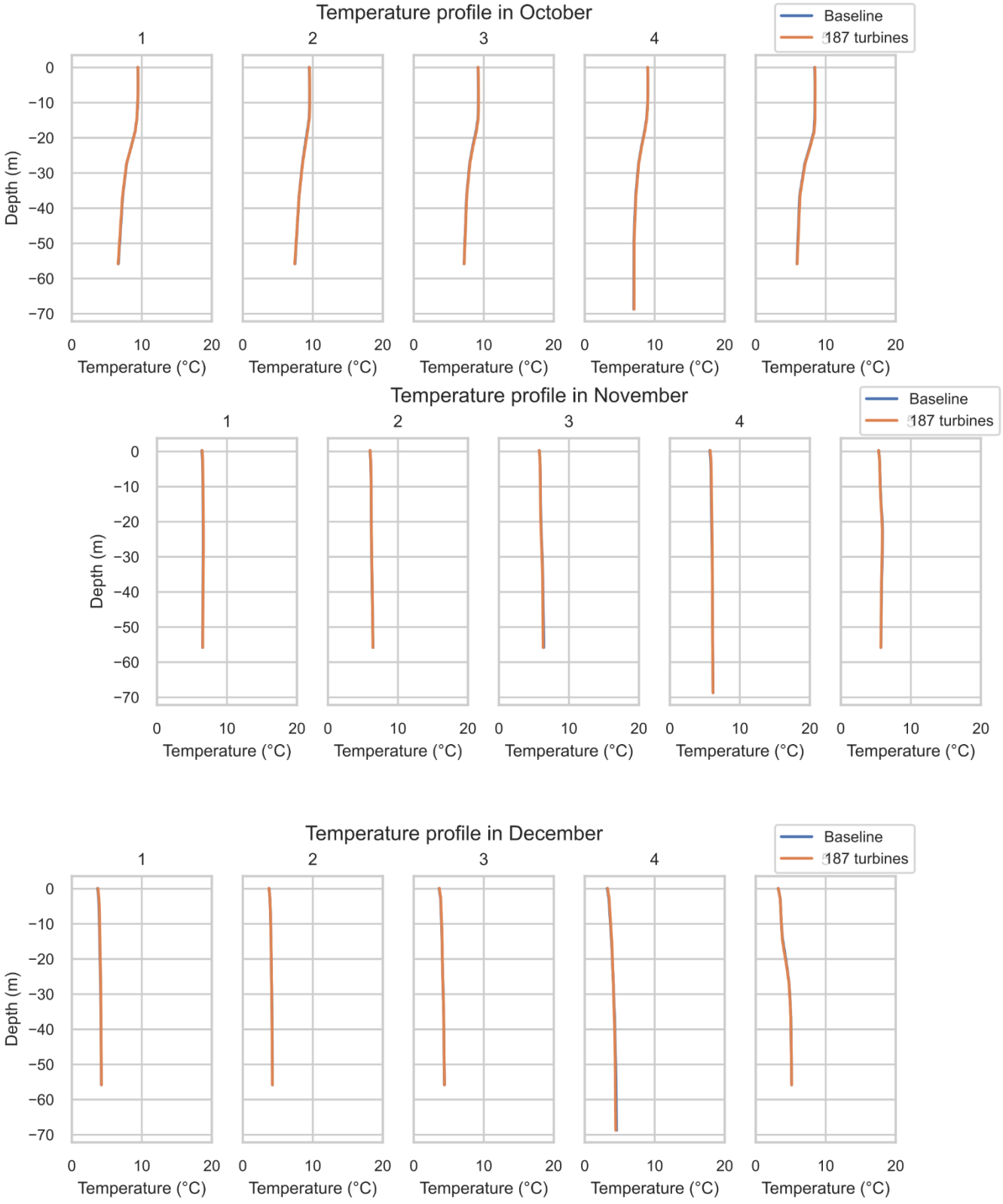

Figure 9.5: Monthly averaged temperature profiles at points 1 to 5 (Figure 8.9) comparing the base, 15MW and 30MW cases.

Appendix 9 Fyrskeppet OWF, June water level